HYDRODYNAMIC FORCES ON OSCILLATING AND NONOSCILLATING SMOOTH CIRCULAR CYLINDERS IN CROSSFLOW

NAVAL SHIP RESEARCH AND DEVELOPMENT CENTER

Bethesda, Md. 20034

HYDRODYNAMIC FORCES ON OSCILLATING AND NONOSCILLATING SMOOTH CIRCULAR CYLINDERS IN CROSSFLOW

by

David W. Coder

SHIP PERFORMANCE DEPARTMENT
RESEARCH AND DEVELOPMENT REPORT

October 1972

Report 3639

The Naval Ship Research and Development Center is a U. S. Navy center for laboratory effort directed at achieving improved sea and air vehicles. It was formed in March 1967 by merging the David Taylor Model Basin at Carderock, Maryland with the Marine Engineering Laboratory at Annapolis, Maryland.

Naval Ship Research and Development Center
Bethesda, Md. 20034

MAJOR NSRDC ORGANIZATIONAL COMPONENTS

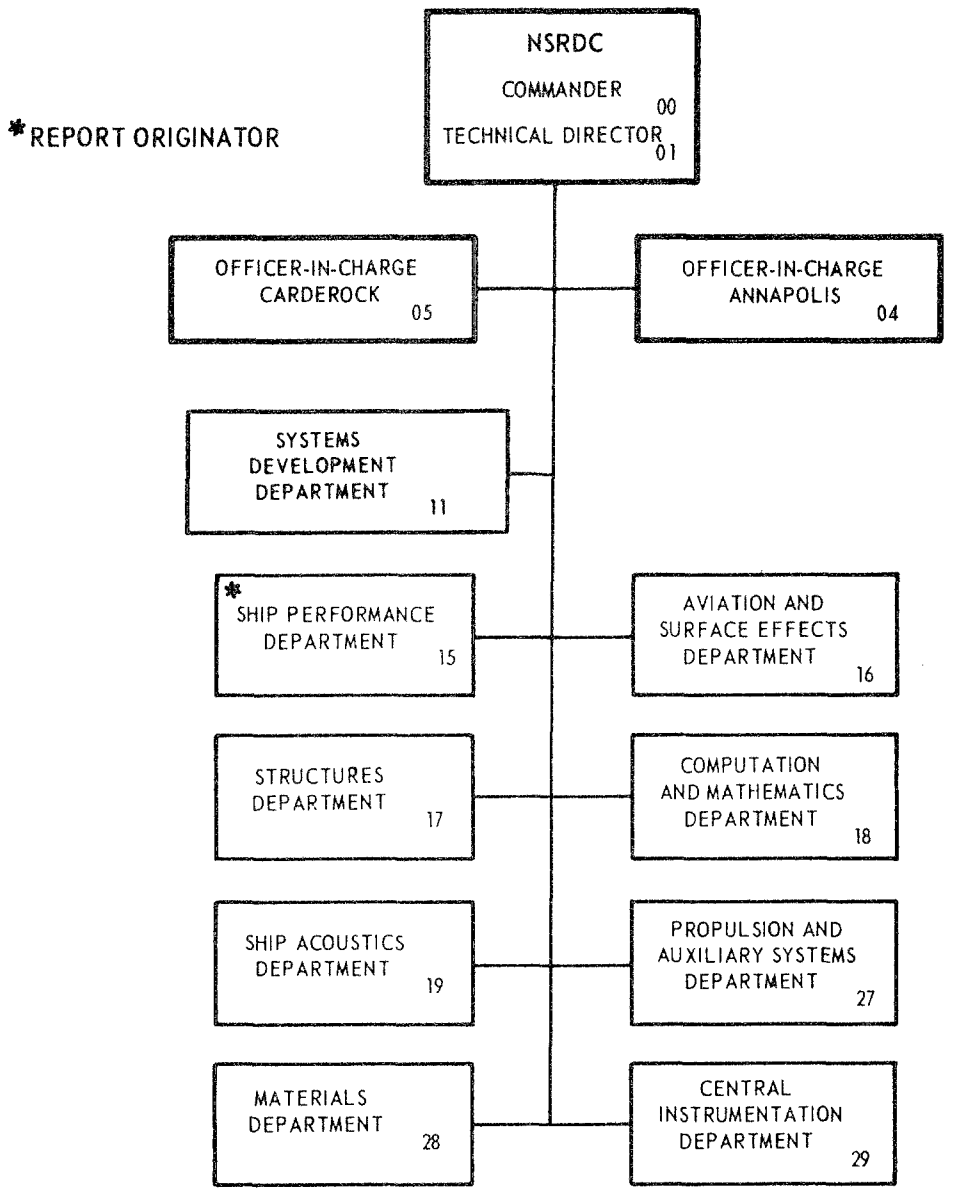

DEPARTMENT OF THE NAVY
NAVAL SHIP RESEARCH AND DEVELOPMENT CENTER
BETHESDA, MD. 20034

HYDRODYNAMIC FORCES ON OSCILLATING AND NONOSCILLATING SMOOTH CIRCULAR CYLINDERS IN CROSSFLOW

by

David W. Coder

October 1972

Report 3639

TABLE OF CONTENTS

LIST OF FIGURES

LIST OF TABLES

NOTATION

A	Frontal area of cylinder
a	Half amplitude of heave oscillation = 0.5 in.
a/d	Amplitude to diameter ratio = 0.0417
C	Generalized coefficient
CMAX	Maximum value obtained in the power spectra used to normalize the figures in Appendix A in engineering units
C_{ave}	Mean value of C during run determined from raw data on tapes
C_D	Drag coefficient = $D/(1/2\ \rho U^2 A)$
C_L	Lift coefficient = $L/(1/2\ \rho U^2 A)$
C_M	Moment coefficient = $M/(1/2\ \rho U^2 Ad)$
C_p	Pressure coefficient = $(p - p_\infty)/(1/2\ \rho U^2)$
C_{p-p}	Maximum possible peak-to-peak value of C determined from the power spectrum analysis = $2\sum_{i=1}^{N} C_i$
$C_{p-p/c}$	Maximum value minus minimum value of C during run determined from raw data on tapes
$C_{p-p/s}$	Repeatable maximum peak-to-consecutive-trough value of C during run from Sanborn oscillograph traces
C_{rms}	Root-mean-square value of C determined from the power spectrum analysis = $0.707\sum_{i=1}^{N} C_i^2$
$C_{rms/c}$	Root-mean-square value of C during run determined from raw data on tapes
C_W	Wave drag coefficient
D	Drag
D_i	i-th component of drag
d	Diameter of cylinder = 12 in.
F	Generalized force
F_n	Froude number = $U/\sqrt{gh}$
f	Frequency of forced oscillation
f_i	Frequency of i-th component

g	Gravitational constant
H	Water basin depth
h	Depth of cylinder
L	Lift
L_i	i-th component of lift
ℓ	Length of dynamometer section = 6 in.
M	Moment around axis of cylinder
M_i	i-th component of moment
p	Local pressure
p_∞	Static pressure
R_n	Reynolds number = Ud/ν
S_f	Strouhal number of forced oscillation
S_{f_i}	Strouhal number of i-th component = $f_i d/U$
T	Temperature of water
T_f	Period of forced oscillation
U	Free stream velocity
$U_{characteristic}$	Characteristic free stream velocity
$W_{( )}$	Maximum percent error in ( )
X_i	Independent variable
ε	Horizontal distance from axis of cylinder to pitching axis
ε/d	Nondimensional distance from axis of cylinder to pitching axis
Θ	Half amplitude of pitch = 1 deg
ν	Viscosity of water
ρ	Density of fluid
ϕ	Angle from leading edge of cylinder

ABSTRACT

A 12-in.-diameter, 6-ft-long cylinder was towed horizontally 4 ft beneath the water surface and perpendicular to the flow. The cylinder was towed at a constant velocity under the following conditions: nonoscillating, oscillating in heave, oscillating in pitch (around the axis of the cylinder), and simultaneously oscillating in pitch and heave. Experimental data on lift, drag, and moment were obtained for Reynolds numbers from about 10^5 to above 10^6. The results show that the oscillations can significantly influence the magnitude of the lift, drag, and moment.

ADMINISTRATIVE INFORMATION

The experimental work was sponsored by the Naval Ship Systems Command (NAVSHIPS) and funded under Subproject S4611 010, Task 11098. The preparation of this report was supported by the Naval Ship Research and Development Center (NSRDC) Training Program and NAVSHIPS Subproject S4627 007, Task 14822.

INTRODUCTION

A cylinder translating through a fluid is subject to a steady drag and unsteady lift and drag forces. These forces are usually converted to coefficient form, or nondimensionalized, by dividing them by the dynamic pressure times the frontal area of the cylinder. These coefficients are functions of Reynolds number (R_n) and have been investigated in many studies some of which are discussed in summary papers by Morkovin,[1] Marris,[2] and others. In the present study, the Reynolds number was varied from about 10^5 to above 10^6 and the pitching moment about the axis of the cylinder was also measured. As far as is known, this is the first time

---

[1]Morkovin, M.V., "Flow around Circular Cylinder--A Kaleidoscope of Challenging Fluid Phenomena," ASME Symposium on Fully Separated Flows (May 1964). A Complete list of references is given on page 77.

[2]Marris, A.W., "A Review on Vortex Streets, Periodic Wakes, and Induced Vibration Phenomena," ASME Paper 62-WA-106 (1962).

that such measurements have been made and reported. Lift, drag, and moment measurements were also made for the cylinder translating at a Reynolds number of 2×10^5, 5×10^5, and 1×10^6 and oscillating in heave (percendicular to the flow) at forced Strouhal numbers (S_f) up to 0.25. Lift and drag measurements were made for the cylinder oscillating in pitch (around the axis of the cylinder) for about the same ranges of Reynolds numbers and forced Strouhal numbers up to 0.40. At a Reynolds number of 1×10^6, data were obtained for simultaneous pitch and heave by pitching the cylinder around the axes d/4 forward and aft of the axis of the cylinder at forced Strouhal numbers up to 0.30. As far as the author knows, the pitching data and the data for simultaneous pitching and heaving are unique.

The data presented in the appendixes were obtained by analyzing the power spectra to obtain "Fourier type" coefficients for the power spectra peak frequencies. These data may be readily used by a designer or engineer to represent the lift, drag, or moment as a series, the major components of which are represented by these "Fourier" coefficients. For example, some of the nonoscillating cylinder data presented in this report have been used as the hydrodynamic input to a digital computer program known as "Structural Analysis by Digital Simulation of Analog Methods" (SAD SAM) to study periscope vibrations.

It is not the intent here to go into much discussion of the physical phenomena that are occurring, but rather to present data for the use of designers and engineers and for the scrutiny of other researchers in fluid mechanics.

DESIGN OF THE EXPERIMENT

EXPERIMENTAL EQUIPMENT

The NSRDC high-speed basin and Carriage 5 were used for the experiment. A pitch heave oscillator (PHO-2) was mounted on the carriage and the model was held horizontally with its axis 4 ft below the surface. The

operational limitations of the oscillator are shown in Figure 1.[3] The heave or pitch amplitude was monitored with a calibrated linear voltage differential transducer (LVDT) mounted in the PHO-2 mechanism.

The experimental cylinder shown attached to the pitch heave oscillator in Figure 2 was 1 ft in diameter and 6 ft long. Since cylinders with length-to-diameter ratios below 6 do not behave as infinite cylinders,[4] 1 ft was the largest diameter that could be used. For diameters much smaller than 1 ft, Reynolds numbers R_n above 10^6 would be difficult to obtain since the necessary velocities would be close to the wavemaking velocity of the high-speed basin and the cavitation inception velocity of the cylinder.

The lift, drag, and moment about the cylinder axis were measured on a short dynamometer section located at the center span of the cylinder. This section "floated" on a dynamometer with small gaps between the section and the rest of the cylinder.

It has been observed by Macovsky[5] that the flow over a cylinder is often three dimensional. Thus, in order to obtain true two-dimensional forces, it would be necessary to make the length of the dynamometer section as short as possible. The natural frequency of the section is inversely proportional to its length. The natural frequencies were kept above 200 Hz so that there would be little interference in the range of frequencies analyzed (0 to 50 Hz). However, from the viewpoint of the dynamometer, the longer section results in the larger forces; thus, more accurate force measurements can be made. It has been suggested by

---

[3]"Instruction Manual: Pitch-Heave Oscillator System," Prepared for Consolidated Systems Corporation, TM 3-3081, David Taylor Model Basin (15 Apr 1964).

[4]Keefe, R.T., "An Investigation of the Fluctuating Forces Acting on a Stationary Circular Cylinder in a Subsonic Stream and of the Associated Sound Field," University of Toronto Institute of Aero. Physics, UTIA Report 76 (Sep 1961).

[5]Macovsky, M.S., "Vortex-Induced Vibration Studies," David Taylor Model Basin Report 1190 (Jul 1958).

Sommerville and Kobett[6] that various size dynamometer sections be used in a series of tests to determine the three-dimensional effects of force cancelling due to phase shifts. True two-dimensional force coefficients may also be determined as a limit to a series. In this case the true two-dimensional lift coefficient could be defined as:

$$C_L = \lim_{\ell \to 0} \frac{1}{\ell} \frac{L}{(1/2)\rho U^2 d}$$

where ℓ is the length of the dynamometer section,

L is the lift,

ρ is the density of the fluid,

U is the free-stream velocity, and

d is the diameter of the cylinder.

It was not feasible to have many sections of different length for this particular experiment because of the cost involved and the difficult design of the dynamometer. Studies by Graham[7] indicate that the correlation length is on the order of 3 diameters in the subcritical regime and 1 diameter in the transition regime. On that basis, therefore, the dynamometer section should be less than 1 diameter in length to ensure a somewhat two-dimensional flow. An estimate of expected forces per unit length on the cylinder was made from existing data of Luistro[8] and Warren.[9]

---

[6]Sommerville, D.E. and D.R. Kobett, "Research and Development Services Covering Wind Induced Oscillations of Vertical Cylinders," Midwest Research Institute, Contract DA-23-072-ORD-1264, Phase Report 2, MRI Project 2190-P (Apr 1959).

[7]Graham, C., "A Survey of Correlation Length Measurements of the Vortex Shedding behind a Circular Cylinder," MIT Engineering Projects Lab Report 76028-1, Prepared under Contract Nonr. 3963(25) (Oct 1966).

[8]Luistro, J.A., "Lift and Drag Coefficients for a Smooth Circular Cylinder at High Reynolds Numbers," David Taylor Model Basin Report 1405 (Nov 1960).

[9]Warren, W.F., "An Experimental Investigation of Fluid Forces on an Oscillating Cylinder," Ph.D. Thesis, University of Maryland (1962).

An estimate of the moment on the cylinder was computed from the lift by finding the gross circulation needed to obtain that lift and then computing the shear force that this circulation would cause on the surface of the cylinder. This shear force would cause a moment about the axis of the cylinder. Given these forces and moments, it was determined that a dynamometer section length of less than 6 in. would cause large interactions in the dynamometer. Accordingly, a length of 6 in. was chosen for the dynamometer section.

One objective of this test was to study the three dimensionality of the flow on the cylinder. The three-dimensional flow for the experimental system would possibly arise from at least four sources: the wake of the cylinder support system (PHO-2 struts), the fact that the cylinder is finite with end plates, misalignment of the cylinder perpendicular to the flow, and inherent three-dimensional effects which would be present in an infinite circular exposed to uniform crossflow. The wake of the supporting PHO-2 struts was reduced by altering the existing rounded noses of the struts so that the insides of the struts were basically flat plates. All of the curvature of the nose section was made to the outside of the struts. It was hoped that this would result in uniform flow along the whole length of the model except for a small boundary layer on the inner side of the struts. The majority of the disturbance to the flow field would be to the outside of the strut. A cylinder length-to-diameter ratio of 6 was chosen in the expectation that this ratio would be large enough to preclude any great three-dimensional effects due to the end plates (PHO-2 struts). It was felt that a region of 4 ft in the middle span of the cylinder would experience incident uniform flow. The PHO-2 was aligned very carefully with a reference line on the carriage. The maximum alignment error of the cylinder normal to the towing direction was much less than 1 deg.

Various spanwise measurements of the flow were made in order to observe the three-dimensional effects. A ring of pressure gages was mounted on the dynamometer section of the cylinder and another ring of pressure gages was located 10 in. away. The correlation length for spanwise effects is on the order of 3 diameters for subcritical Reynolds numbers, from 1 to 6 diameters for transition Reynolds numbers, 1/2 diameter for transcritical

Reynolds numbers.[7] Hot film anemometers were placed spanwise over one-half of the cylinder in such a manner that at least two would lie within the correlation length for all three Reynolds number regimes. The correlation length for supercritical is the smallest, so this spacing had to be 0.5d/2 = 3 in. Several additional hot film anemometers were placed on the other side of the cylinder to check symmetry and for additional information. The location of gages is shown in Figure 3.

The hot film aneometers were all located at an angle of 78 deg; this allowed these transducers to be moved from 72 to 88 deg by rotation of the cylinder. According to Cahn,[10] the separation point on a circular cylinder for subcritical flow lies between these two values. Thus, it was felt that the use of these transducers would enable the separation point to be located in this flow regime.

The type of hot film aneometer used on the test was the end-mounted cylindrical type.* The gage consists basically of two wires set parallel along the axis of a glass cylinder with a thin platinum film mounted on the end of the cylinder across the ends of the two wires. This glass cylinder was then mounted in the end of a stainless steel tube 0.095 in. in diameter and 1 1/8 in. long. The gages were mounted in the test cylinder with the end of the gage flush with the surface of the cylinder. The gage subtended an angle of less than 1 deg of the test cylinder. The gage resistance was between 10 and 15 Ω. A resistor of about 85 to 90 Ω was connected in series with the gage to form the active arm of a 100 Ω bridge. The bridge was powered and balanced by an ENDEVCO constant-current signal-conditioning unit.

The gages operate on the principle of a change in resistance due to temperature change. The heat transfer of the I^2R heat generation in the gage is mostly transferred to the water. This heat transfer to the water

---

[10] Cahn, R.D., "The Nature of Flow Separation from a Circular Cylinder Near the Critical Reynolds Number," Masters Thesis, University of Maryland, Aeronautical Engineering Department (1963).

* Obtained from Lintronic Laboratory, Silver Spring, Maryland.

is greatly dependent on the flow properties. Thus, as the flow properties change, the heat transfer changes, changing the operating temperature of the gage. The changes in resistance due to the temperature change result in a resistance imbalance in the bridge which will then give rise to a voltage output.

A rough calibration of the hot film gages was done by inserting the gages into a pipe in which water was displaced by a piston. The results showed that some of the gages had as much as twice the sensitivity of others. However, this fact caused no difficulty since it had been planned to use these gages for qualitative data only.

Because of their cost, the number of these pressure gages was limited to about ten. Two rings of five each were placed at angles of 70, 85, 100, 115, and 130 deg from the leading edge. The gages were placed at these angles in order to have one gage before the separation point for subcritical Reynolds numbers (less than 75 deg according to Cahn[10]) and the rest in the wake. The wake area was of most interest since this is the region of vortex shedding and the pressure distribution in front of the separation region is very close to the potential flow distribution. The gages were placed 15 deg apart since the cylinder could be rotated 6 deg down and 10 deg up. This would allow pressures to be measured over the whole surface from 64 to 140 deg.

The pressure transducers used for the experiment were modified PT3 pressure gages designed and built by NSRDC. The gages are cylindrical in shape with a diameter of 1/4 in. and a length of about 1/4 in. The immediate pressure sensor is a thin metal diaphragm on the end of the cylinder which deflects slightly when exposed to pressure. A four-active-arm, strain-gage bridge made of 500-Ω semiconducting resistance strain gages is mounted on the diaphragm. The bridge was powered by a special low current (3 ma) power supply. The calibration of the gages was done by inserting them into an airtight system which was comprised of a pressure generator (bellows) and a parallel manometer to read the pressure in the system. The gages were mounted in the model such that the diaphragm was exposed to the flow and flush with the surface of the cylinder. The 1/4-in. flat diaphragm on the 1-ft-diameter cylinder subtended an angle of slightly more than 2 deg.

The carriage velocity was determined from a calibrated rotopulser on the wheel of the carriage. An accelerometer was mounted in the test section to monitor possible vibration and to serve as a backup for the LVDT whenever the cylinder was oscillated.

A block diagram of the electronic instrumentation used to condition and record the transducer outputs is shown in Figure 4.

SUMMARY OF EXPERIMENTAL PROGRAM

The primary independent variables for the experiment were carriage velocity and frequency of oscillation. These two parameters were varied during testing to obtain data for Reynolds numbers from 10^4 to above 10^6 and oscillating Strouhal numbers from 0 to 2. Heave runs were made at Reynolds numbers of 0, 10^5, 2×10^5, 5×10^5 and 1×10^6 with an amplitude-to-diameter ratio of 0.0417. Pitch runs were made at Reynolds numbers of 0, 10^5, 2×10^5, 5×10^5, and 1×10^6 with an amplitude of 1 deg with pitching axis coinciding with the axis of the cylinder. At a Reynolds number of 1×10^6, simultaneous pitch and heave runs were made by positioning the pitching axis at a horizontal distance of ±0.25 diameters from the axis of the cylinder and pitching with an amplitude of 1 deg.

ERROR ANALYSIS

The estimated maximum percent errors in the measurement of the constants and variables in the experiment are listed in Table 1. These maximum percent errors in the nondimensional numbers and coefficients were calculated from the equation[11]

$$W_c^2 = \left(\frac{\partial C}{\partial x_1}\right)^2 W_{x_1}^2 + \left(\frac{\partial C}{\partial x_2}\right)^2 W_{x_2}^2 + \ldots$$

[11] Schenck, H., "Theories of Engineering Experimentation," McGraw-Hill Book Company, Inc., New York (1961).

TABLE 1 - EXPERIMENTAL ERROR

X_i					W_{X_i}/X_i
Variable	Symbol	Values	Measurement Technique	Estimated Max. Error or Deviation from Value	Max. Percent Error
Frontal Area of Test Section	A	0.5 ft^2	A = d x ℓ	---	0.053
Heave Half Amplitude	a	0.5 in.	Oscilloscope	0.010 in.	2.0
Drag on Test Section	D	-0.0334 v/lb at x 1k -0.0167 v/lb at x 500 -0.00663 v/lb at x 200	Pre- and Post-Calibration of Dynamometer with Static Weights	0.0018 v/lb at x 1k 0.0011 v/lb at x 500 0.00033 v/lb at x 200	6.59
Diameter of Cylinder	d	12 in.	Micrometer	0.005 in.	0.042
Frequency of Oscillation	f	0.02 to 4 Hz	$f = 1/T_f$	---	0.5f (hz)
Frequency of i-th component	f_i	0 to 50 Hz	Half-Interval Size for Power Spectrum	0.0244 hz	$2.44/f_i$ (hz)
Depth to Axis of Cylinder	h	4 ft	Scale	0.125 in.	0.261
Lift on Test Section	L	0.0625 v/lb at x 1k 0.0312 v/lb at x 500 0.0124 v/lb at x 200	Pre- and Post-Calibration of Dynamometer with Static Weights	0.0016 v/lb at x 1k 0.0009 v/lb at x 500 0.0002 v/lb at x 200	2.88
Length of Test Section	ℓ	6 in.	Micrometer	0.002 in.	0.033
Moment on Test Section	M	0.1419 v/in-lb at x 1k 0.0728 v/in-lb at x500 0.0281 v/in-lb at x200	Pre- and Post-Calibration of Dynamometer with Static Weights	0.0011 v/in-lb at x 1k 0.0027 v/in-lb at x500 0.0001 v/in-lb at x200	3.71
Pressure	p	0 to 5 psi	Pressure Gage (pre- and post-cal)	0.01 psi	1/p (psi)
Temperature of Water	T	71 to 74 F	Thermometer	0.5 F	0.70
Period of Oscillation	T_f	0.25 to 50 sec	Counter	0.005 sec	$0.5/T_f$ (sec)
Carriage Velocity	U	0 to 15 fps	Wheel & Magnetic Pickup	0.017 fps	1.7/U (fps)
Eccentricity to Pitching Axis	ε	3 in.	Micrometer	0.005 in.	0.167
Pitch Half Amplitude	θ_o	1 deg	Oscilloscope	0.02 deg	2.0
Viscosity of Water	ν	1.002 to 1.041 x 10^5 ft^2-sec	From Temp. Measurement	0.006 to 0.007 x 10^5 ft^2 sec	0.7
Density of Water	ρ	1.935 $\frac{lb\text{-}sec^2}{ft^4}$	Assumed Constant Oven Temp. Range	0.001 $\frac{lb\text{-}sec^2}{ft^4}$	0.05

where W_C is the maximum percent error in C,

W_{x_i} is the maximum percent error in x_i,

C is the coefficient or nondimensional number, and

$x_1, x_2, \cdots$ are independent variables.

The coefficients and nondimensional numbers used to analyze the data are defined as

a/d Half amplitude to diameter ratio,

C_D Drag coefficient = $D/(1/2\ \rho U^2 A)$,

C_L Lift coefficient = $L/(1/2\ \rho U^2 A)$,

C_M Moment coefficient = $M/(1/2\ \rho U^2 Ad)$,

C_p Pressure coefficient = $(p - p_\infty)/(1/2\ \rho U^2)$

F_n Froude number = $U/\sqrt{gh}$,

R_n Reynolds number = $\frac{Ud}{\nu}$

S_f Strouhal number of forced oscillation = $\frac{fd}{U}$, and

S_{f_i} Strouhal number of i-th component = $\frac{f_i d}{U}$

Therefore,

$$\frac{W_{a/d}}{a/d} = \left[\left(\frac{W_a}{a}\right)^2 + \left(\frac{W_d}{d}\right)^2\right]^{1/2} = \left[(2.0)^2 + (0.042)^2\right]^{1/2} \approx 2.0$$

$$\frac{W_{C_D}}{C_D} = \left[\left(\frac{W_D}{D}\right)^2 + \left(\frac{W_\rho}{\rho}\right)^2 + 4\left(\frac{W_U}{U}\right)^2 + \left(\frac{W_A}{A}\right)^2\right]^{1/2}$$

$$= \left[(6.59)^2 + (0.05)^2 + 4\left(\frac{1.7}{U}\right)^2 + (0.053)^2\right]^{1/2}$$

$$\approx \left[(6.59)^2 + 4\left(\frac{1.7}{U}\right)^2\right]^{1/2}$$

$$\frac{W_{C_L}}{C_L} = \left[\left(\frac{W_L}{L}\right)^2 + \left(\frac{W_\rho}{\rho}\right)^2 + 4\left(\frac{W_U}{U}\right)^2 + \left(\frac{W_A}{A}\right)^2\right]^{1/2}$$

$$= \left[(2.88)^2 + (0.05)^2 + 4\left(\frac{1.7}{U}\right)^2 + (0.053)^2\right]^{1/2}$$

$$\approx \left[(2.88)^2 + 4\left(\frac{1.7}{U}\right)^2\right]^{1/2}$$

$$\frac{W_{C_M}}{M} = \left[\left(\frac{W_M}{M}\right)^2 + \left(\frac{W_\rho}{\rho}\right)^2 + 4\left(\frac{W_U}{U}\right)^2 + \left(\frac{W_A}{A}\right)^2 + \left(\frac{W_d}{d}\right)^2\right]^{1/2}$$

$$= \left[(3.71)^2 + (0.05)^2 + 4\left(\frac{1.7}{U}\right)^2 + (0.053)^2 + (0.042)^2\right]^{1/2}$$

$$\approx \left[(3.71)^2 + 4\left(\frac{1.7}{U}\right)^2\right]^{1/2}$$

$$\frac{W_{C_p}}{C_p} = \left[\left(\frac{W_p}{p}\right)^2 + \left(\frac{W_\rho}{\rho}\right)^2 + 4\left(\frac{W_U}{U}\right)^2\right]^{1/2}$$

$$= \left[\left(\frac{1}{p}\right)^2 + (0.05)^2 + 4\left(\frac{1.7}{U}\right)^2\right]^{1/2}$$

$$\approx \left[\left(\frac{1}{p}\right)^2 + 4\left(\frac{1.7}{U}\right)^2\right]^{1/2}$$

$$\frac{W_{F_n}}{F_n} = \left[\left(\frac{W_U}{U}\right)^2 + \frac{1}{4}\left(\frac{W_h}{h}\right)^2\right]^{1/2}$$

$$= \left[\left(\frac{1.7}{U}\right)^2 + \frac{1}{4}(0.261)^2\right]^{1/2}$$

$$\frac{W_{R_n}}{R_n} = \left[\left(\frac{W_U}{U}\right)^2 + \left(\frac{W_d}{d}\right)^2 + \left(\frac{W_\nu}{\nu}\right)^2\right]^{1/2}$$

$$= \left[\left(\frac{1.7}{U}\right)^2 + (0.042)^2 + (0.7)^2\right]^{1/2}$$

$$\approx \left[\left(\frac{1.7}{U}\right)^2 + (0.7)^2\right]^{1/2}$$

$$\frac{W_{S_f}}{S_f} = \left[\left(\frac{W_f}{f}\right)^2 + \left(\frac{W_d}{d}\right)^2 + \left(\frac{W_U}{U}\right)^2\right]^{1/2}$$

$$= \left[(0.5f)^2 + (0.042)^2 + \left(\frac{1.7}{U}\right)^2\right]^{1/2}$$

$$\approx \left[(0.5f)^2 + \left(\frac{1.7}{U}\right)^2\right]^{1/2}$$

$$W_{S_{f_i}} = \left[\left(\frac{W_{f_i}}{f_i}\right)^2 + \left(\frac{W_d}{d}\right)^2 + \left(\frac{W_U}{U}\right)^2\right]^{1/2}$$

$$= \left[\left(\frac{2.44}{f_i}\right)^2 + (0.042)^2 + \left(\frac{1.7}{U}\right)^2\right]^{1/2}$$

$$\approx \left[\left(\frac{2.44}{f_i}\right)^2 + \left(\frac{1.7}{U}\right)^2\right]^{1/2}$$

The estimated maximum experimental errors in the coefficients and nondimensional numbers were calculated from the above equations and are shown as a function of Reynolds number and frequency in Figure 5.

WAVE DRAG CALCULATION

The wave drag of the cylinder was calculated from the following equations:[12]

$$C_W = \frac{\pi^2 d^3}{H^3}\left[\frac{\xi^3 \cosh^2 (1 - h/H)\xi}{\sinh 2\xi - \xi}\right]$$

$$F_n^2 \xi = \tanh \xi$$

where C_W is the wave drag coefficient,

d is the cylinder diameter = 1 ft,

h is the cylinder depth = 4 ft,

H is the water basin depth = 16 ft,

F_n is the Froude number based on basin depth = $U/(gH)^{1/2}$, and

g is the gravitational constant.

---

[12]Sretensky, L.N., "Motion of a Cylinder under the Surface of a Heavy Fluid," NACA TM 1335 (Aug 1953).

The wave drag coefficient is shown as a function of Froude number in Figure 6.

BLOCKAGE CALCULATION

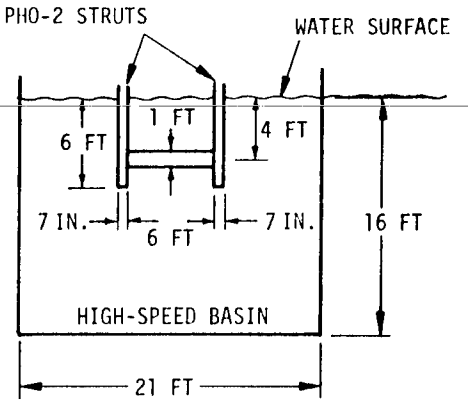

Frontal area of PHO-2 struts = 2 x 6 ft x 7/12 ft = 7 ft^2

Frontal area of cylinder = 1 ft x 6 ft = 6 ft^2

Total blockage area = 13 ft^2

Frontal area of high speed basin = 21 ft x 16 ft = 336 ft^2

Blockage area ratio = 13/336 = 0.0387

The blockage is 3.87 percent. This means that the characteristic flow velocity will be slightly higher than the carriage velocity, or

$$U_{characteristic} \approx 1.04\ U$$

DATA ANALYSIS

DATA REDUCTION

The data recorded on analog tape during the experiment were digitized by using the SDS 910 computer of the Computation Mathematics Department (CMD) at NSRDC. The effective scan rate per channel of 400 points per second allowed analysis of the data up to 100 Hz. The digital data for the lift, drag, moment, and pressures were analyzed by using the IBM 7090 digital computer of the CMD. The computer analysis program was based on an existing CMD program which uses the Fast Fourier Transform (FFT) technique

to calculate the power spectrum. (The program has recently been converted for use with the CDC 6700 digital computer at NSRDC.) The mean value, maximum value, minimum value, mean square value, root mean-square value, and power spectrum data were calculated for a sampling of (2^{13}) points, corresponding to 20.48 sec in the center of each set of data.

Coefficients were then defined as

C_{ave} = mean value during run

$C_{p\text{-}p/c}$ = maximum value - minimum value

$C_{rms/c}$ = root-mean-square value

The computer program was modified to further analyze the power spectrum. The 20 largest power spectrum peaks not more than 20 dB below the largest peak in the range between 0 and 50 Hz were determined. The power near each of the peaks was determined by integration. The limits of integration were (1) either the points at which the power spectrum failed to decrease monotonically giving away from the peak, or (2) the points at which the power spectrum value dropped to 20 dB below the peak value (1 percent of peak value), whichever came first. The square root of the powers determined in this manner represents force or moment coefficients associated with the peak frequencies. The peak frequency and associated coefficient were calculated and printed out as well as the left end, right end, bandwidth of integration, and the Strouhal number of the peak frequency. From these coefficients, the known electronic noise at predetermined frequencies as determined from a zero velocity and frequency run was subtracted out, and the maximum possible value ($C_{p\text{-}p}$) and the root-mean-square value (C_{rms}) were obtained from

$$C_{p\text{-}p} = 2\sum_{i=1}^{N} C_i$$

$$C_{rms} = 0.707\left[\sum_{i=1}^{N} C_i^{\,2}\right]^{1/2}$$

where N is generally 20 less the number of power spectrum peaks due to noise.

The data analysis described above was augmented in the case of the lift on the nonoscillating cylinder by data obtained from the Sanborn oscillograph strip charts. These data supply additional information on the character of the lift and allow the data in this report to be compared with those of other studies (this has been done by Wang[13]). The Sanborn data were examined to obtain peak-to-consecutive-trough values. The maximum values that were repeated several times during the run are reported and labeled "$C_{p\text{-}p/s}$." A schematic is given to help clarify the data analysis techniques used; see Figure 7.

DYNAMOMETER CORRECTIONS FOR OSCILLATING CONDITIONS

A series of oscillation experiments was performed at zero velocity in order to determine the inertial terms which would later be subtracted from the data. Inertial loading of the moment gage during pitching, lift gage during heaving, and moment and lift gages during pitching and heaving were determined. The dynamometer was balanced before the experiment to eliminate the load on the lift gage during pitching. However, the dynamometer could not be simultaneously balanced to eliminate the rest of the dynamometer interactions. All of these interaction forces and moments except the interaction moment during heaving showed a simple dependence on the square of the forcing frequency. Thus

$$F \propto f^2 = \left(\frac{S_f U}{d}\right)^2 \propto S_f^{\,2}\, U^2$$

---

[13]Wang, H.T., "Survey of the Magnitude and Correlation of the Lift Force Acting on a Nonoscillating Circular Cylinder," NSRDC Report 3335 (in review).

where F represents any interaction force or moment,

f is the frequency,

S_f is the Strouhal number of forced oscillation,

U is the free-stream velocity, and

d is the diameter of the cylinder.

If the force or moment is nondimensionalized by its appropriate term, then

$$C \propto \frac{F}{U^2} \propto \frac{S_f{}^2 U^2}{U^2} \propto S_f{}^2$$

The resulting interaction force or moment coefficients (C) are seen to have a simple dependence on the square of the forced Strouhal number. This is shown in Figures 8, 9, and 10a. The interaction moment due to heaving is not a simple function of frequency and so the above simplification cannot be made. The interaction moment due to heaving is shown versus forced frequency in Figure 10b. From the data in Figure 10b, the interaction moment coefficients due to heaving were determined as a function of forced Strouhal numbers for the various Reynolds numbers tested and are presented in Table 2.

EXPERIMENTAL RESULTS AND DISCUSSION

GENERAL REMARKS

The dynamometer data are considered the most interesting of the data collected. These data were reduced first; the coefficients reported in this section have not been corrected for wave drag or blockage effect. One plot is presented of the pressure data obtained on the dynamometer section for the nonoscillating cylinder at various Reynolds numbers. Some of the hot film data were useful in determining the flow separation angle on the

TABLE 2 - HEAVE EFFECT ON MOMENT GAGE

	← $R_n = 10^6$ →		← 5×10^5 →		← 2×10^5 →		← $R_n = 10^5$ →	
f (Hz)	S_f	$C_M \times 10^3$	S_f	$C_M \times 10^3$	S_f	$C_M \times 10^3$	S_f	$C_M \times 10^3$
0.44	0.044	0.0167	0.088	0.0668	0.220	0.4175	0.400	1.67
0.50	0.050	0.0168	0.100	0.0672	0.250	0.4200		
0.60	0.060	0.0195	0.120	0.0780	0.300	0.4875		
0.75	0.075	0.0273	0.150	0.1092	0.375	0.6825		
0.80	0.080	0.0358	0.160	0.1432	0.400	0.8950		
0.90	0.090	0.0417	0.180	0.1668				
1.00	0.100	0.0649	0.200	0.2596				
1.10	0.110	0.0714	0.220	0.2856				
1.25	0.125	0.0797	0.250	0.3188				
1.50	0.150	0.0931	0.300	0.3724				
1.80	0.180	0.1013	0.320	0.4052				
2.00	0.200	0.1126	0.400	0.4504				
2.20	0.220	0.1236						
2.50	0.250	0.1436						
3.00	0.300	0.1880						
4.00	0.400	0.3443						

cylinder. These hot films and the critical Reynolds number data have been compared with other experimental and theoretical work and are presented separately.[14]

NONOSCILLATING CYLINDER

The results of the nonoscillating cylinder experiment are given in Appendixes A and B and Figures 11-15. The power spectra of the lift given in Appendix A for various Reynolds numbers showed single peaks for Reynolds numbers below 2.5×10^5. Above this Reynolds number, multiple peaks for the lift were found. The power spectra for the drag and moment indicated multiple peaks for the range of Reynolds numbers from 2.5×10^5 to 1.5×10^6.

Although the power spectra plots given in Appendix A show the character of the lift, drag, and moment, the quantitization of the power spectrum data as described in the section on data analysis makes these data more usable and reveals added information on the character of the data signals. For example, the power spectrum of the lift for Run 13 showed the largest peak at 0.29 Hz and the second largest peak at 0.78 Hz. The peak value at 0.78 Hz was less than 80 percent of the peak value at 0.29 Hz. However a comparison of the power around the two peaks indicates that the power around 0.78 Hz was slightly greater than that around 0.29 Hz. Thus, the maximum peak was considered to be at 0.78 Hz.

The data obtained from further analysis of the power spectra are tabulated in Appendix B. Some of the smaller peaks visible on the power spectra plots are occasionally not represented in the tabulated data. These peaks were either not one of the maximum 20 peaks in the range of frequencies from 0 to 50 Hz or were more than 20 dB below the maximum peak in that range. The maximum possible values (C_{p-p}) and the root-mean-square values (C_{rms}) calculated from the power spectrum data and tabulated in Appendix B are presented in Figures 11-14.

---

[14]Coder, D.W., "Location of Separation on a Circular Cylinder in Cross-flow as a Function of Reynolds Number," NSRDC Report 3647 (Nov 1971).

The lift coefficients $(C_L)_{p-p}$ and $(C_L)_{rms}$ are shown in Figure 11a. The solid lines are hand-faired curves drawn through the data points. The dotted lines are from "supercritical" data obtained in a wind-tunnel by Fung.[15] The data of this report are in agreement with the Fung peak values, but somewhat smaller than the Fung root-mean-square values. The lift data of this report were compared with data from many other studies cited by Wang.[13] The lift curves exhibited large dips for Reynolds numbers from about 1.5 to 5.0 x 10^5. This is the so-called "transition regime" that begins at the critical Reynolds number and ends at the beginning of the "transcritical regime" where the flow becomes somewhat independent of Reynolds number. From the lift data it appears that the critical Reynolds number is about 1.5 x 10^5 and the transcritical regime starts at 5.0 x 10^5. The hot film data[14] indicated a critical Reynolds number of about 2.5 x 10^5 on the cylinder away from the dynamometer section. There is evidence that the critical Reynolds number on the dynamometer section was somewhat smaller due to the rougher aluminum surface.

The character of the lift in the subcritical regime (below the critical Reynolds number) is that it is composed of one component whose Strouhal number is about 0.2. The magnitude of the lift decreases in the transition regime and the number of components increases as the transcritical regime is approached. Thus, in the subcritical and the beginning of the transition regime where the lift has only one component, the repeatable peak-to-peak values of the lift coefficient as determined from the Sanborn oscillograph traces $(C_L)_{p-p/s}$ should agree well with $(C_L)_{p-p}$ determined from the power spectrum. This was the case for Reynolds numbers up to about 2.5 x 10^5 as shown in Figure 11b. For Reynolds numbers of 4.0 x 10^5 and larger, $(C_L)_{p-p/s}$ was much lower than $(C_L)_{p-p}$, which is to be expected whenever the number of lift components increase.

The premise used to compute C_{p-p} from the power spectrum by simply adding the magnitudes of the components is that if the components were

---

[15] Fung, Y.C., "Fluctuating Lift and Drag Acting on a Cylinder in a Flow at Supercritical Reynolds Numbers," IAS Paper 60-6 (Jan 1960).

completely independent of each other (i.e., have no consistent phase angle relationship with each other), the components would add up to this maximum value at some time. If there happens to be some phase relationship between some of the components, they can only add up to some value smaller than this. Therefore, this value may be regarded as the maximum possible value. The root-mean-square values calculated from the power spectrum should be very accurate since phase differences are not a factor in determining rms values. The maximum peak-to-peak values $(C_L)_{p-p/c}$ and root-mean-square values $(C_L)_{rms/c}$ obtained directly from the raw data were in good agreement with $(C_L)_{p-p}$ and $(C_L)_{rms}$, respectively, for Reynolds numbers of 5.0×10^5 and above as shown in Figure 11b. The noise in the data made the values of $(C_L)_{p-p/c}$ and $(C_L)_{rms/c}$ worthless for smaller Reynolds numbers. The noise overode the data signal and showed up on a log-log plot of coefficient versus Reynolds number as a straight line of slope -2. The data distorted by noise are connected with dotted straight lines of slope -2 to show this effect; see Figure 11b.

The Strouhal number of the largest component of the lift is plotted versus Reynolds number in Figure 12. In the subcritical and transition regimes, the Strouhal number was about 0.2 up to $R_n = 2.0 \times 10^5$. For $R_n = 4.0 \times 10^5$ and larger, the Strouhal number dropped below 0.2 to a rough average value of 0.12. The Strouhal numbers corresponding to the Fung power spectra peaks are included in Figure 12 and confirm this decrease in Strouhal number.

The average, the peak-to-peak, and the root-mean-square drag coefficients $(C_D)_{ave}$, $(C_D)_{p-p}$, and $(C_D)_{rms}$, respectively, are shown in Figure 13 for Reynolds numbers from 4×10^5 to 1.5×10^6. The root-mean-square values remained about constant in this regime, but the peak-to-peak and average values showed a slight drop for Reynolds number below 5×10^5. The root-mean-square values compared favorably with the Fung values, but the Fung mean values which should correspond to $(C_D)_{ave}$ were only one-half as large. However, the data agreed well with average values reported by Luistro.[8] Unfortunately, Fung does not report peak-to-peak values of the drag to compare with $(C_D)_{p-p}$.

The moment coefficient data given in Figure 14 are unique as far as this author knows. The data show that the root-mean-square value of moment coefficient remained constant for Reynolds numbers from 4×10^5 to 1.5×10^6, whereas the peak-to-peak values showed a slight continual increase over this range.

The pressure on the dynamometer section is given for various Reynolds numbers in Figure 15.

CYLINDER OSCILLATING IN HEAVE

As shown in Figures 16-23, the lift, drag, and moment were influenced by oscillation of the cylinder in heave. The peak-to-peak and root-mean-square lift coefficients for Reynolds numbers of 2×10^5, 5×10^5, and 1×10^6 first reduced to a minimum as the Strouhal number of heave oscillation was increased to about 0.15. The lift then increased to its maximum value at a Strouhal number of about 0.2. This characteristic of the lift has been observed for lower Reynolds numbers by Warren[9] and Bishop and Hassan.[16] In the supercritical regime, Fung[15] oscillated his cylinder at amplitude-to-diameter ratios up to 0.0395 but the Strouhal numbers of heave oscillation were less than 0.09, well below the range of the present study.

For a Reynolds number of 2×10^5, the average drag increased about 30 percent whenever the cylinder was oscillated. However, at the higher Reynolds numbers of 5×10^5 and 1×10^6, the average drag decreased with oscillation. The peak-to-peak and root-mean-square values appeared to decrease for Strouhal numbers of heave up to about 0.15. For $R_n = 5 \times 10^5$ they increased again up to $S_f = 0.18$ and decreased for higher S_f. The same was true for $R_n = 10^6$ except that there was an extra dip at $S_f = 0.20$.

The moment coefficients for $R_n = 5 \times 10^5$ and 1×10^6 showed a significant dip at $S_f = 0.20$.

---

[16] Bishop, R.E.D. and A.Y. Hassan, "The Lift and Drag Forces on a Circular Cylinder Oscillating in a Flowing Fluid," Proc. of the Royal Society, A, Vol. 277, pp. 51-75 (1963).

CYLINDER OSCILLATING IN PITCH

Oscillating the cylinder in pitch also affects the lift and drag coefficients as shown in Figures 24-29. As far as this author knows, these data are unique. For a Reynolds number of 2×10^5, the effect due to oscillation in pitch appears similar to that of heave (dotted line on Figure 24) but not as drastic. The troughs and peaks located at Strouhal numbers of about 0.15 and 0.20, respectively, were the same as for heave. For a Reynolds number of 5×10^5, the troughs and peaks were more to the left of those for heave and occurred at about 0.1 and 0.15, respectively, as shown in Figure 25. The shape of the curves for pitch in Figure 26 for $R_n = 1 \times 10^6$ was completely different from those for heave. The dramatic changes in the pitch curves occurred for Strouhal numbers of pitch less than 0.15, where few data points were taken. It would be well to repeat this experiment to obtain more measurements in this low Strouhal number range.

For a Reynolds number of 2×10^5, the average drag shown in Figure 27 was increased due to oscillation in pitch, just as was the case for heave. However, unlike heave, the effect of pitch oscillation on the average drag was negligible for the larger Reynolds numbers of 5×10^5 and 1×10^6 as shown in Figures 28 and 29. The unsteady drag for pitching appeared to be very similar to that for heave for $R_n = 5 \times 10^5$, but somewhat different for $R_n = 1 \times 10^6$.

CYLINDER OSCILLATING IN PITCH AND HEAVE

Oscillating the cylinder at a half amplitude of 1 deg around axes ±0.25 diameter from its axis resulted in simultaneous pitching and heaving. The two motions were pitching at a half amplitude of 1 deg and heaving at an amplitude-to-diameter ratio of 0.00437. The difference in motion between locating the pitching axis forward (+) or aft (-) of the cylinder axis may be stated in terms of motion of the most forward point of the cylinder relative to its most aft point. For $\varepsilon/d = +0.25$, the most aft point moved a distance three times as far as the most forward point. For $\varepsilon/D = -0.25$, the most forward point moved three times as far as the most aft point.

The data for the lift during simultaneous pitching and heaving (Figures 30 and 31) showed no easily identifiable trends, not behaving like either the pitching results or the heaving results. However, the drag data in Figures 32 and 33 showed a definite correlation with the heave data.

SUMMARY AND CONCLUSION

The lift, drag, and moment were measured on nonoscillating and oscillating cylinders for Reynolds numbers from 10^5 to 10^6. Because of the sensitivity of the dynamometer, data at some of the lower Reynolds numbers were not obtainable. These data could be obtained by making the dynamometer more sensitive and repeating the appropriate parts of the experiment. Some data, however, were obtained for each of the subcritical, transitional, and transcritical regimes of fluid flow. The data are presented in the appendixes as mean values, peak-to-peak values, root-mean-square values, and unsteady components at discrete frequencies. This allows the data to be used easily by the designer. It is unfortunate that previous investigators did not present their unsteady data in a similar manner so that further comparisons with the data in this report could be made. Where comparisons were possible, the mean values, peak-to-peak values, and root-mean-square values reported herein were in general agreement with selected data existing in the literature.

The mean drag and peak-to-peak and root-mean-square lift and drag for the nonoscillating cylinder exhibited the general trends observed by other investigators (i.e., the drop and subsequent rise to a lower level of the coefficients in the transition regime). The peak-to-peak and root-mean-square moment coefficients, which have not been measured previously, behaved similar to the lift and drag where meaningful measurements were made in the transition and transcritical regimes. The coefficients increased significantly for Reynolds numbers from 4×10^5 to about 6×10^5 and then tended to flatten out at higher Reynolds numbers.

Taken collectively, the data for the oscillating cylinder show that the forces and moments may be significantly affected by oscillation depending on the oscillation frequency. The most significant effects were seen near a forced Strouhal number of 0.2, the Strouhal number of vortex

shedding for the subcritical regime! Whether it was a peak or a trough at this Strouhal number, the effect was generally more pronounced the lower the Reynolds number (i.e., of the three Reynolds numbers 2×10^5, 5×10^5, and 1×10^6). The phenomenon of pronounced influence near this Strouhal number has been observed and reported in the literature for lift and drag for heaving in the subcritical regime. It appears that this effect also occurs above the critical Reynolds number, but to a lesser extent with increasing Reynolds number. It has been shown here that this effect is seen in the moment also.

In contrast to heaving motion, pitching motion resulted in smaller deviations (peaks and troughs) in the peak-to-peak and root-mean-square values of the lift and drag for the lowest Reynolds number of 2×10^5. The oscillating Strouhal number for significant deviations during pitching decreased from 0.2 for $R_n = 2 \times 10^5$ to near 0.15 for $R_n = 5 \times 10^5$ to near 0.1 or below for $R_n = 1 \times 10^6$, whereas the significant oscillating Strouhal number for heaving remained about 0.2 for all three Reynolds numbers.

The average drag coefficient at $R_n = 2 \times 10^5$ was increased somewhat for oscillation in either pitch or heave. For $R_n = 5 \times 10^5$ and 1×10^6, the mean drag was reduced by heaving, whereas pitching motion appeared to have little, if any, effect.

For oscillation in pitch and heave simultaneously at $R_n = 1 \times 10^6$, the unsteady lift was quite different depending on whether the axis of rotation was forward or aft of the axis of the cylinder. The peak-to-peak and root-mean-square values were higher when the axis of rotation was forward. Although the lift values for combined motion were not similar to either pitch or heave (except possibly the root-mean-square values for aft oscillation), the mean, peak-to-peak, and root-mean-square values for drag at $R_n = 1 \times 10^6$ were very similar to the values for heaving alone.

ACKNOWLEDGMENTS

The author gratefully acknowledges the assistance of Mr. W.G. Souders and Mr. H.D. Harper in conducting the experiments and that of Miss L. Dutcher in writing the data reduction computer programs. The author also wishes to thank Dr. A. Borden, formerly of NSRDC, and Dr. C.L. Sayre, of the University of Maryland, who gave guidance during the study.

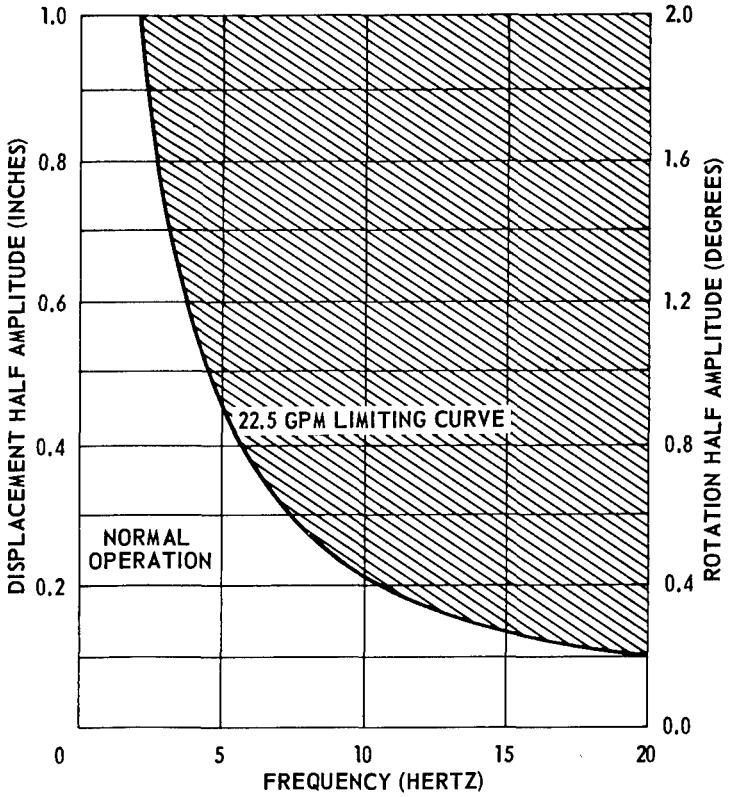

Figure 1 - Operational Limitations of Pitch Heave Oscillator PHO-2

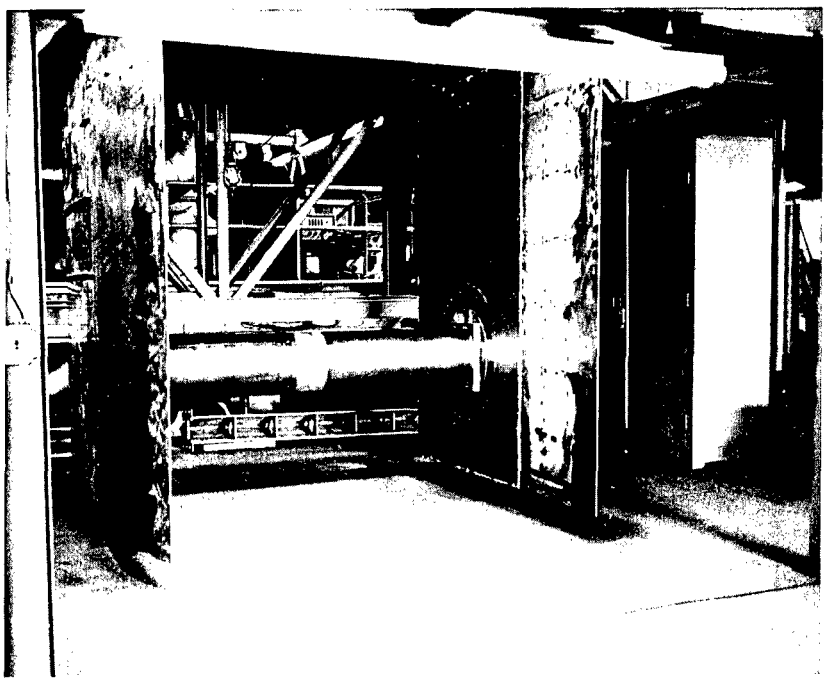

Figure 2 - 12-Inch-Diameter Cylinder Mounted on PHO-2 Struts

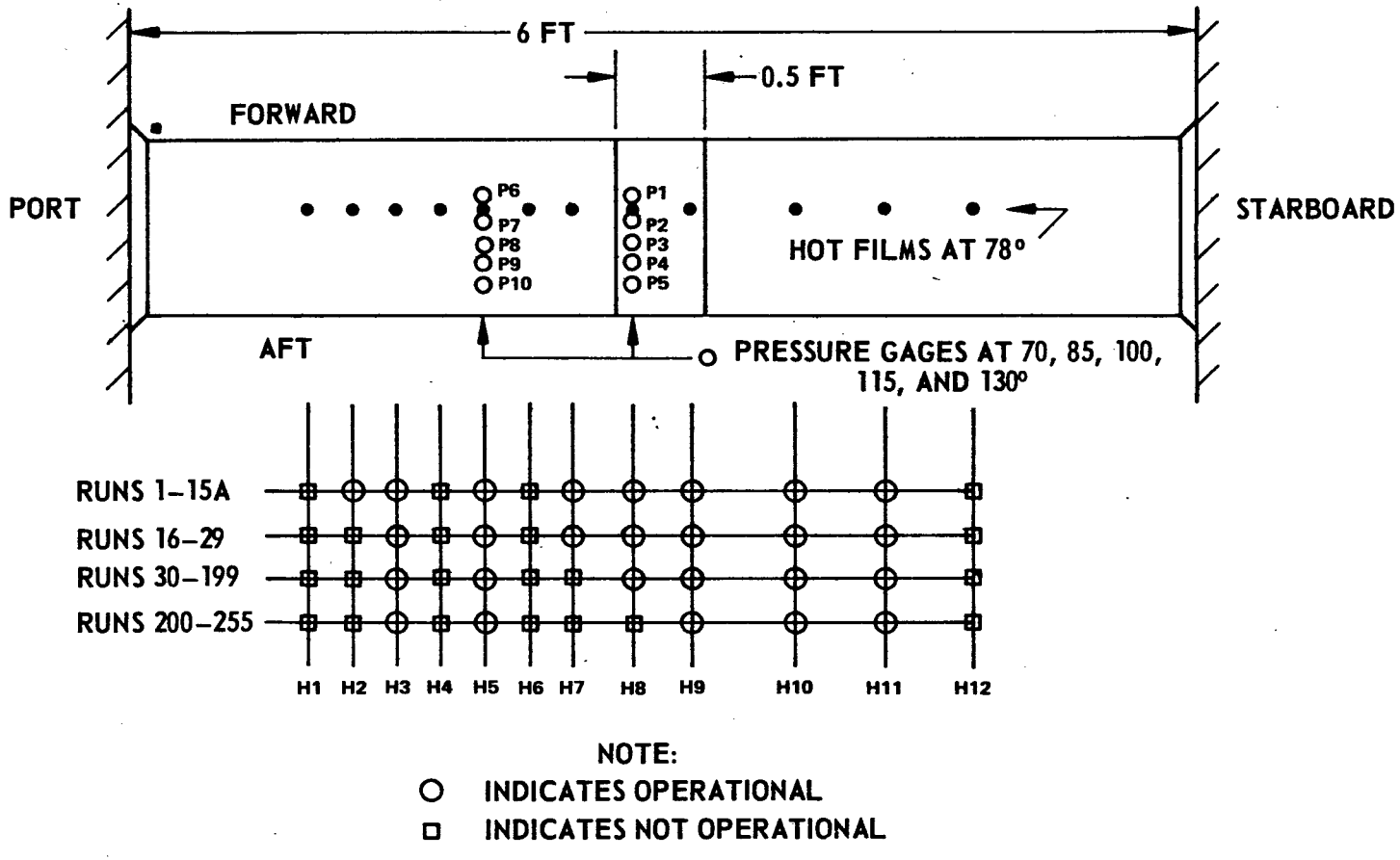

Figure 3 - Location of Hot Films and Pressure Gages on the 12-Inch-Diameter Cylinder

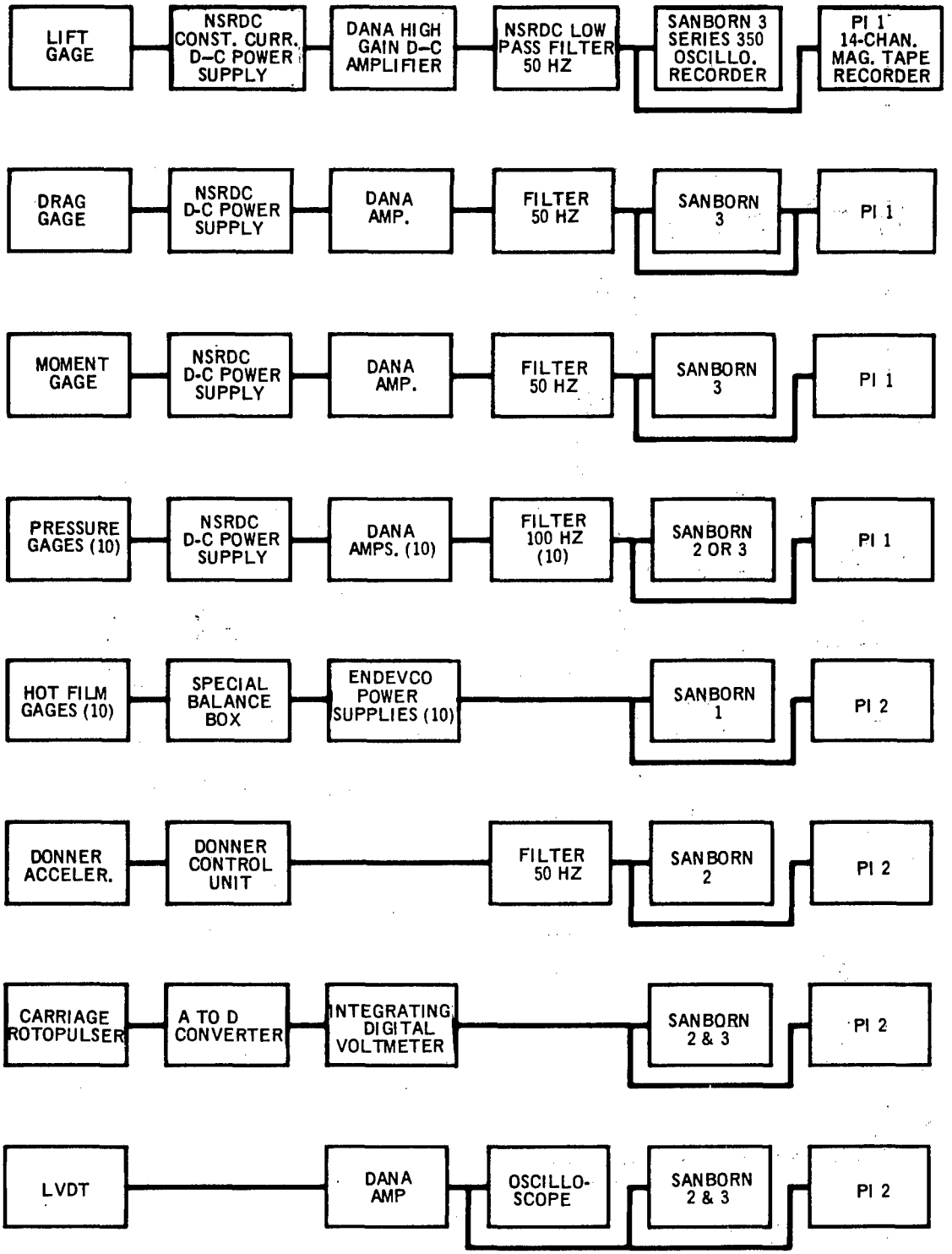

Figure 4 - Details of the Electronic Instrumentation

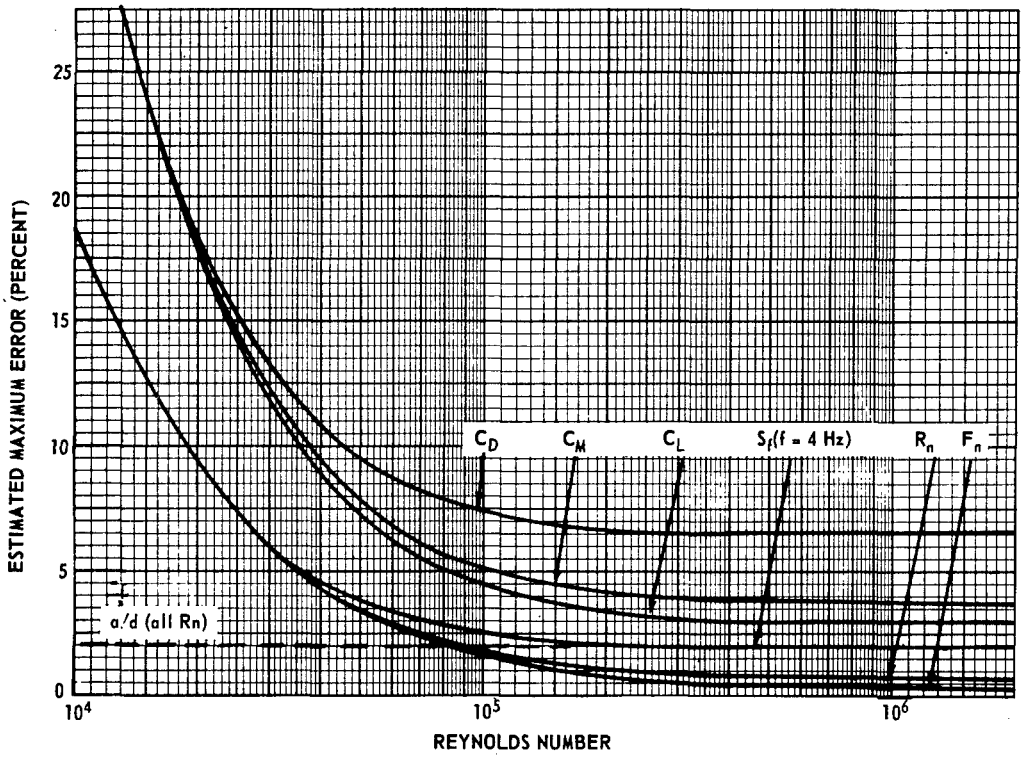

Figure 5a - For Various Coefficients and Nondimensional Numbers versus Reynolds Number

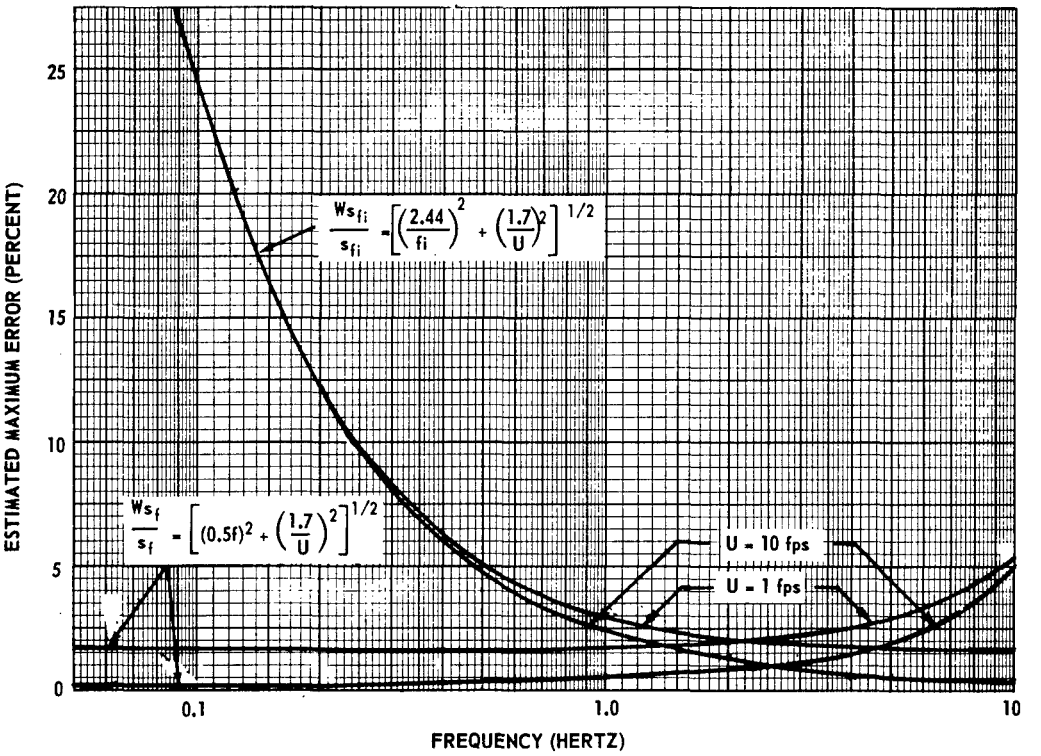

Figure 5b - For Nondimensional Frequencies versus Frequency

Figure 5 - Estimated Maximum Experimental Error in the Coefficients and Nondimensional Numbers

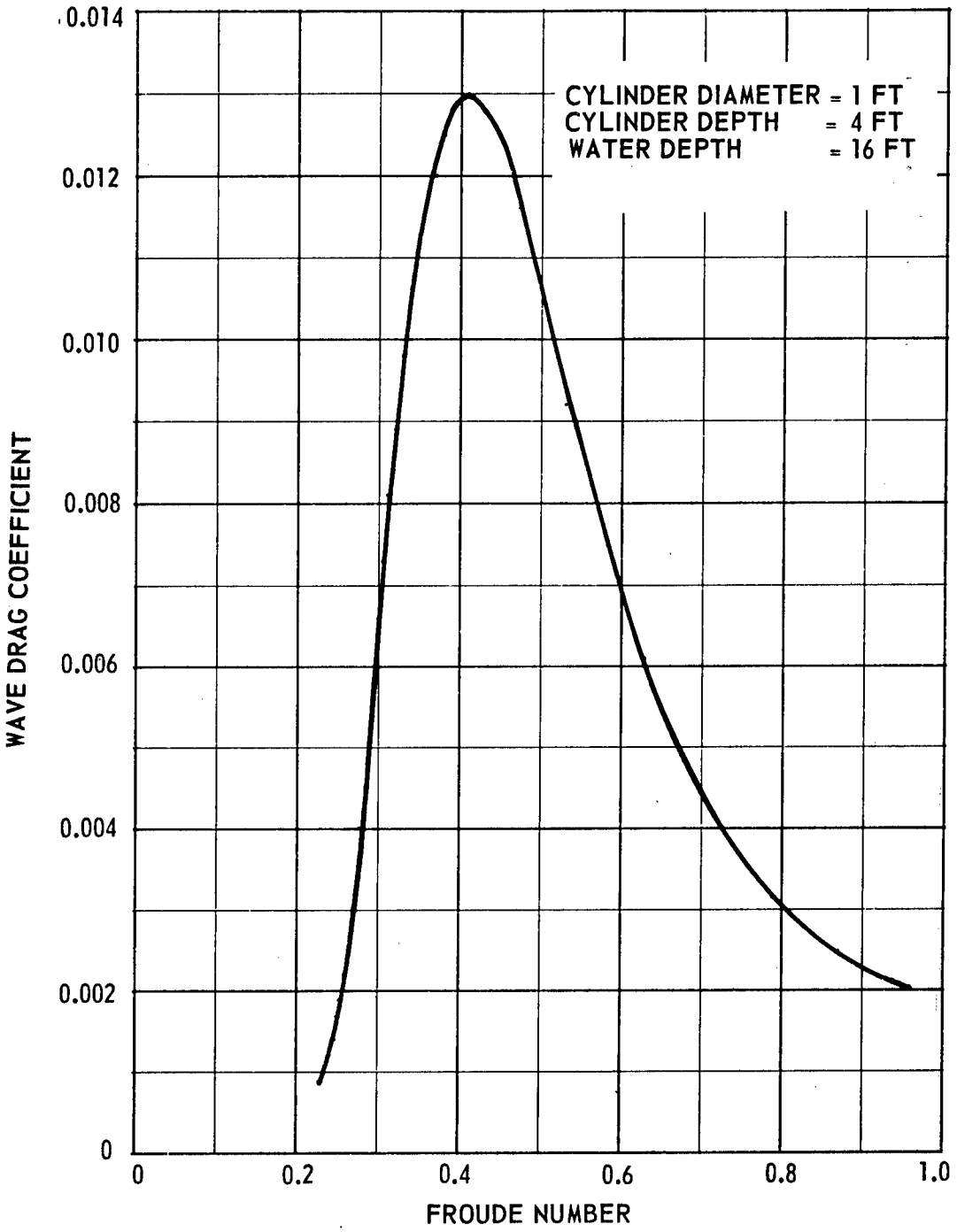

Figure 6 - Wave Drag Coefficient versus Froude Number

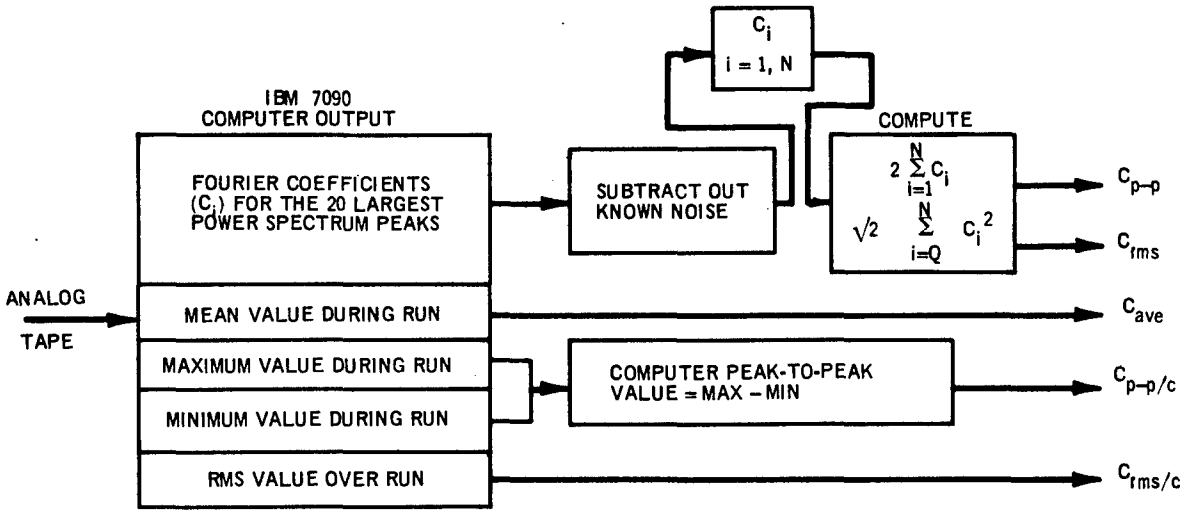

COMPUTER DATA ANALYSIS

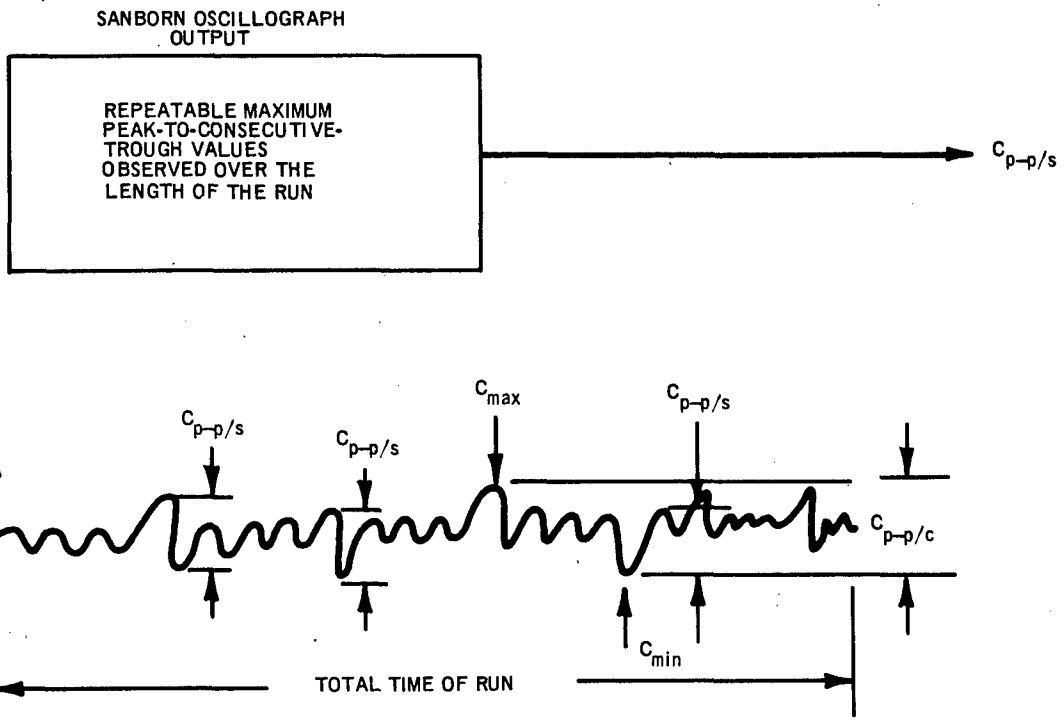

SANBORN OSCILLOGRAPH DATA ANALYSIS

Figure 7 - Summary of Data Analysis Techniques

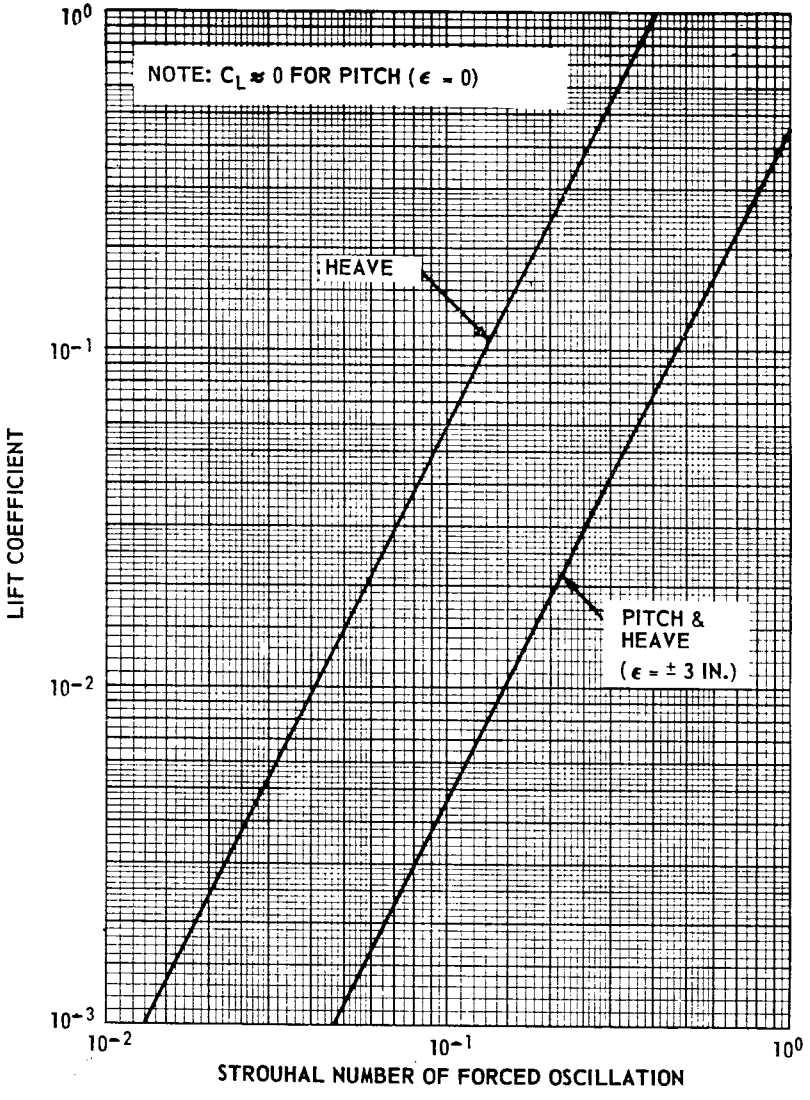

Figure 8 - Dynamometer Interaction for Lift Gage under Various Modes of Cylinder Oscillation

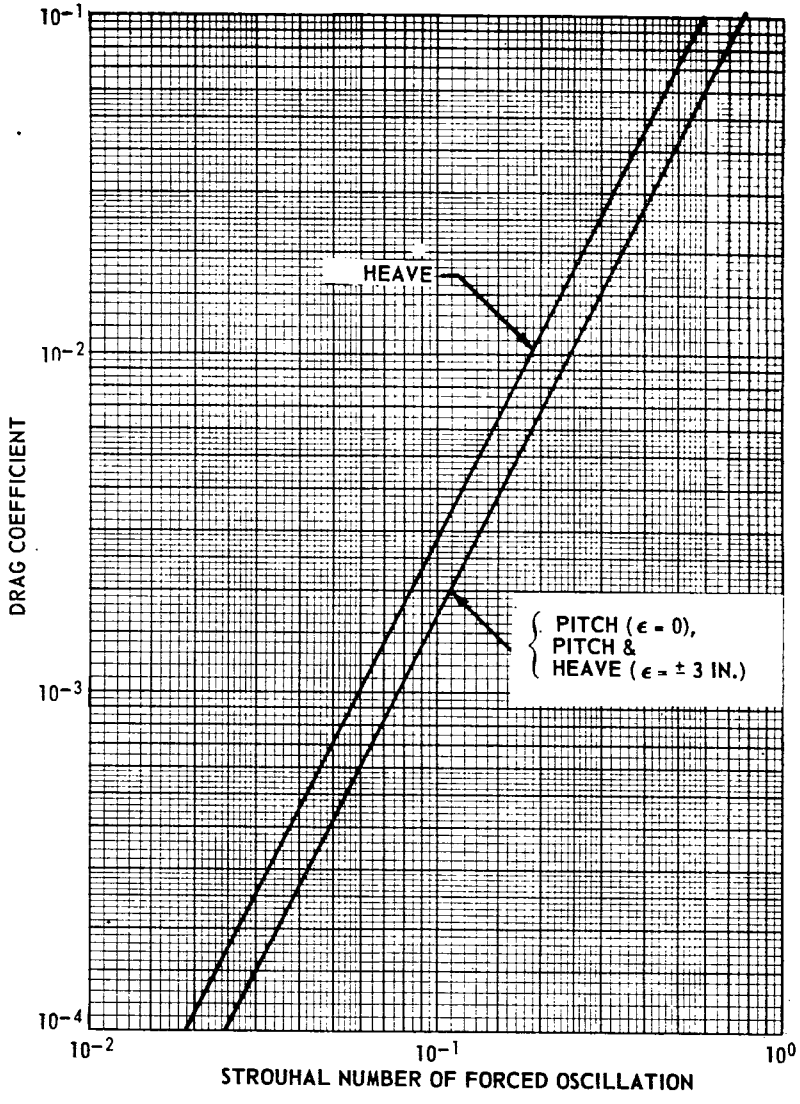

Figure 9 - Dynamometer Interaction for Drag Gage under Various Modes of Cylinder Oscillation

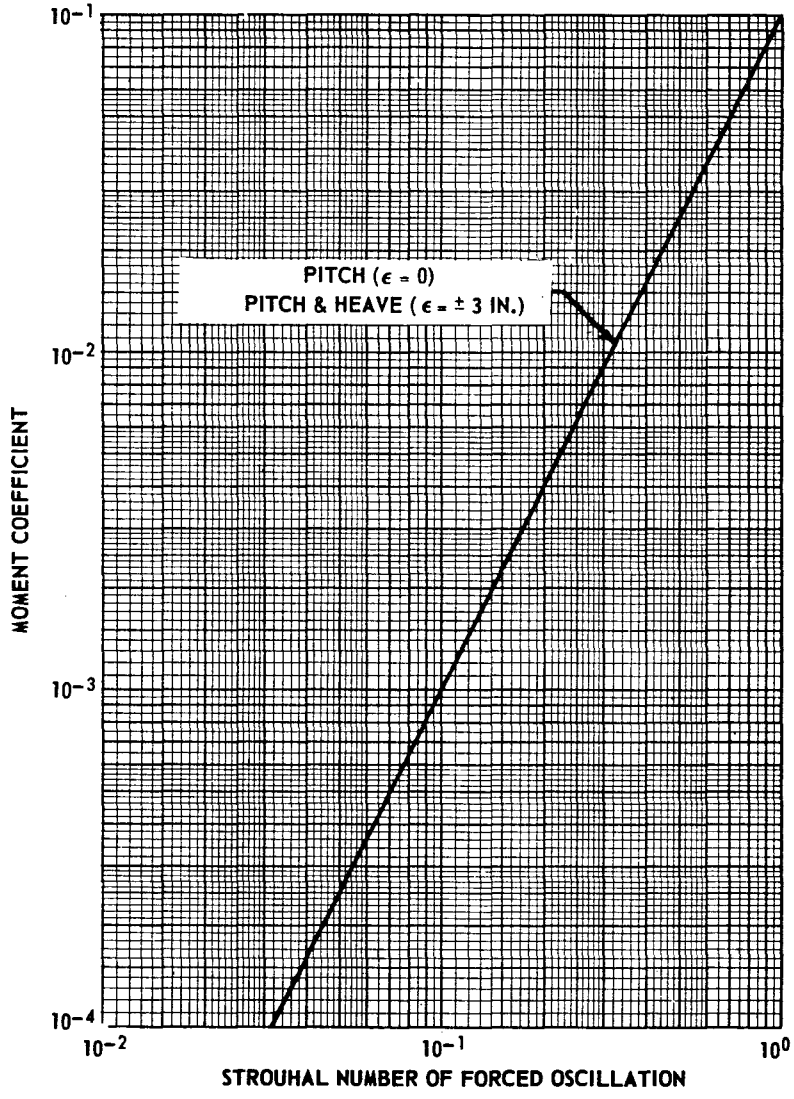

Figure 10a - For Cylinder Oscillating in Pitch or Pitch and Heave

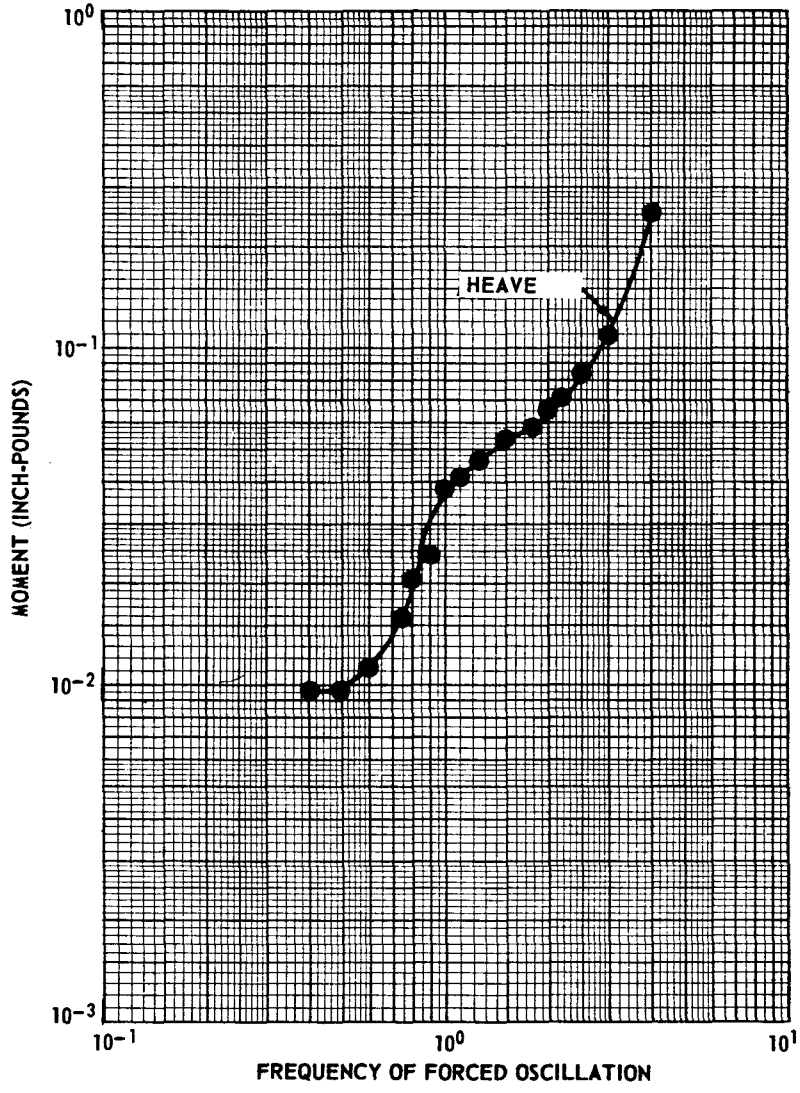

Figure 10b - For Cylinder Oscillating in Heave

Figure 10 - Dynamometer Interaction for Moment Gage

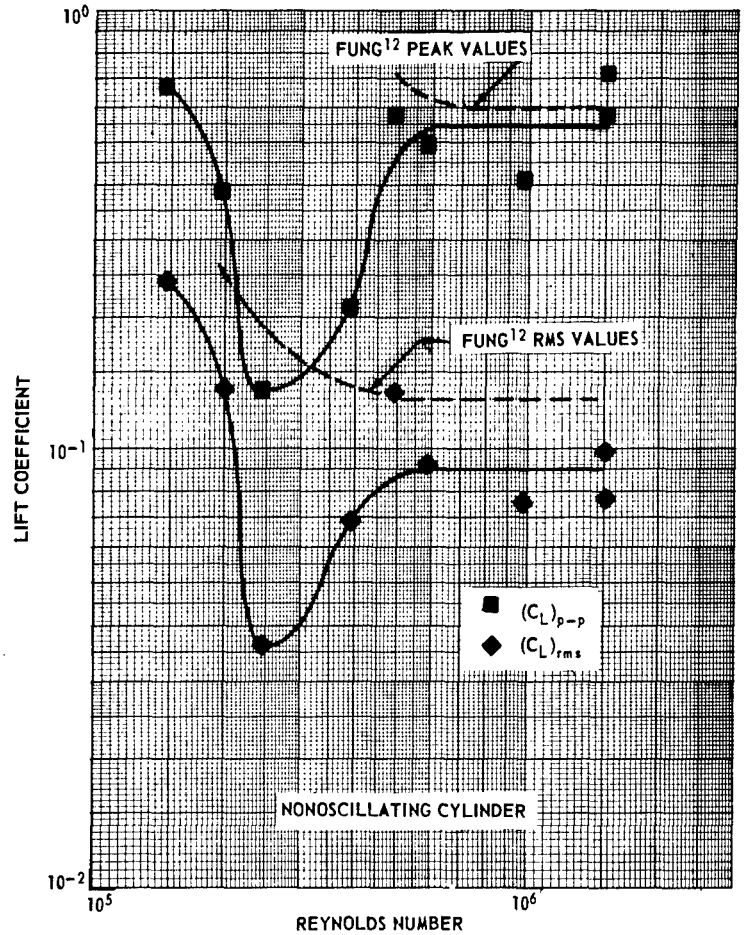

Figure 11a - For the Nonoscillating Cylinder

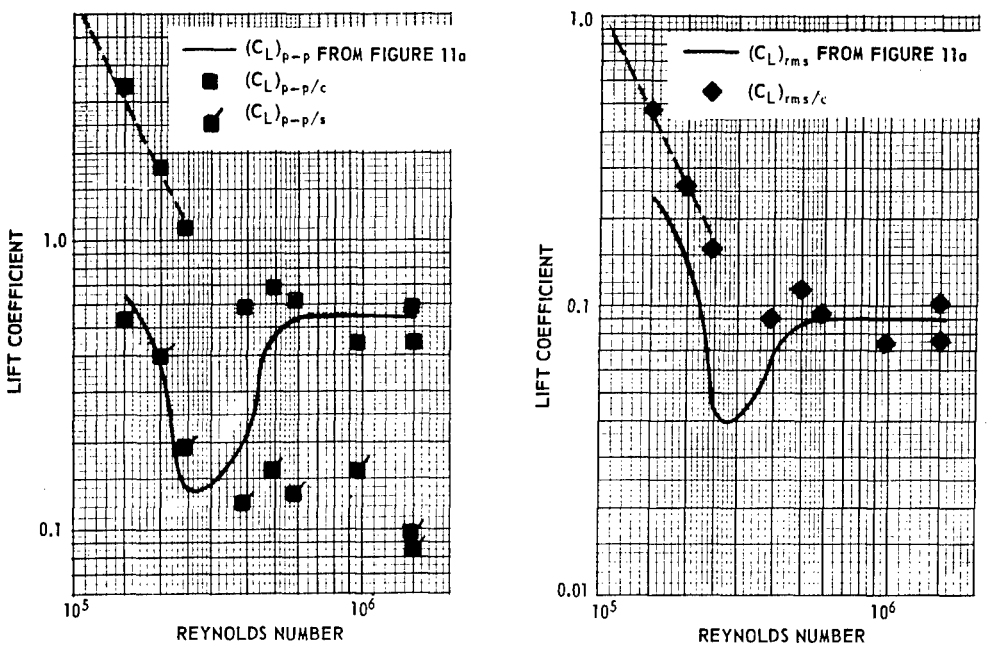

Figure 11b - Comparison of the Various Methods of Determining Lift Coefficient

Figure 11 - Lift Coefficient versus Reynolds Number

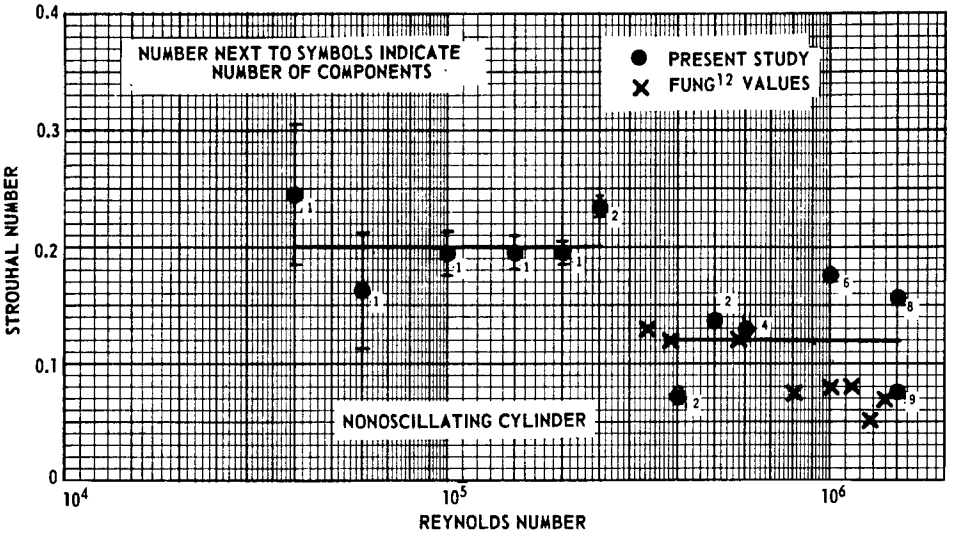

Figure 12 - Strouhal Number for the Major Lift Component versus Reynolds Number for the Nonoscillating Cylinder

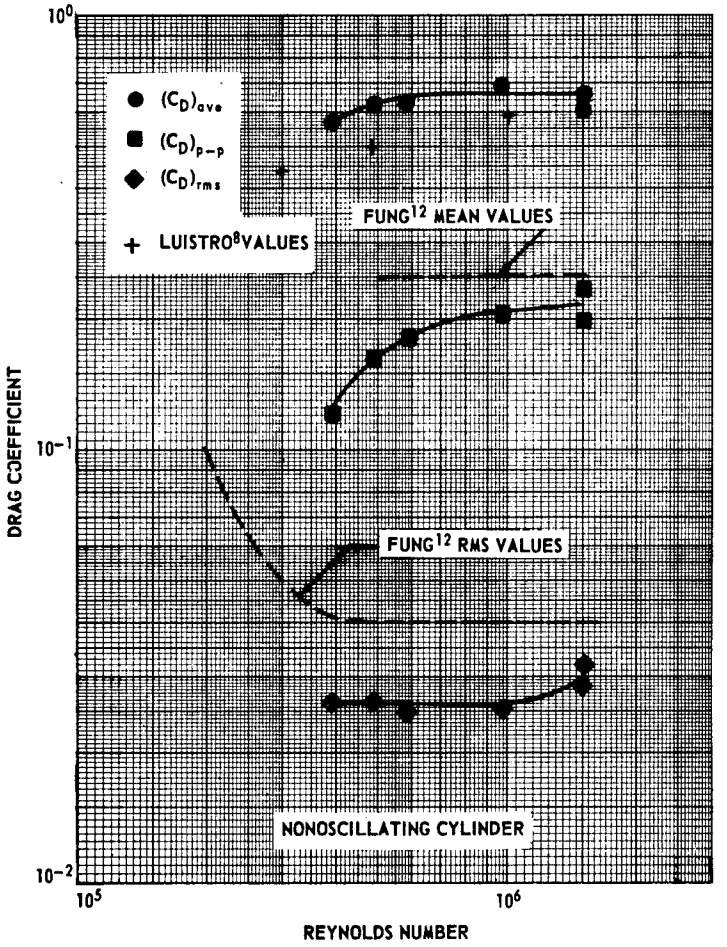

Figure 13 - Drag Coefficient versus Reynolds Number for the Nonoscillating Cylinder

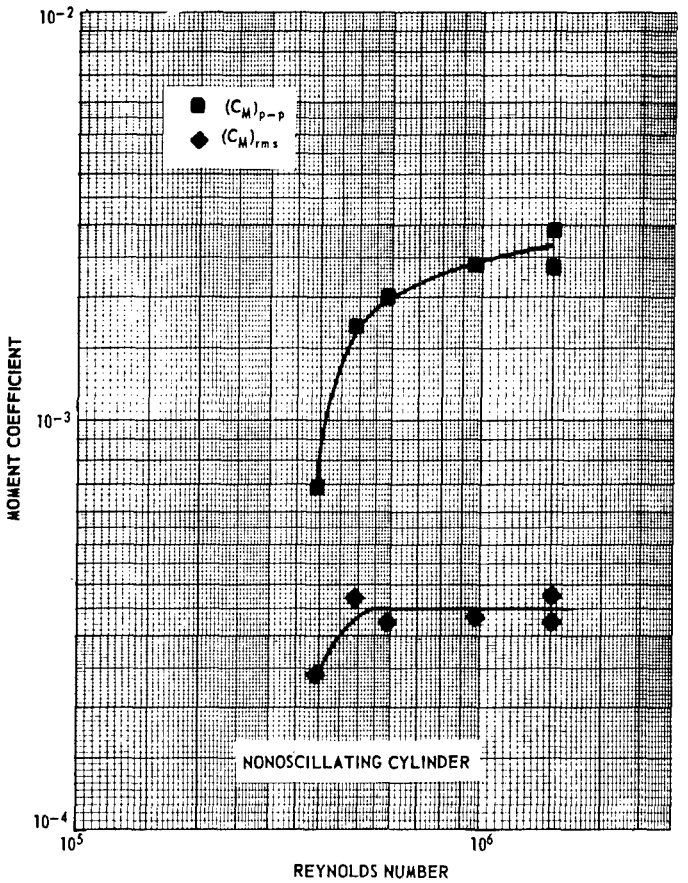

Figure 14 - Moment Coefficient versus Reynolds Number for the Nonoscillating Cylinder

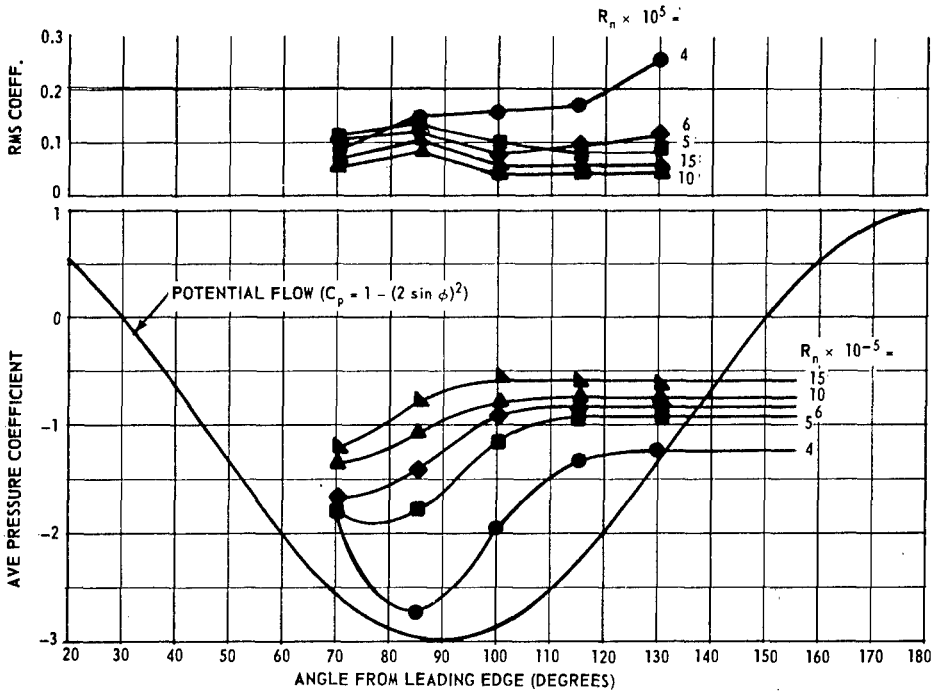

Figure 15 - Pressure Coefficient on the Dynamometer Section for Various Reynolds Numbers for the Nonoscillating Cylinder

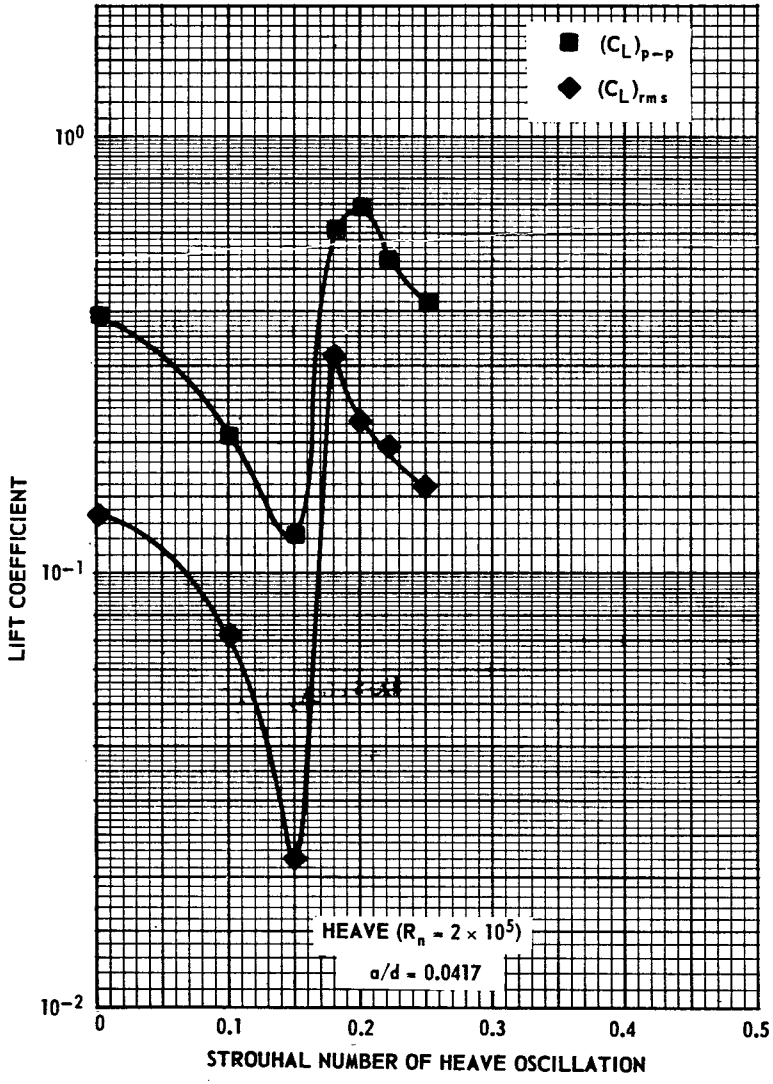

Figure 16 - Lift Coefficient for Heave at $R_n = 2 \times 10^5$

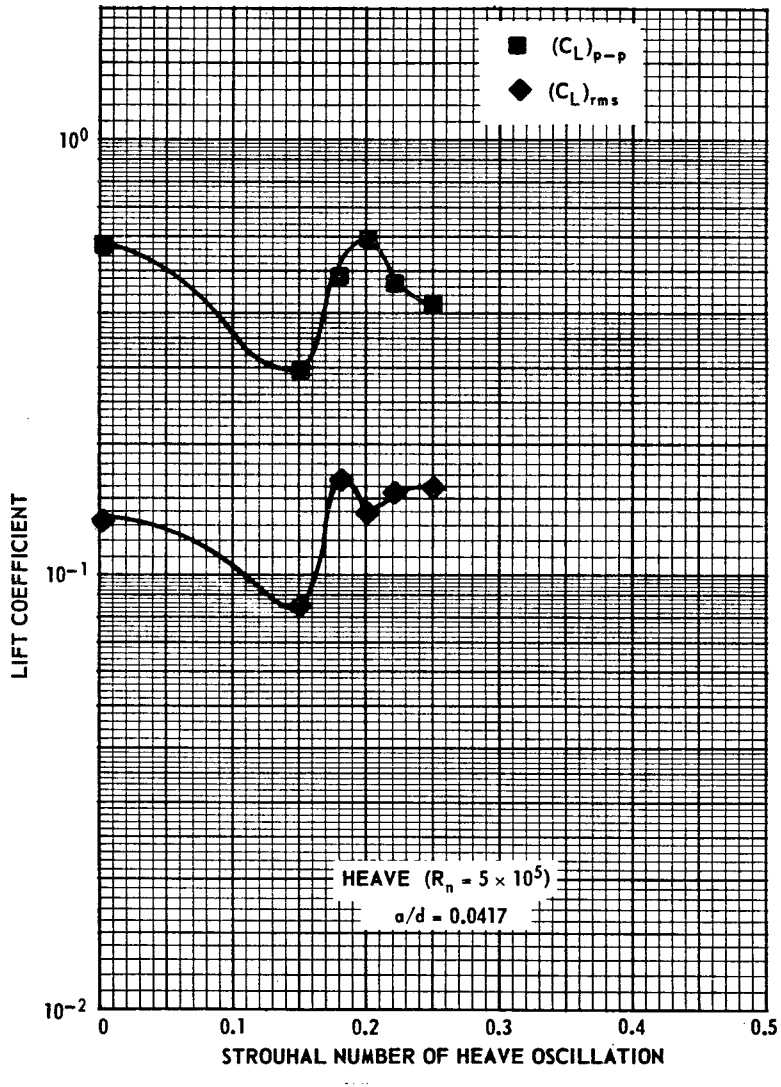

Figure 17 - Lift Coefficient for Heave at $R_n = 5 \times 10^5$

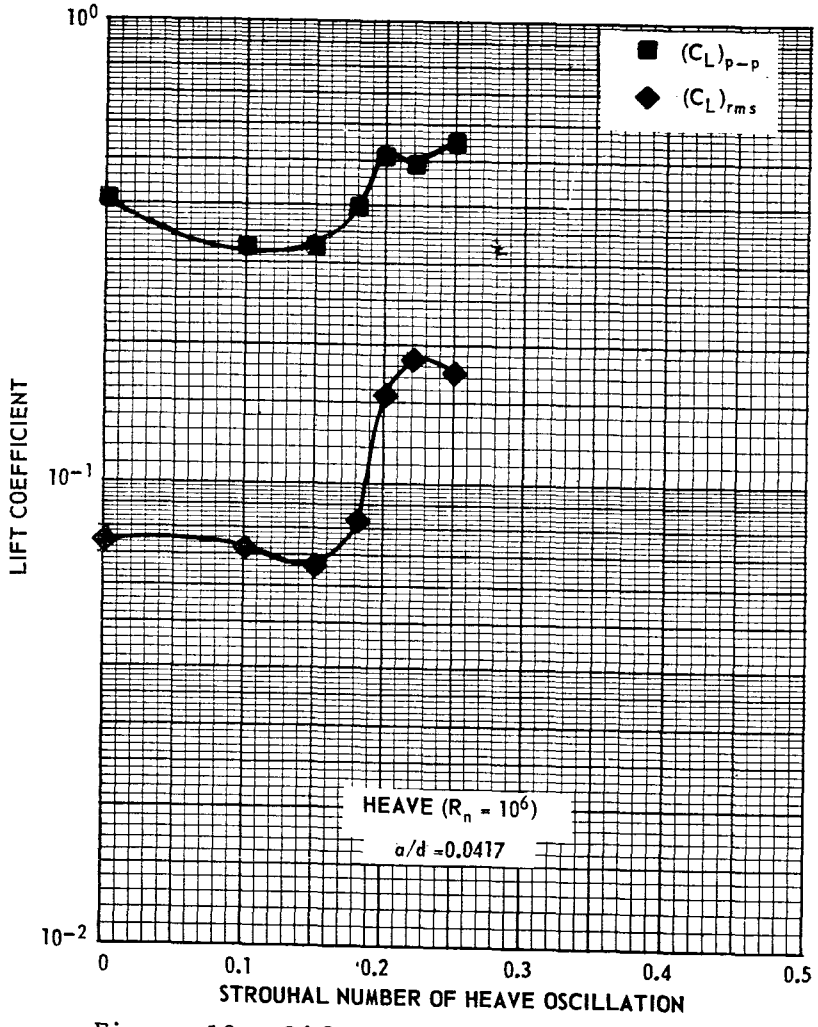

Figure 18 - Lift Coefficient for Heave at $R_n = 1 \times 10^6$

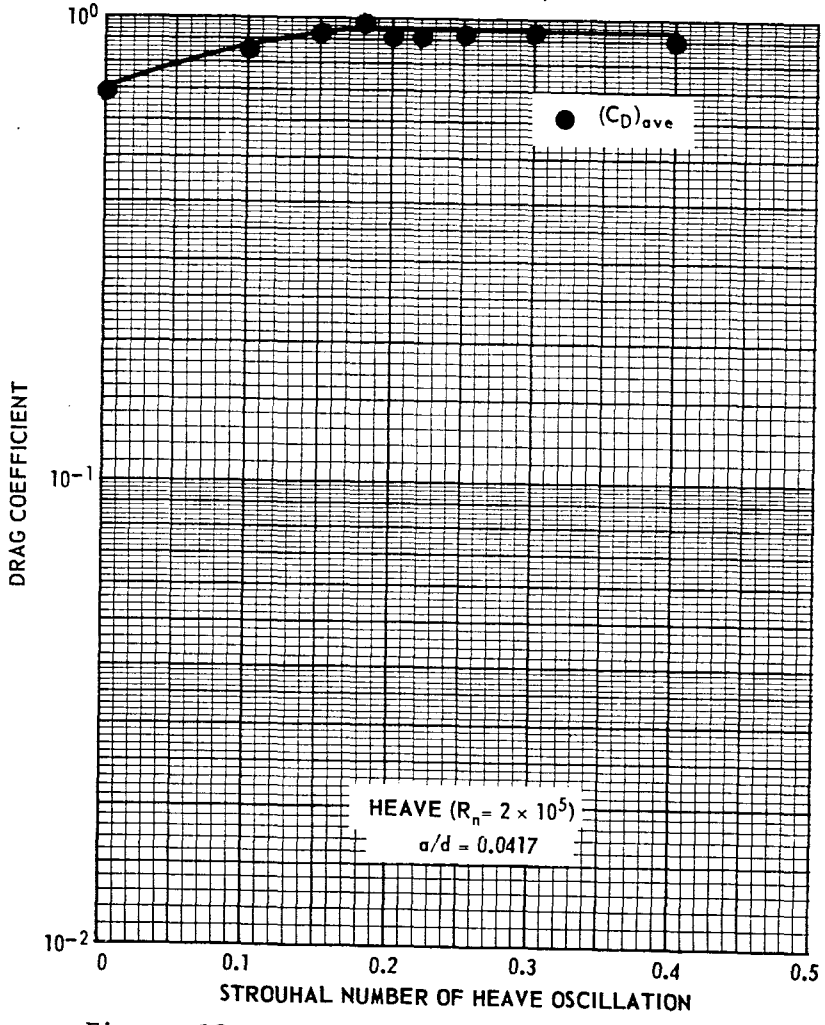

Figure 19 - Drag Coefficient for Heave at $R_n = 2 \times 10^5$

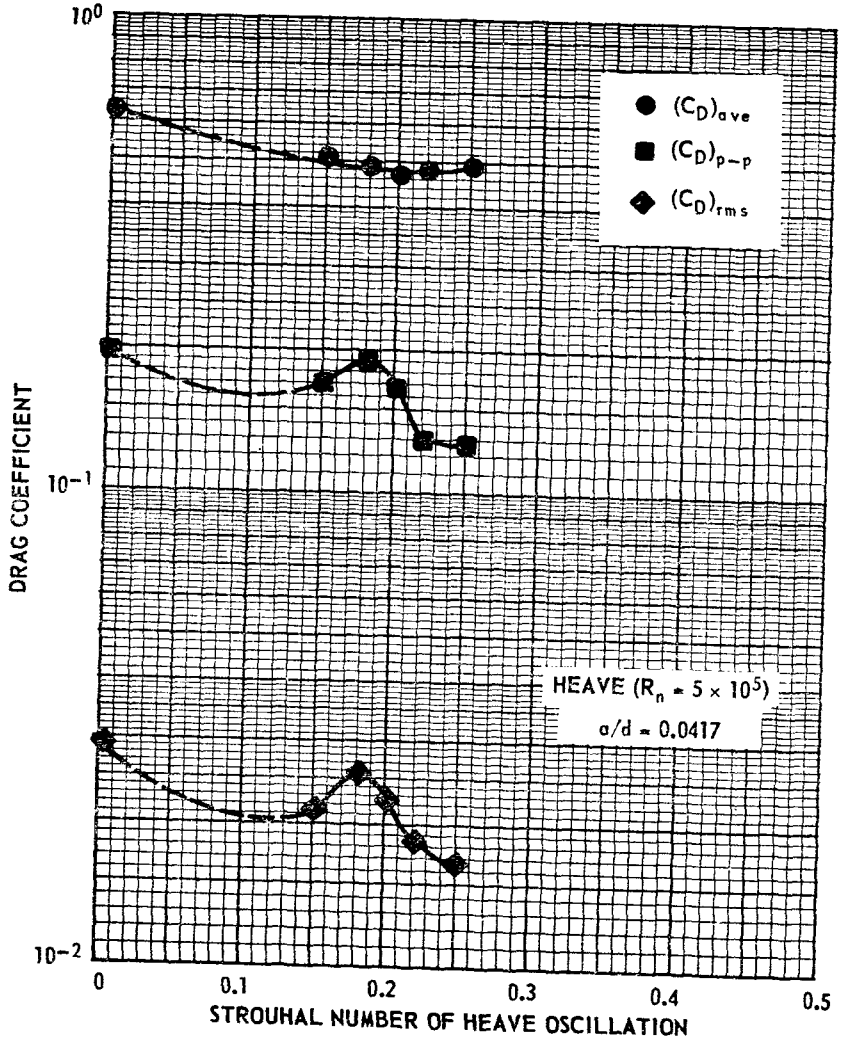

Figure 20 - Drag Coefficient for Heave at $R_n = 5 \times 10^5$

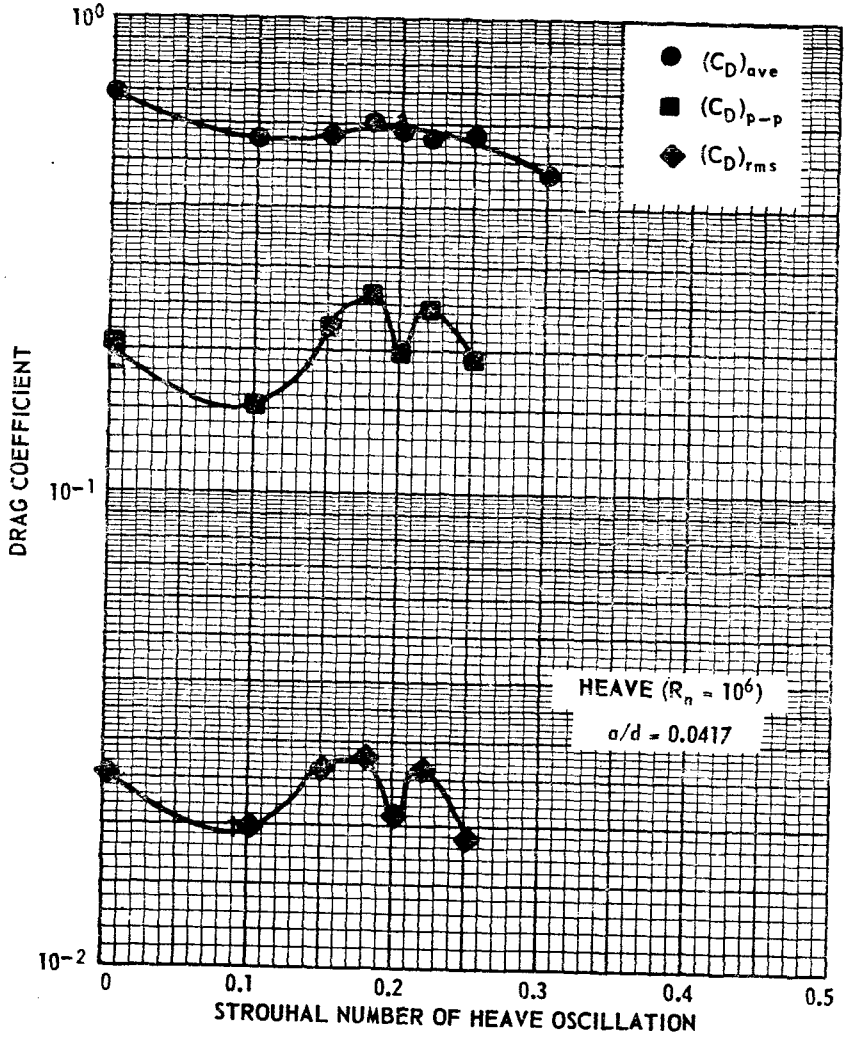

Figure 21 - Drag Coefficient for Heave at $R_n = 1 \times 10^6$

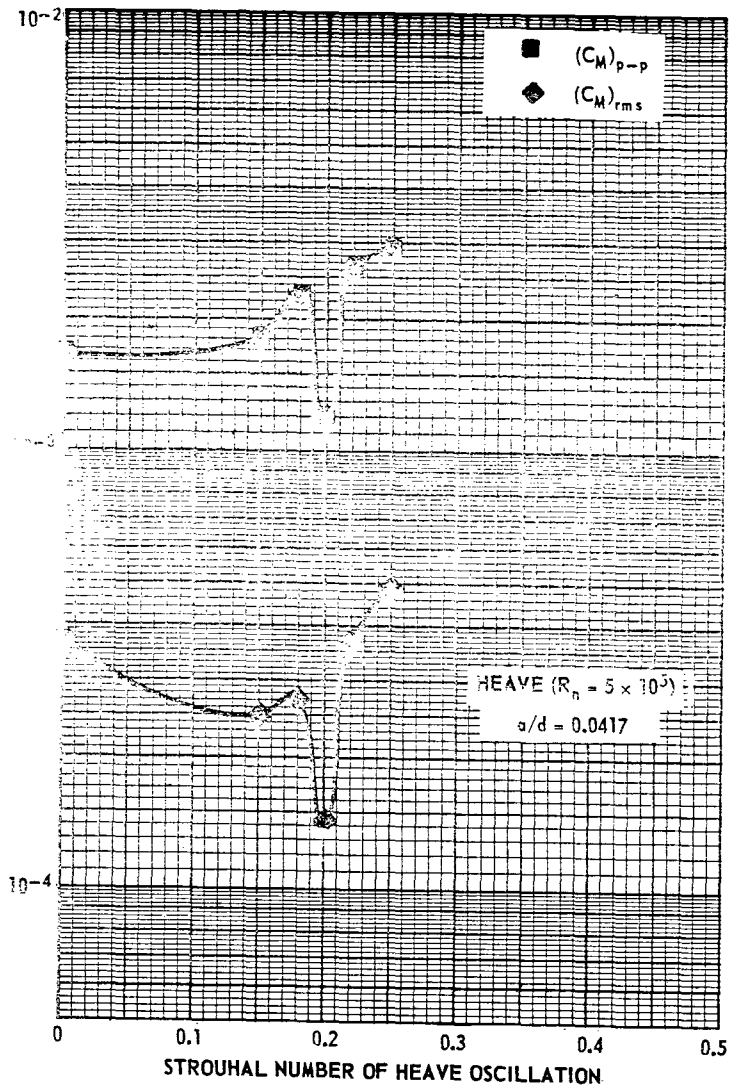

Figure 22 - Moment Coefficient for Heave at $R_n = 5 \times 10^5$

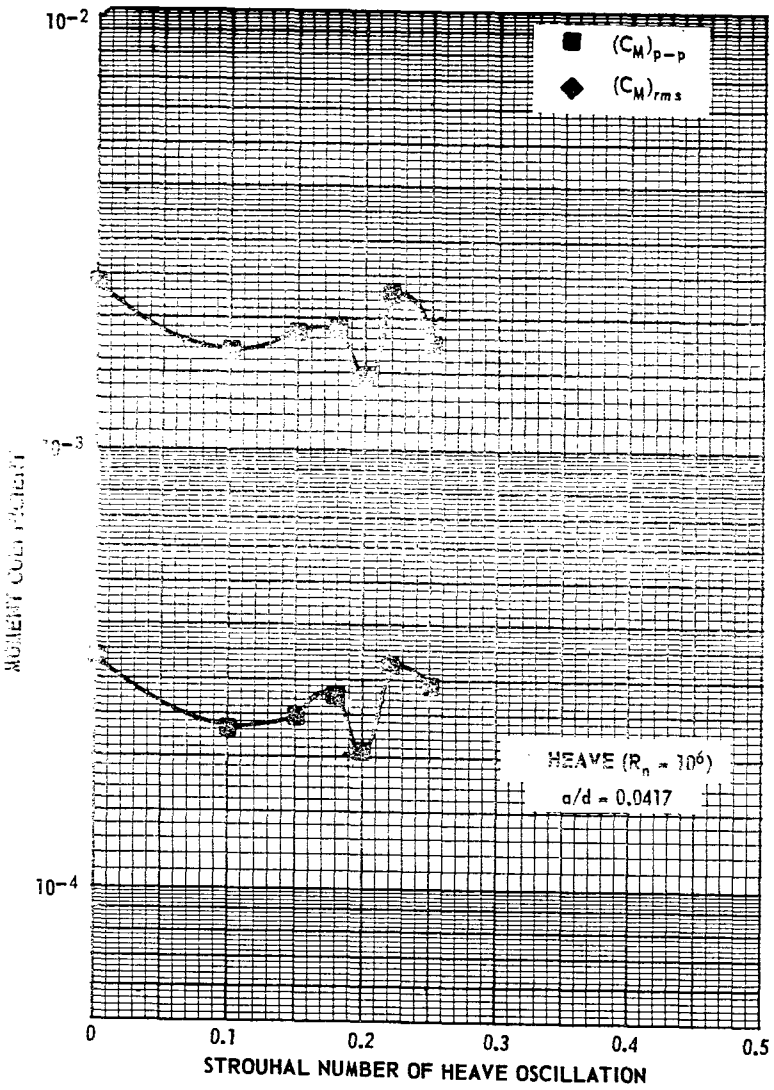

Figure 23 - Moment Coefficient for Heave at $R_n = 1 \times 10^6$

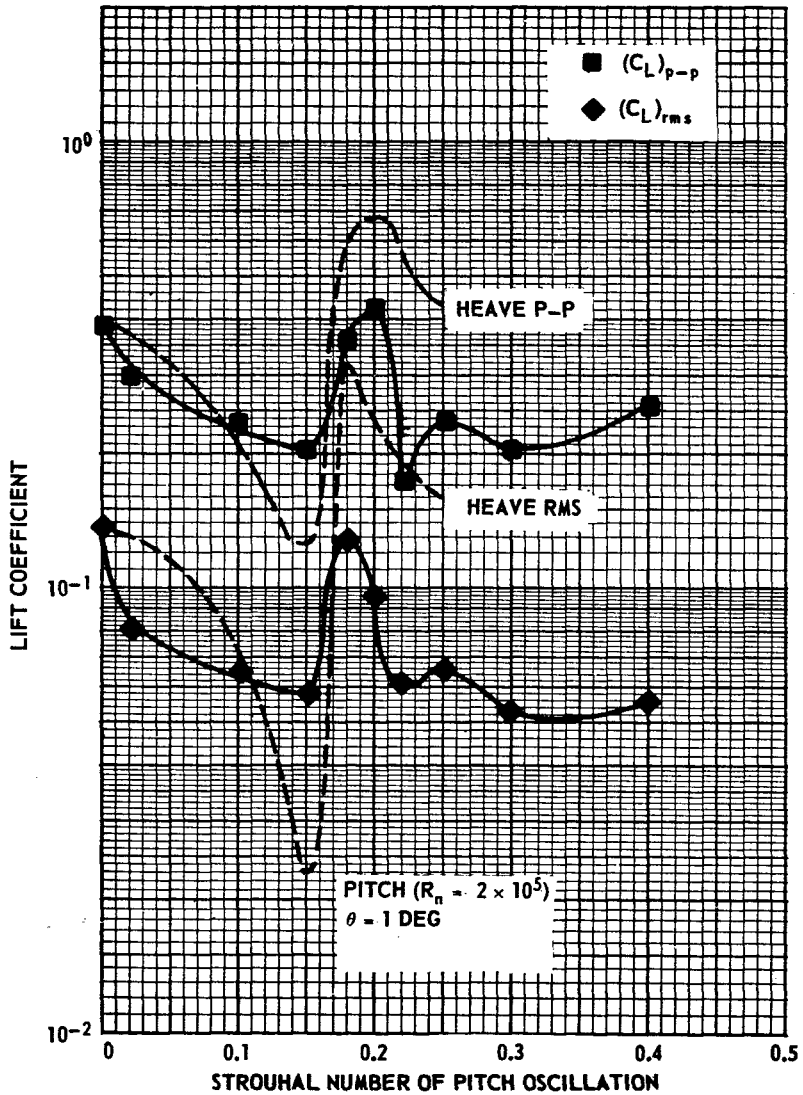

Figure 24 - Lift Coefficient for Pitch at $R_n = 2 \times 10^5$

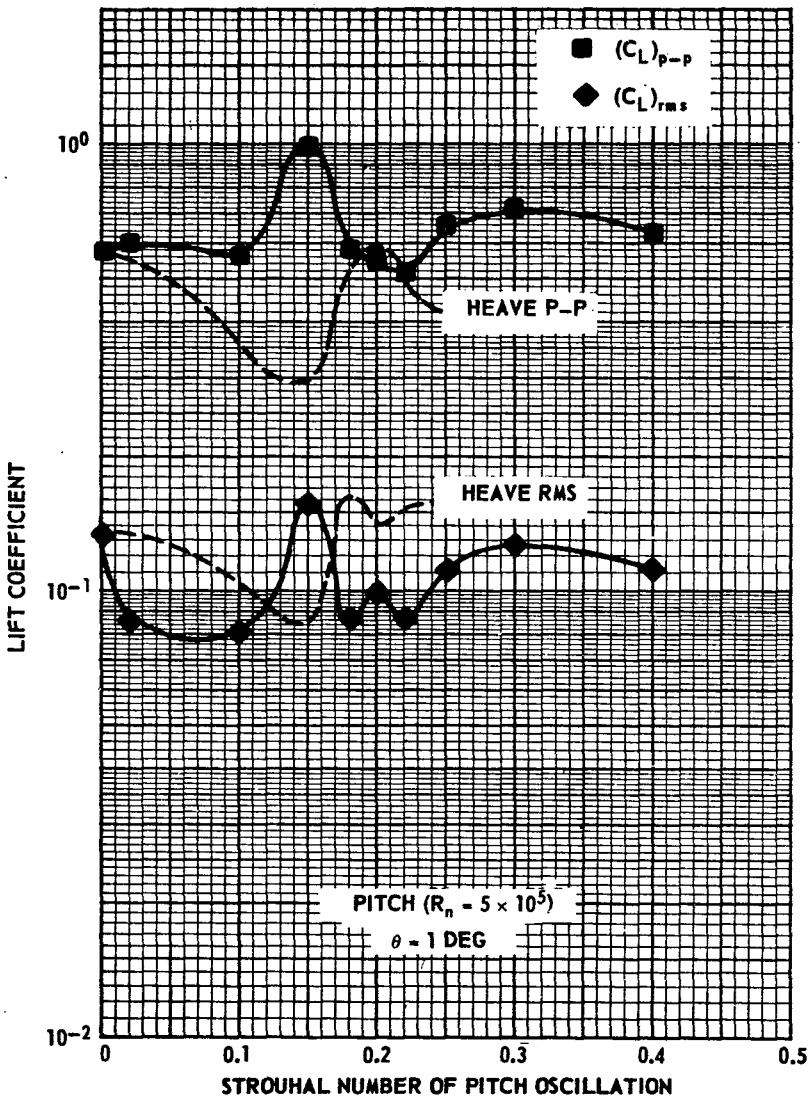

Figure 25 - Lift Coefficient for Pitch at $R_n = 5 \times 10^5$

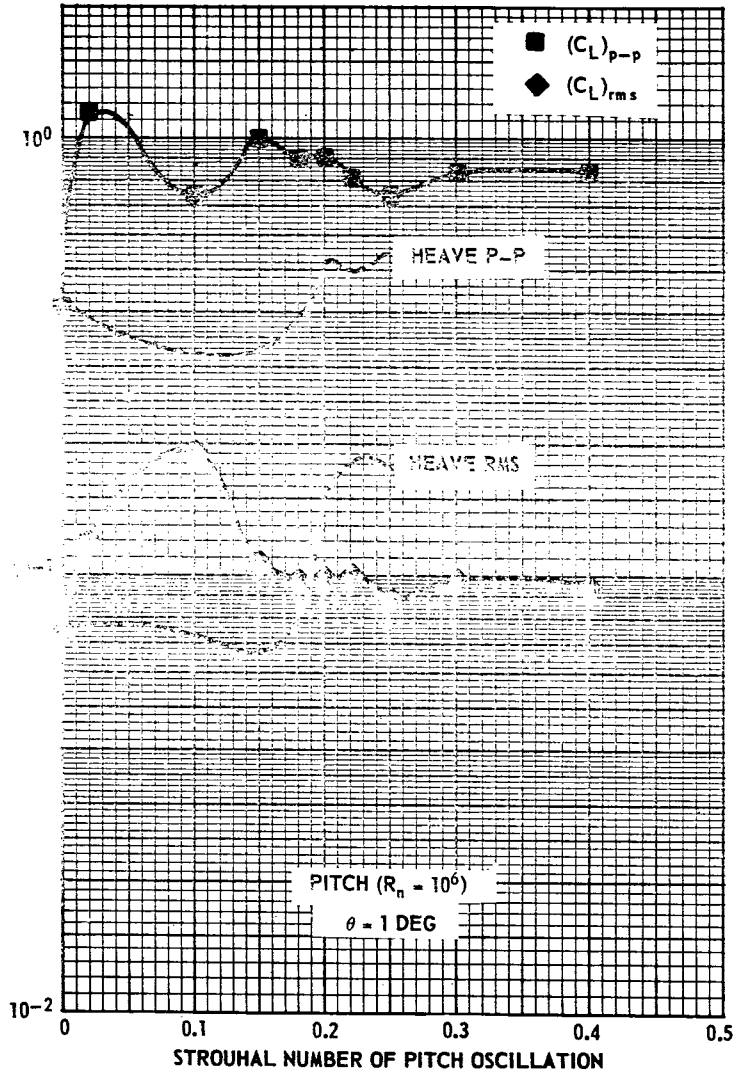

Figure 26 - Lift Coefficient for Pitch at $R_n = 1 \times 10^6$

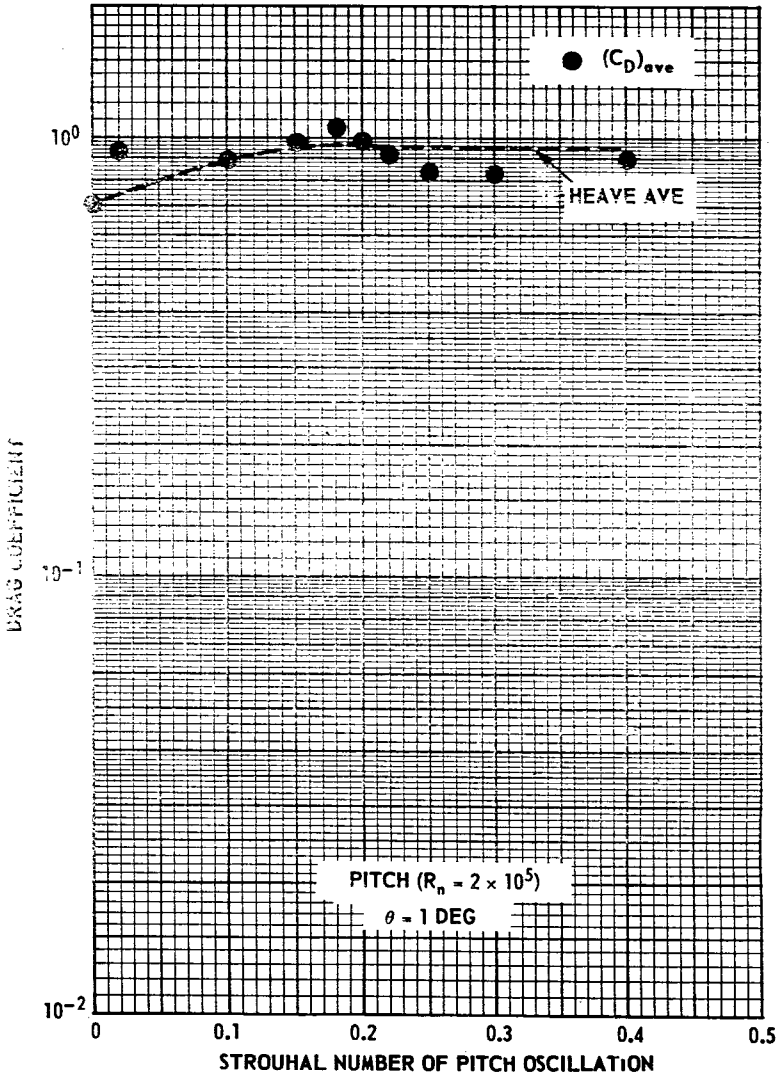

Figure 27 - Drag Coefficient for Pitch at $R_n = 2 \times 10^5$

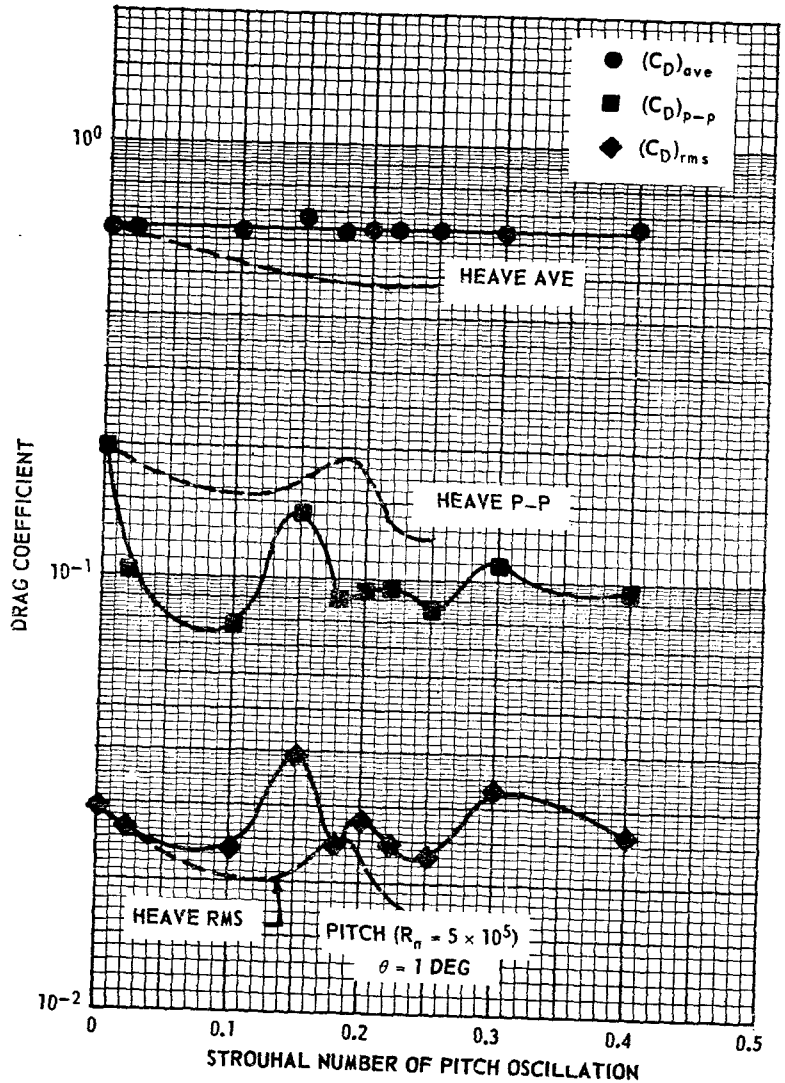

Figure 28 - Drag Coefficient for Pitch at $R_n = 5 \times 10^5$

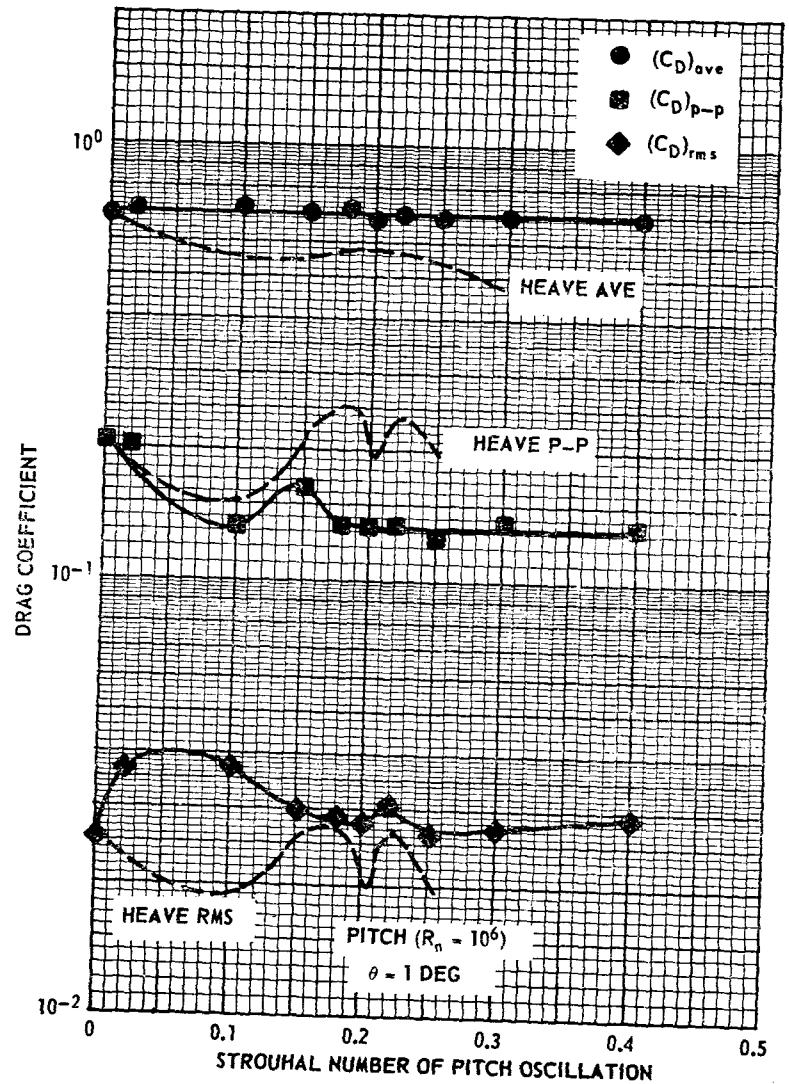

Figure 29 - Drag Coefficient for Pitch at $R_n = 1 \times 10^6$

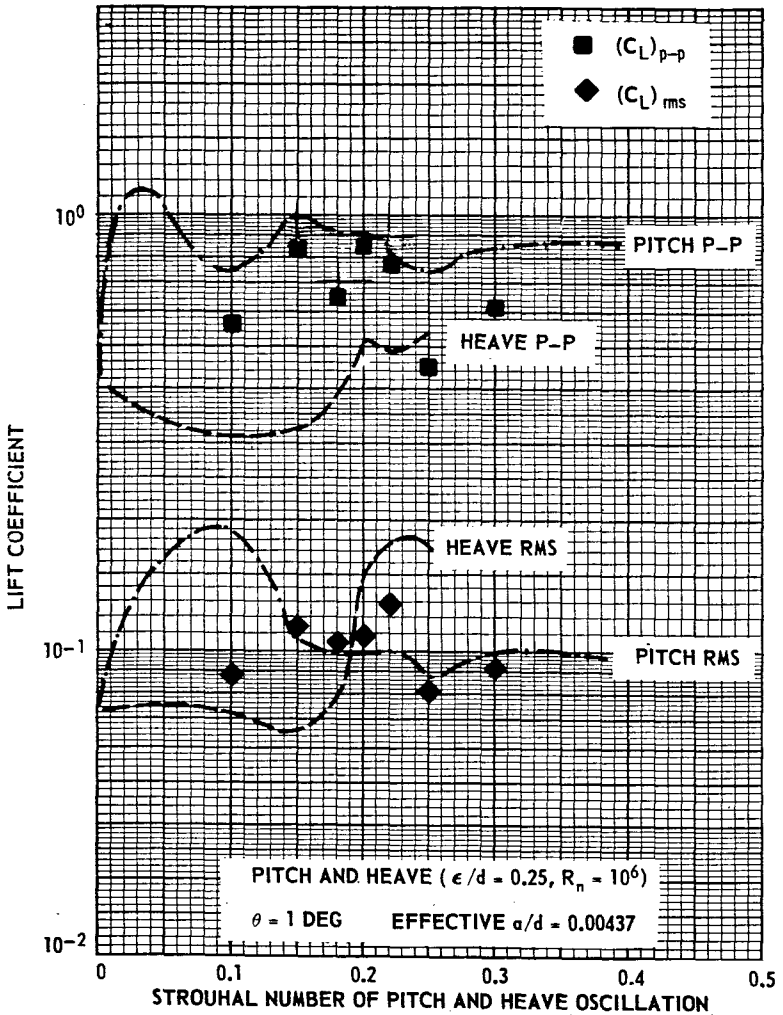

Figure 30 - Lift Coefficient for Pitch and Heave at ε/d =+0.25 and R_n = 1 x 10^6

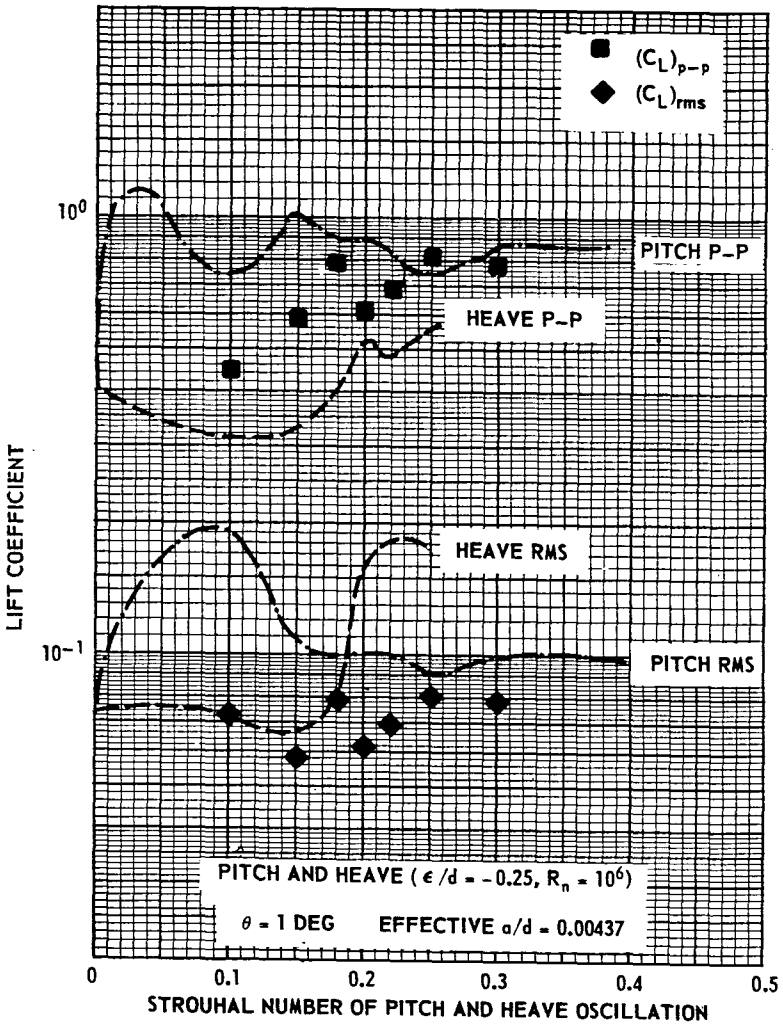

Figure 31 - Lift Coefficient for Pitch and Heave at ε/d =-0.25 and R_n = 1 x 10^6

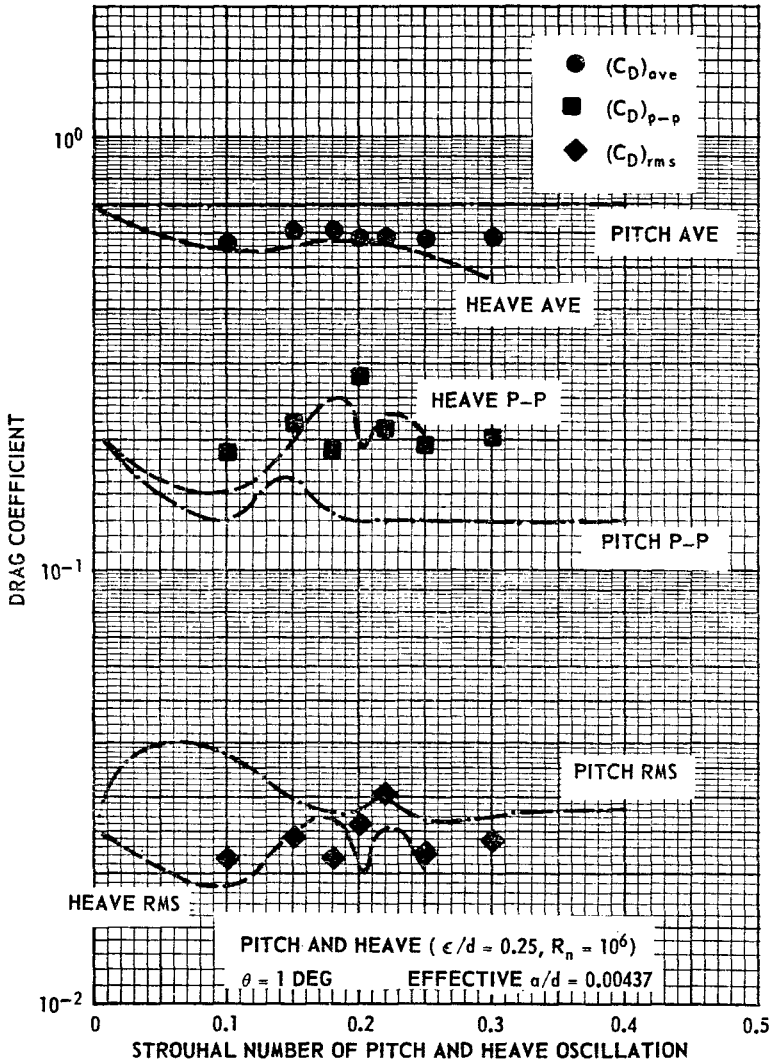

Figure 32 - Drag Coefficient for Pitch and Heave at ϵ/d =+0.25 and R_n = 1 x 10^6

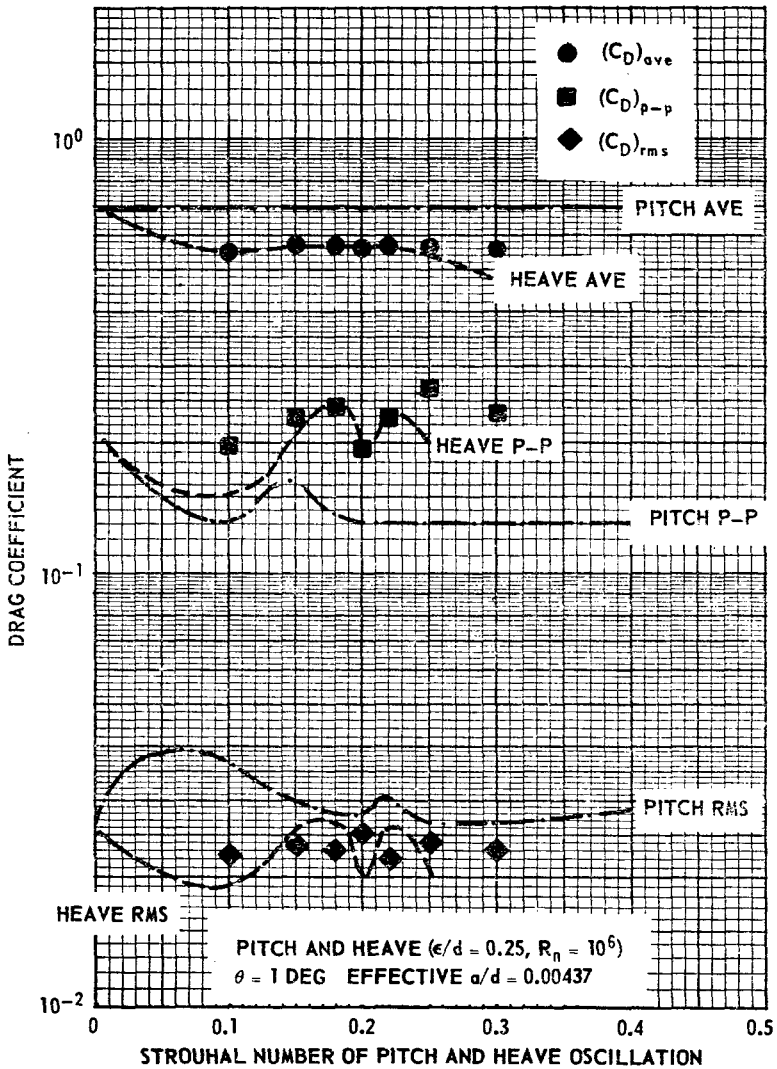

Figure 33 - Drag Coefficient for Pitch and Heave at ϵ/d =-0.25 and R_n = 1 x 10^6

APPENDIX A

POWER SPECTRA OF LIFT, DRAG, AND MOMENT FOR THE NONOSCILLATING CYLINDER

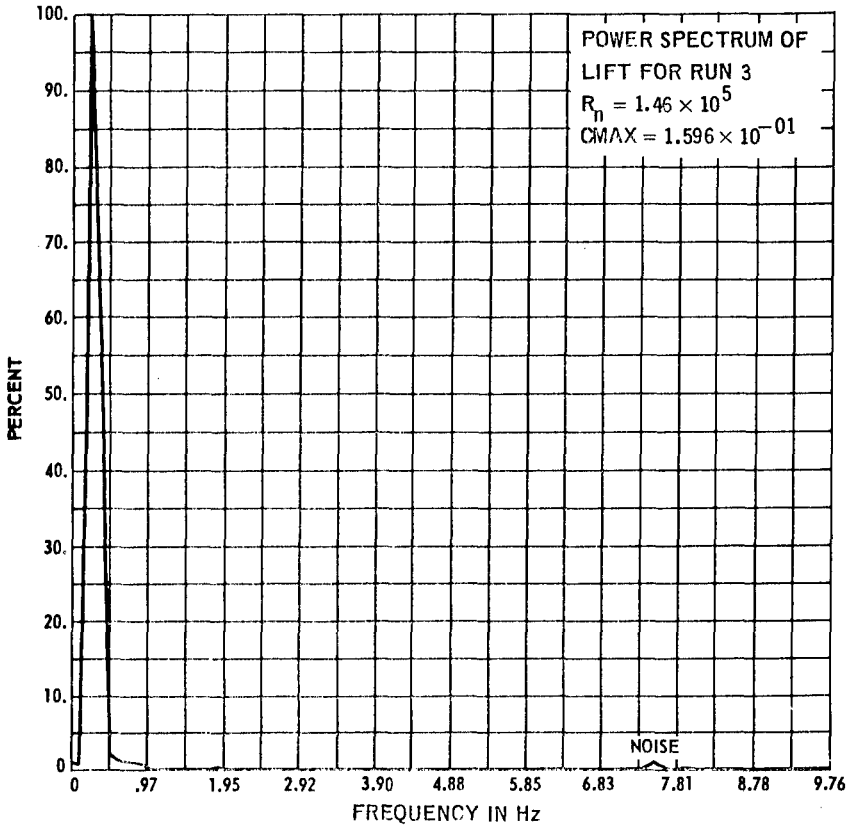
POWER SPECTRUM OF
LIFT FOR RUN 3
$R_n = 1.46 \times 10^5$
CMAX = 1.596×10^{-01}
PERCENT
100.
90.
80.
70.
60.
50.
40.
30.
20.
10.
0
NOISE
0
.97
1.95
2.92
3.90
4.88
5.85
6.83
7.81
8.78
9.76
FREQUENCY IN Hz

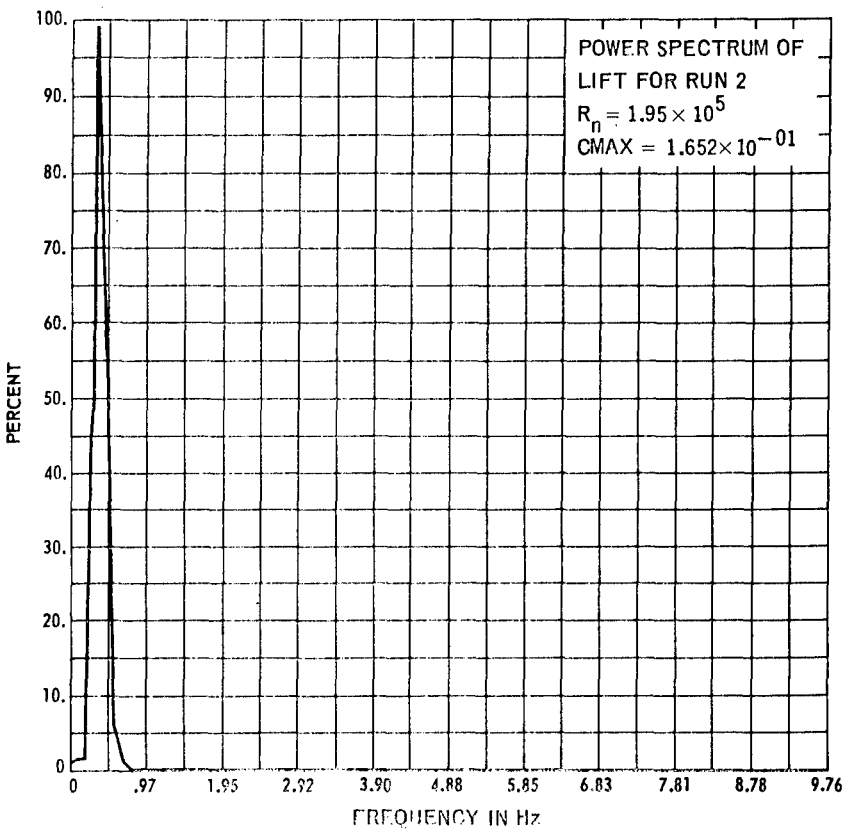
POWER SPECTRUM OF
LIFT FOR RUN 2
$R_n = 1.95 \times 10^5$
CMAX = 1.652×10^{-01}
PERCENT
100.
90.
80.
70.
60.
50.
40.
30.
20.
10.
0
0
.97
1.95
2.92
3.90
4.88
5.85
6.83
7.81
8.78
9.76
FREQUENCY IN Hz

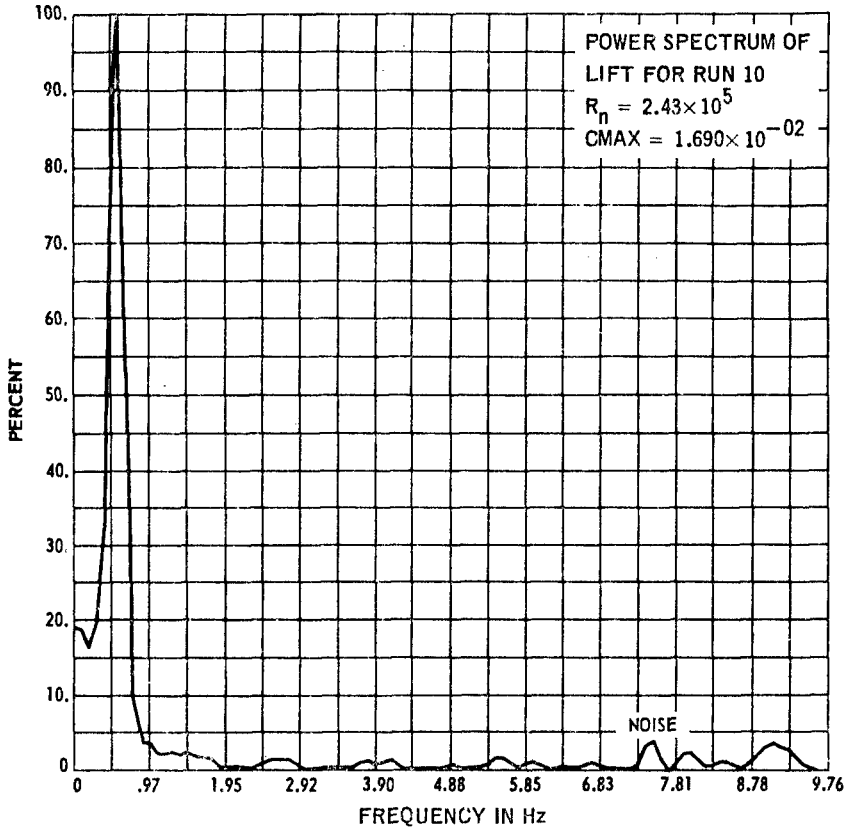
POWER SPECTRUM OF
LIFT FOR RUN 10
$R_n = 2.43\times10^5$
CMAX = 1.690×10^{-02}
NOISE
PERCENT
100.
90.
80.
70.
60.
50.
40.
30.
20.
10.
0
0
.97
1.95
2.92
3.90
4.88
5.85
6.83
7.81
8.78
9.76
FREQUENCY IN Hz

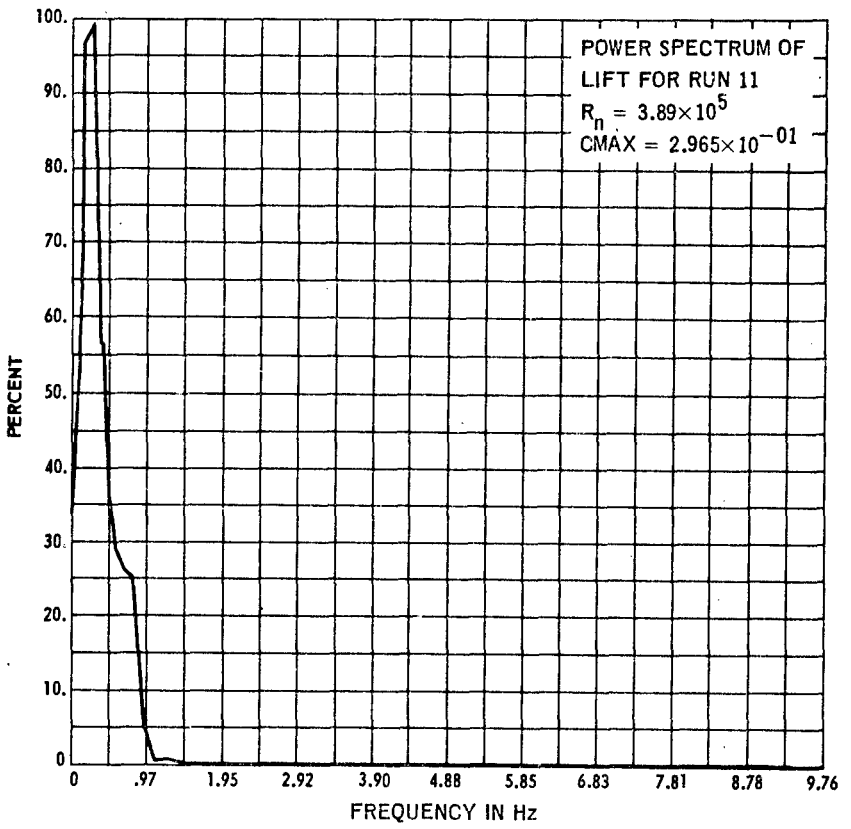
POWER SPECTRUM OF
LIFT FOR RUN 11
$R_n = 3.89\times10^5$
CMAX = 2.965×10^{-01}
PERCENT
100.
90.
80.
70.
60.
50.
40.
30.
20.
10.
0
0
.97
1.95
2.92
3.90
4.88
5.85
6.83
7.81
8.78
9.76
FREQUENCY IN Hz

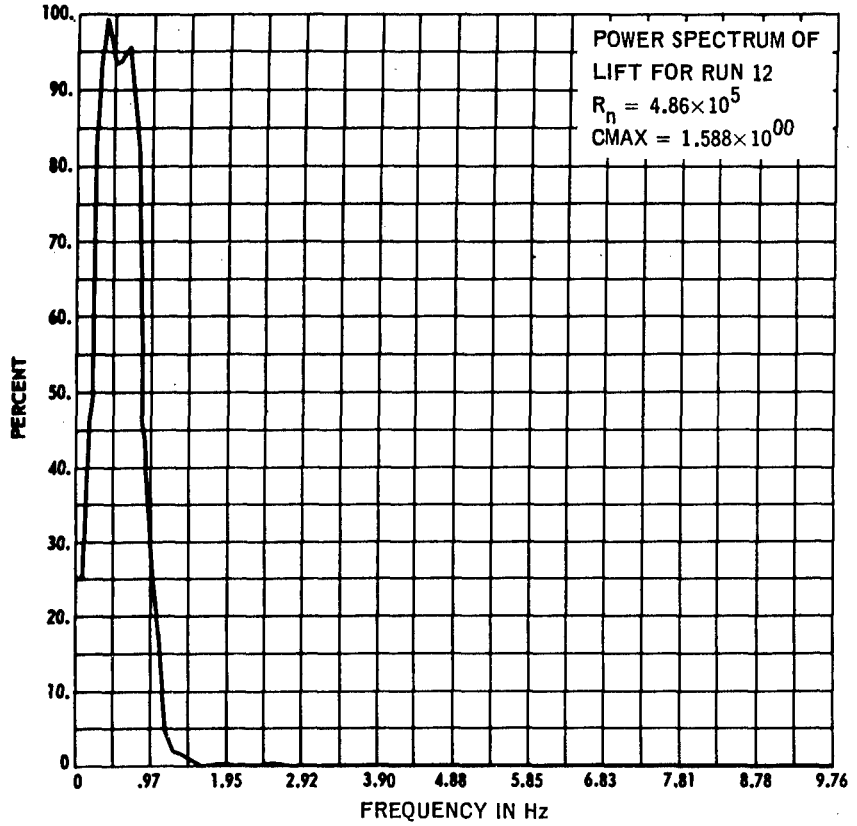
POWER SPECTRUM OF
LIFT FOR RUN 12
$R_n = 4.86\times10^5$
CMAX = 1.588×10^{00}
PERCENT
100.
90.
80.
70.
60.
50.
40.
30.
20.
10.
0
0
.97
1.95
2.92
3.90
4.88
5.85
6.83
7.81
8.78
9.76
FREQUENCY IN Hz

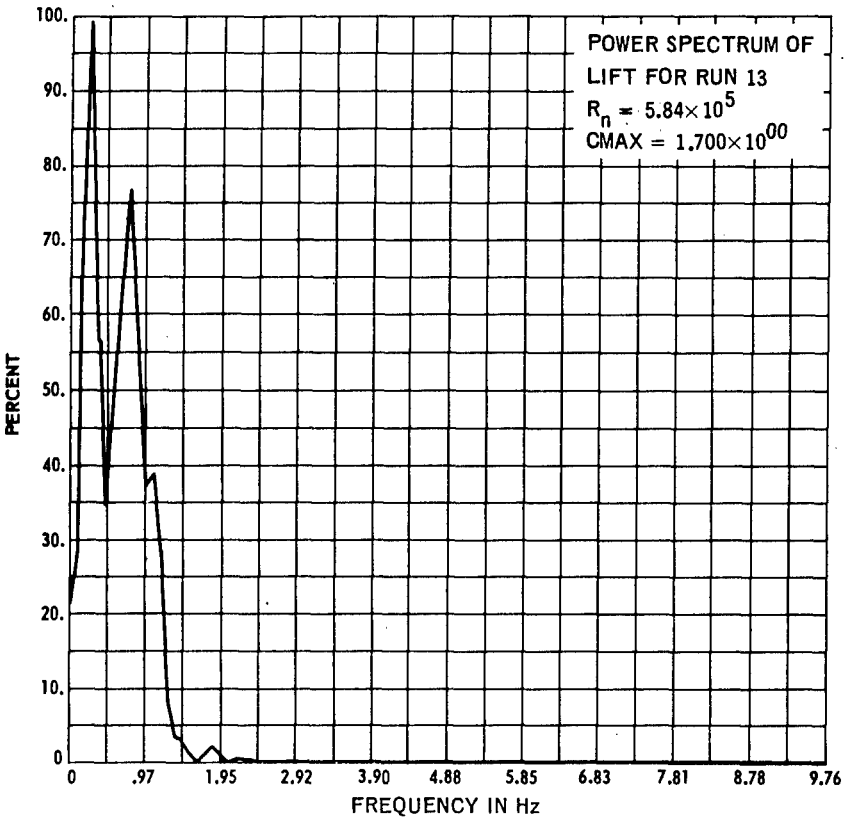
POWER SPECTRUM OF
LIFT FOR RUN 13
$R_n = 5.84\times10^5$
CMAX = 1.700×10^{00}
PERCENT
100.
90.
80.
70.
60.
50.
40.
30.
20.
10.
0
0
.97
1.95
2.92
3.90
4.88
5.85
6.83
7.81
8.78
9.76
FREQUENCY IN Hz

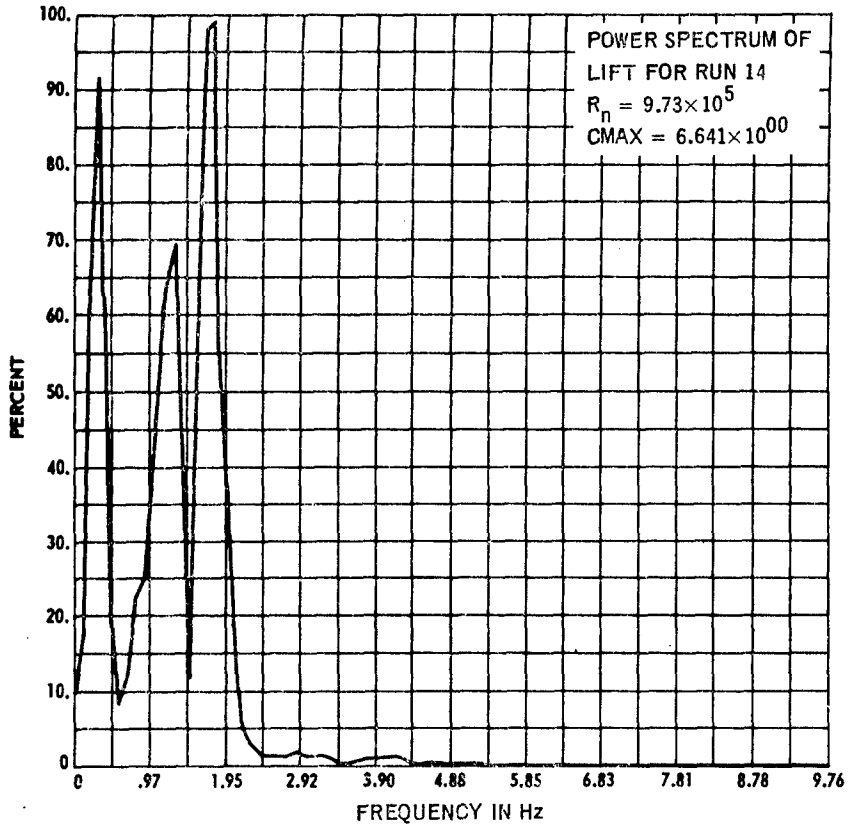
POWER SPECTRUM OF
LIFT FOR RUN 14
$R_n = 9.73\times10^5$
CMAX = 6.641×10^{00}
PERCENT
100.
90.
80.
70.
60.
50.
40.
30.
20.
10.
0
0
.97
1.95
2.92
3.90
4.88
5.85
6.83
7.81
8.78
9.76
FREQUENCY IN Hz

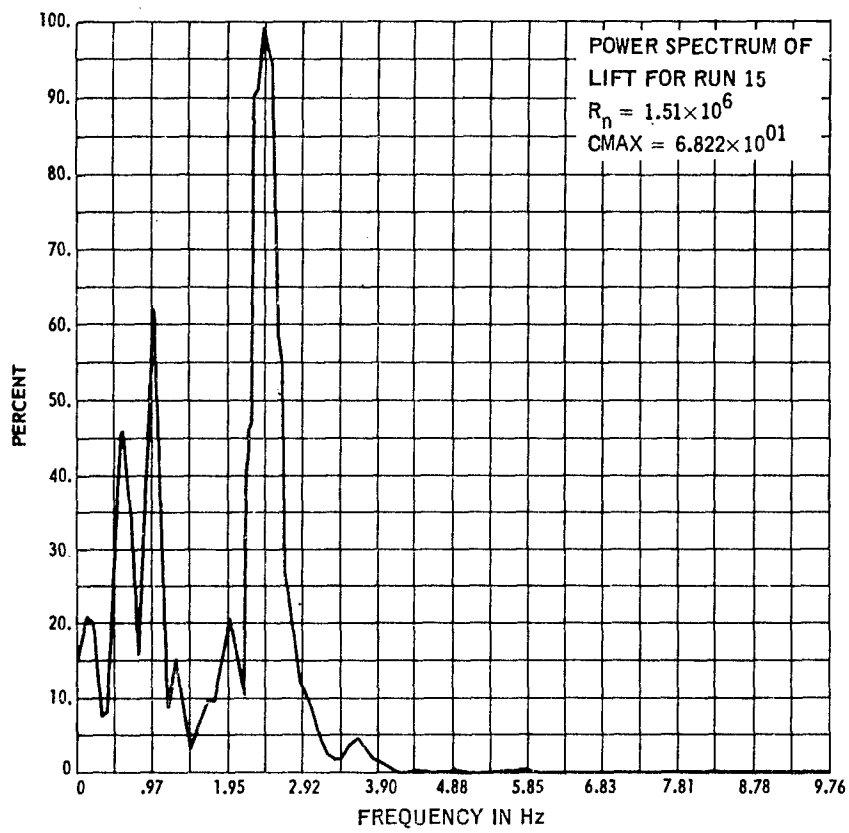
POWER SPECTRUM OF
LIFT FOR RUN 15
$R_n = 1.51\times10^6$
CMAX = 6.822×10^{01}
PERCENT
100.
90.
80.
70.
60.
50.
40.
30.
20.
10.
0
0
.97
1.95
2.92
3.90
4.88
5.85
6.83
7.81
8.78
9.76
FREQUENCY IN Hz

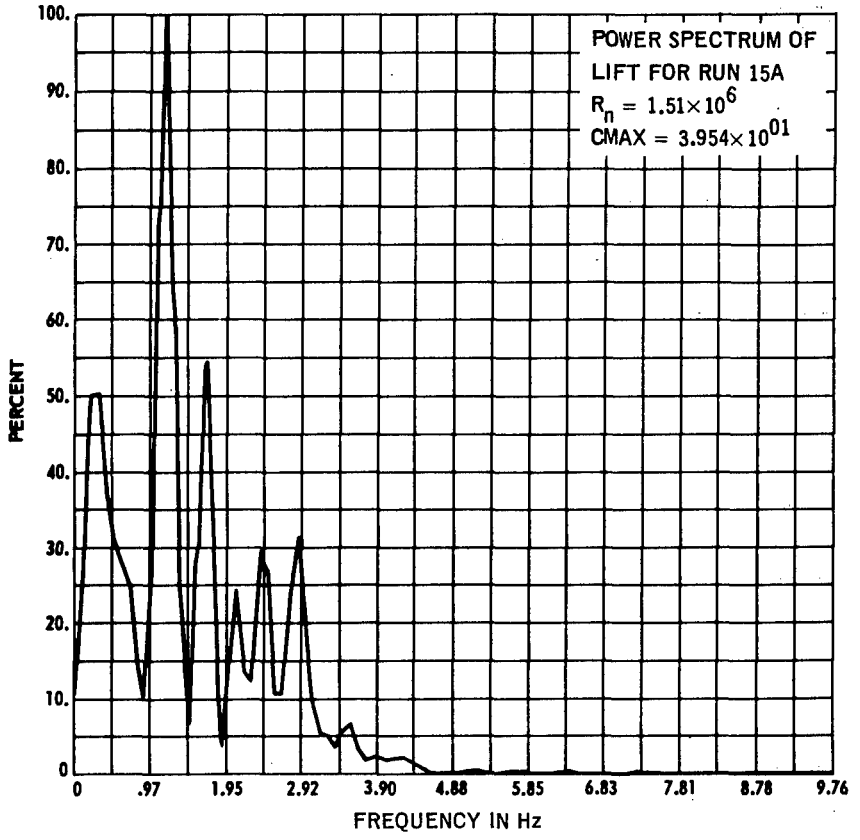
POWER SPECTRUM OF
LIFT FOR RUN 15A
$R_n = 1.51\times10^{6}$
CMAX = 3.954×10^{01}
PERCENT
100.
90.
80.
70.
60.
50.
40.
30.
20.
10.
0
0
.97
1.95
2.92
3.90
4.88
5.85
6.83
7.81
8.78
9.76
FREQUENCY IN Hz

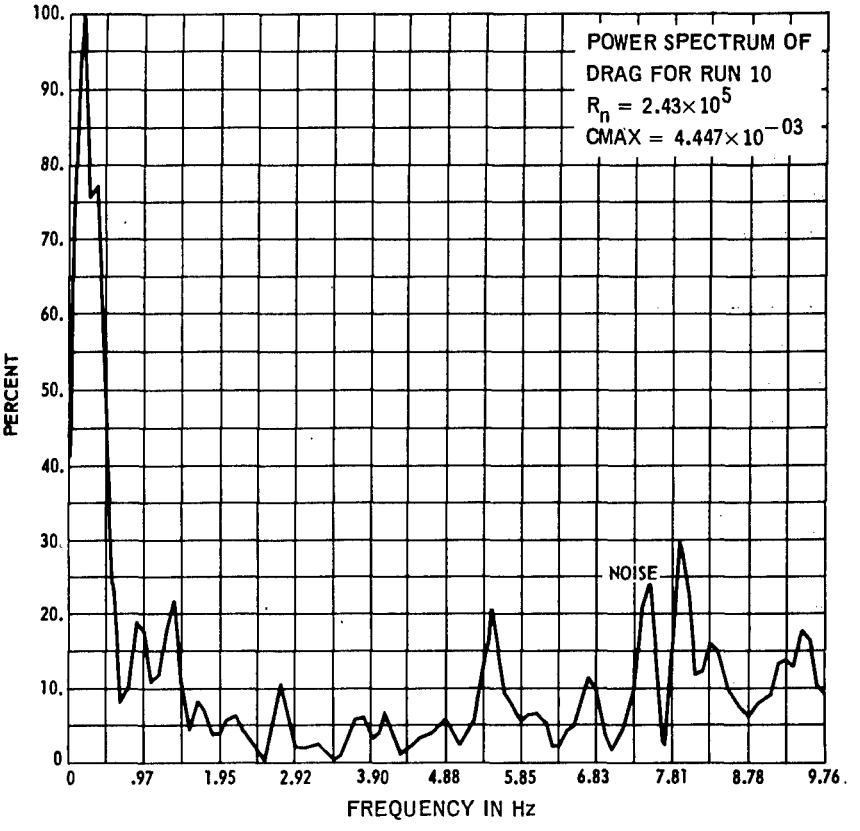
POWER SPECTRUM OF
DRAG FOR RUN 10
$R_n = 2.43\times10^{5}$
CMAX = 4.447×10^{-03}
NOISE
PERCENT
100.
90.
80.
70.
60.
50.
40.
30.
20.
10.
0
0
.97
1.95
2.92
3.90
4.88
5.85
6.83
7.81
8.78
9.76
FREQUENCY IN Hz

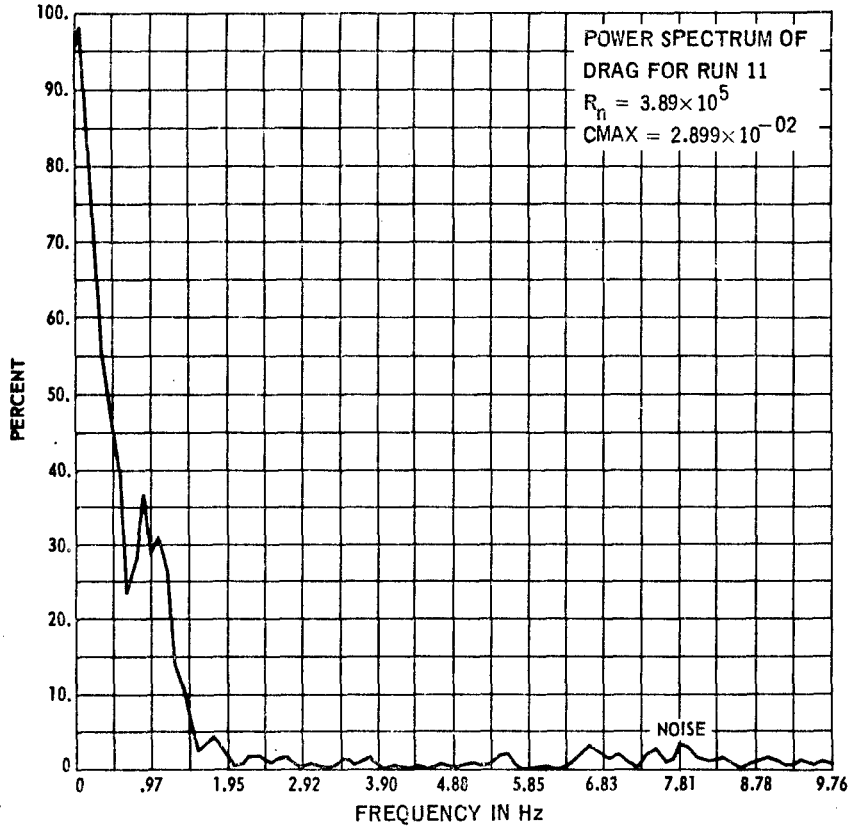
POWER SPECTRUM OF
DRAG FOR RUN 11
$R_n = 3.89 \times 10^5$
CMAX = 2.899×10^{-02}
PERCENT
100.
90.
80.
70.
60.
50.
40.
30.
20.
10.
0
NOISE
0
.97
1.95
2.92
3.90
4.88
5.85
6.83
7.81
8.78
9.76
FREQUENCY IN Hz

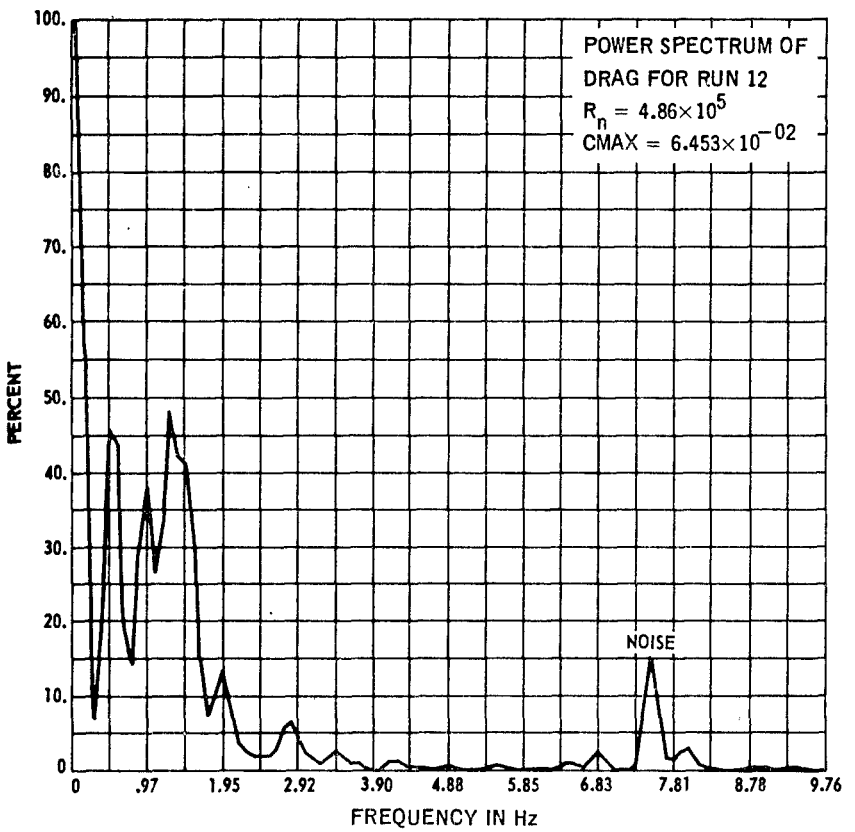
POWER SPECTRUM OF
DRAG FOR RUN 12
$R_n = 4.86 \times 10^5$
CMAX = 6.453×10^{-02}
PERCENT
100.
90.
80.
70.
60.
50.
40.
30.
20.
10.
0
NOISE
0
.97
1.95
2.92
3.90
4.88
5.85
6.83
7.81
8.78
9.76
FREQUENCY IN Hz

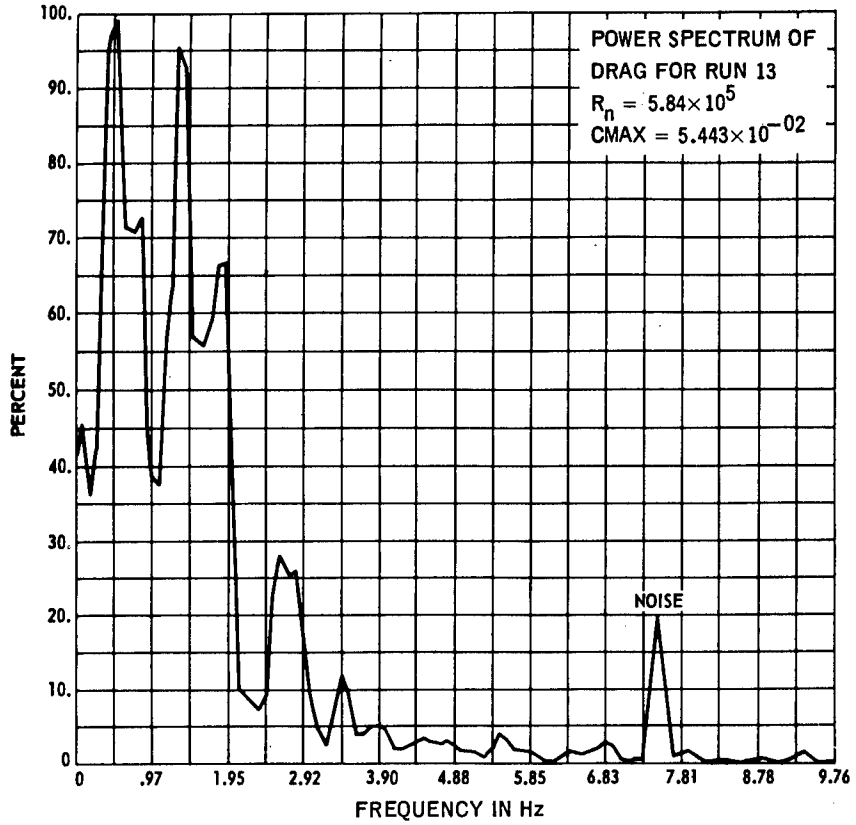
POWER SPECTRUM OF
DRAG FOR RUN 13
$R_n = 5.84\times10^{5}$
CMAX = 5.443×10^{-02}
PERCENT
100.
90.
80.
70.
60.
50.
40.
30.
20.
10.
0
NOISE
0
.97
1.95
2.92
3.90
4.88
5.85
6.83
7.81
8.78
9.76
FREQUENCY IN Hz

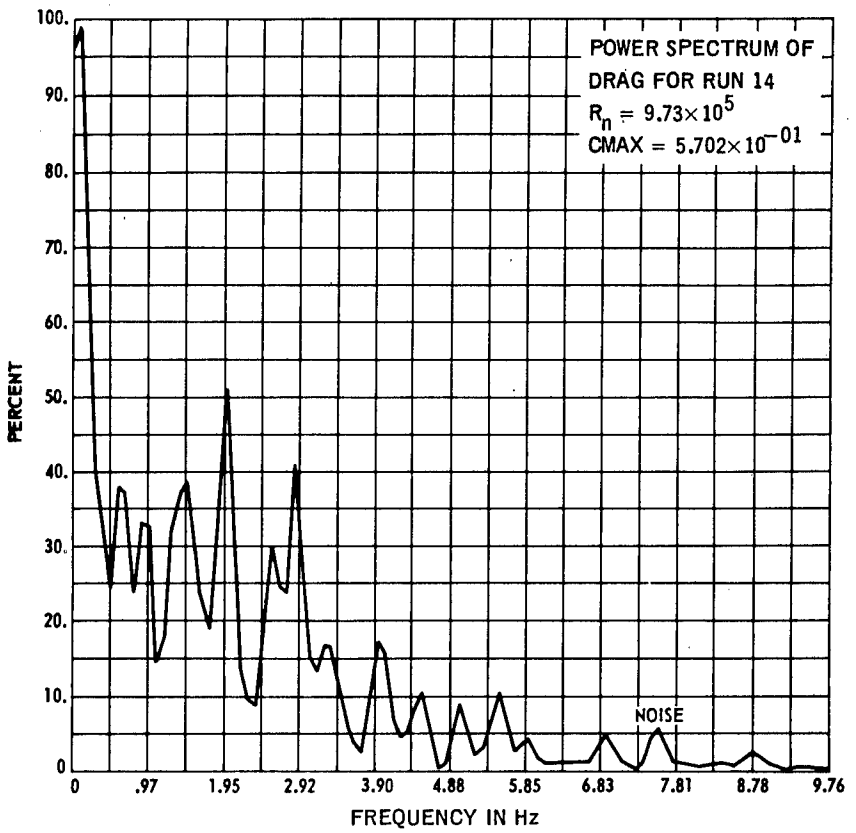
POWER SPECTRUM OF
DRAG FOR RUN 14
$R_n = 9.73\times10^{5}$
CMAX = 5.702×10^{-01}
PERCENT
100.
90.
80.
70.
60.
50.
40.
30.
20.
10.
0
NOISE
0
.97
1.95
2.92
3.90
4.88
5.85
6.83
7.81
8.78
9.76
FREQUENCY IN Hz

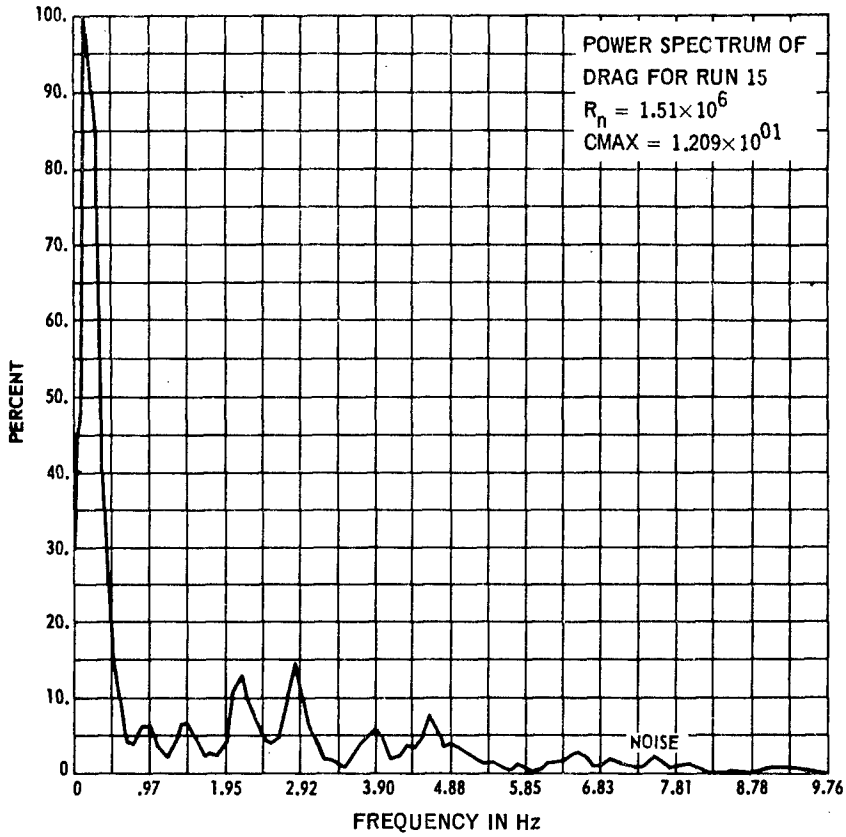
POWER SPECTRUM OF
DRAG FOR RUN 15
$R_n = 1.51\times10^6$
CMAX = 1.209×10^{01}
NOISE
PERCENT
100.
90.
80.
70.
60.
50.
40.
30.
20.
10.
0
0
.97
1.95
2.92
3.90
4.88
5.85
6.83
7.81
8.78
9.76
FREQUENCY IN Hz

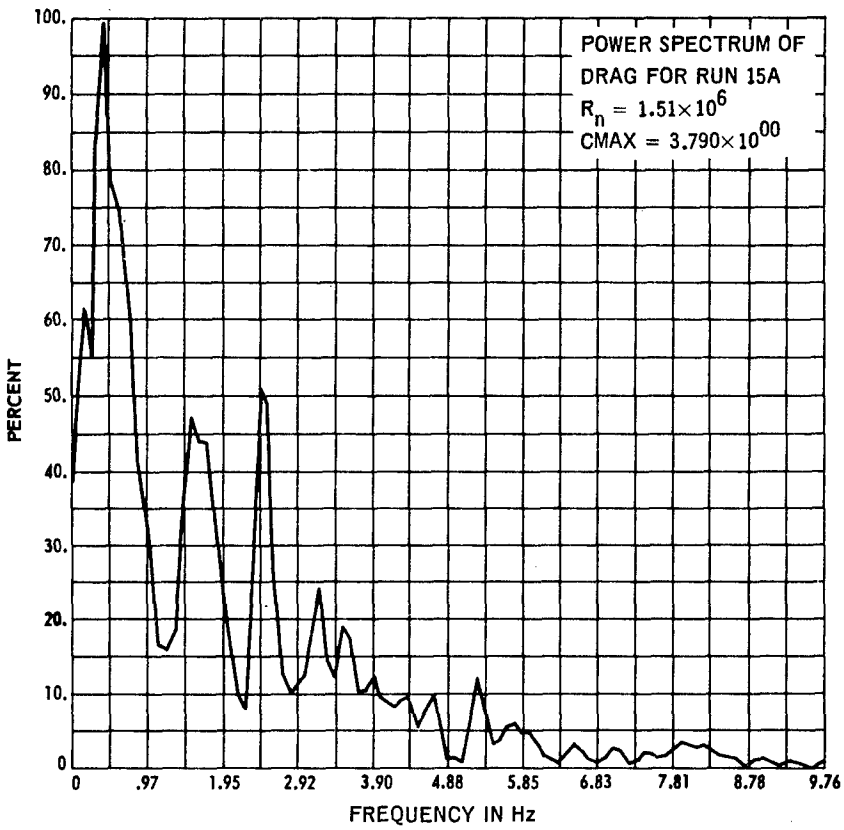
POWER SPECTRUM OF
DRAG FOR RUN 15A
$R_n = 1.51\times10^6$
CMAX = 3.790×10^{00}
PERCENT
100.
90.
80.
70.
60.
50.
40.
30.
20.
10.
0
0
.97
1.95
2.92
3.90
4.88
5.85
6.83
7.81
8.78
9.76
FREQUENCY IN Hz

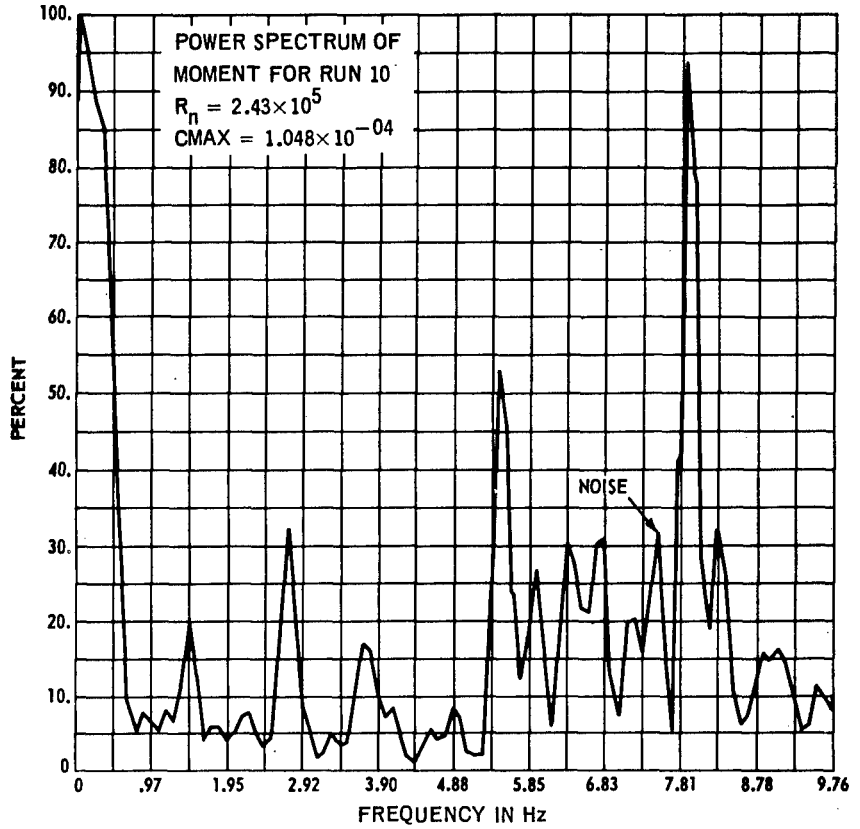
POWER SPECTRUM OF
MOMENT FOR RUN 10
$R_n = 2.43\times10^{5}$
CMAX = 1.048×10^{-04}
NOISE
PERCENT
100.
90.
80.
70.
60.
50.
40.
30.
20.
10.
0
0
.97
1.95
2.92
3.90
4.88
5.85
6.83
7.81
8.78
9.76
FREQUENCY IN Hz

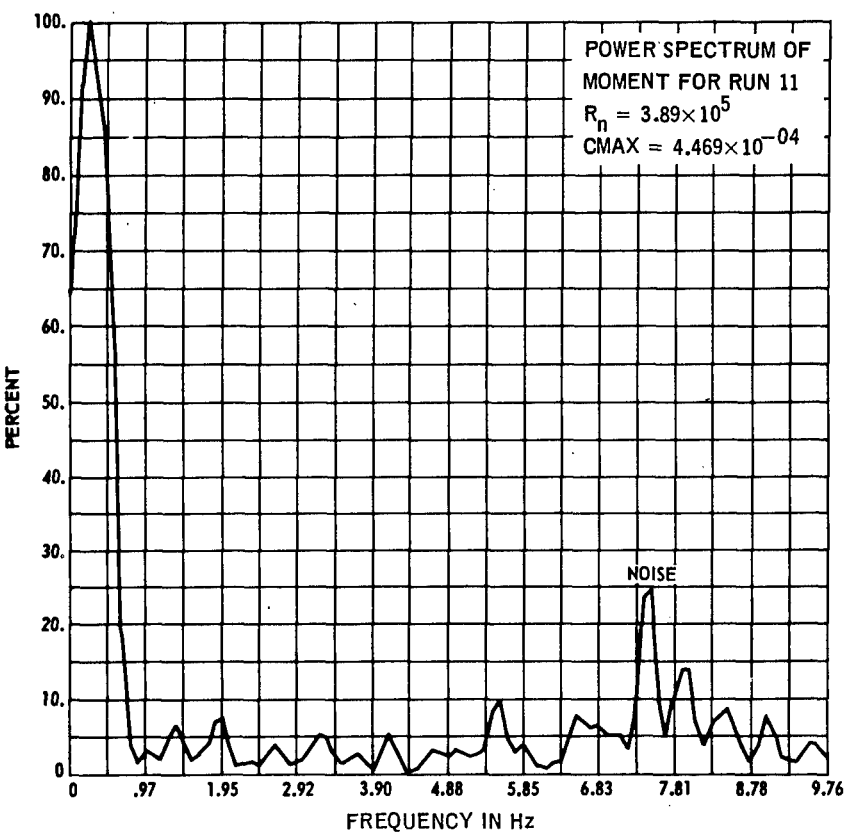
POWER SPECTRUM OF
MOMENT FOR RUN 11
$R_n = 3.89\times10^{5}$
CMAX = 4.469×10^{-04}
NOISE
PERCENT
100.
90.
80.
70.
60.
50.
40.
30.
20.
10.
0
0
.97
1.95
2.92
3.90
4.88
5.85
6.83
7.81
8.78
9.76
FREQUENCY IN Hz

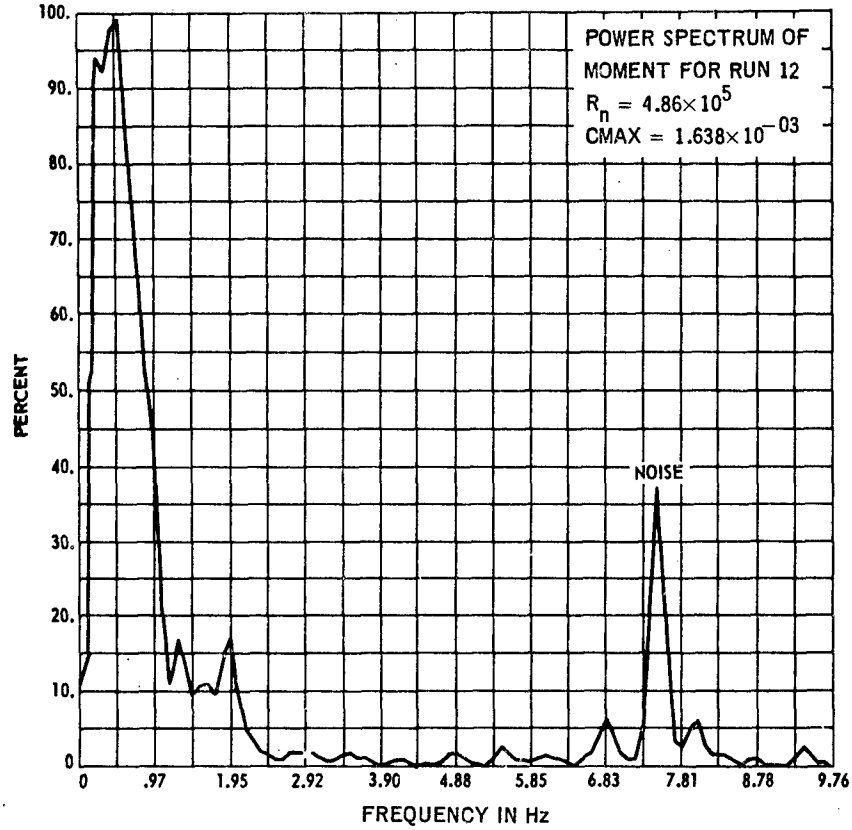
POWER SPECTRUM OF
MOMENT FOR RUN 12
$R_n = 4.86\times10^5$
CMAX = 1.638×10^{-03}
NOISE
PERCENT
100.
90.
80.
70.
60.
50.
40.
30.
20.
10.
0
0
.97
1.95
2.92
3.90
4.88
5.85
6.83
7.81
8.78
9.76
FREQUENCY IN Hz

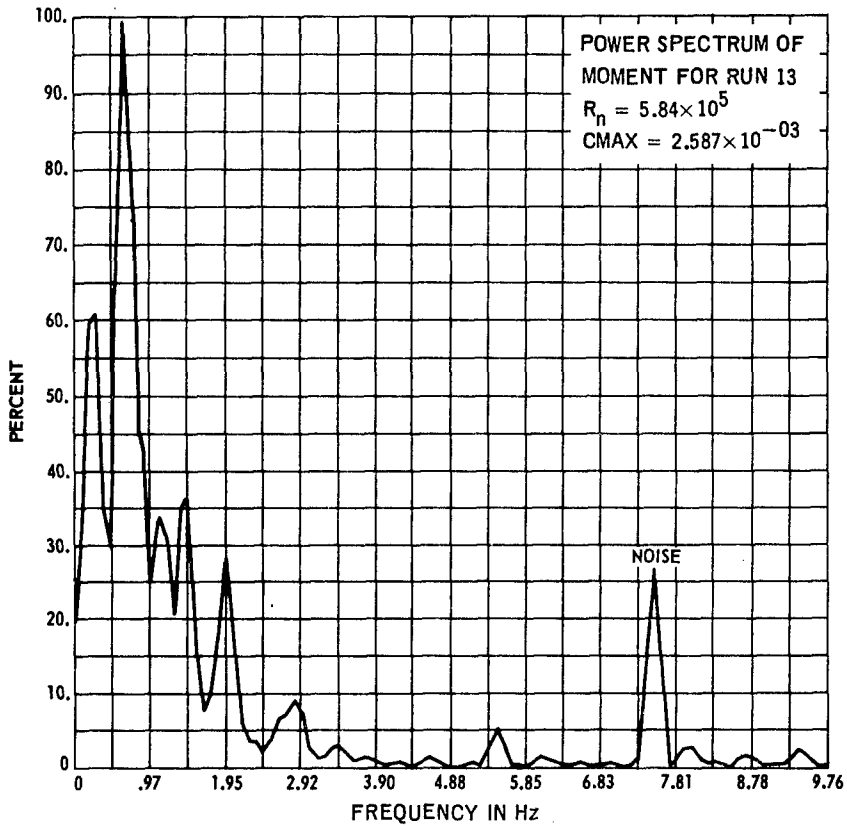
POWER SPECTRUM OF
MOMENT FOR RUN 13
$R_n = 5.84\times10^5$
CMAX = 2.587×10^{-03}
NOISE
PERCENT
100.
90.
80.
70.
60.
50.
40.
30.
20.
10.
0
0
.97
1.95
2.92
3.90
4.88
5.85
6.83
7.81
8.78
9.76
FREQUENCY IN Hz

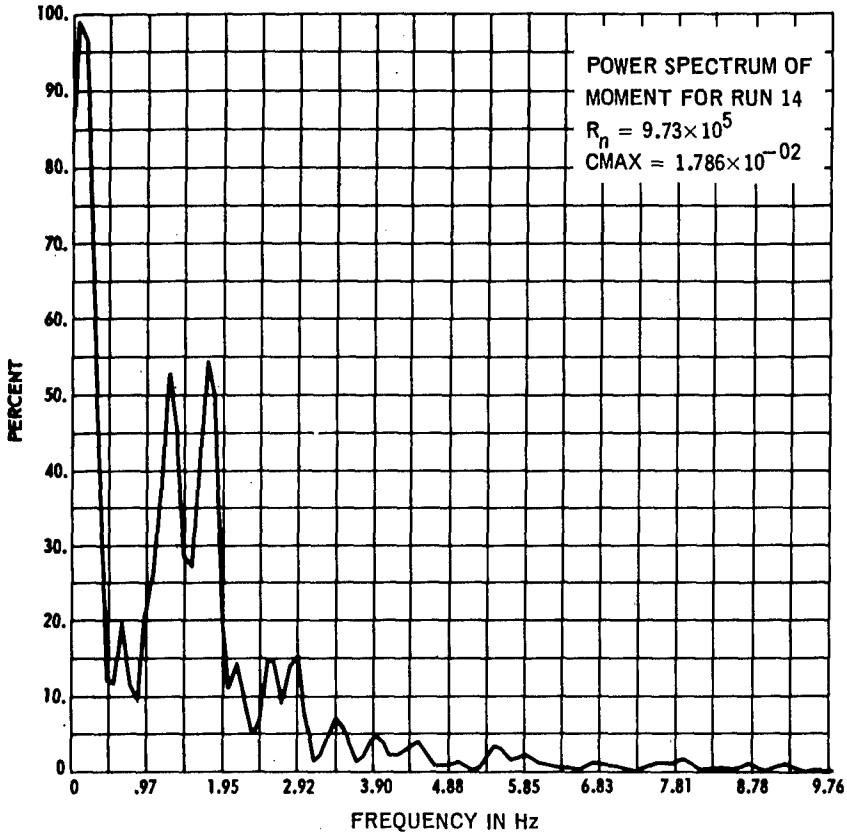
POWER SPECTRUM OF
MOMENT FOR RUN 14
$R_n = 9.73\times10^{5}$
CMAX = 1.786×10^{-02}
PERCENT
100.
90.
80.
70.
60.
50.
40.
30.
20.
10.
0
0
.97
1.95
2.92
3.90
4.88
5.85
6.83
7.81
8.78
9.76
FREQUENCY IN Hz

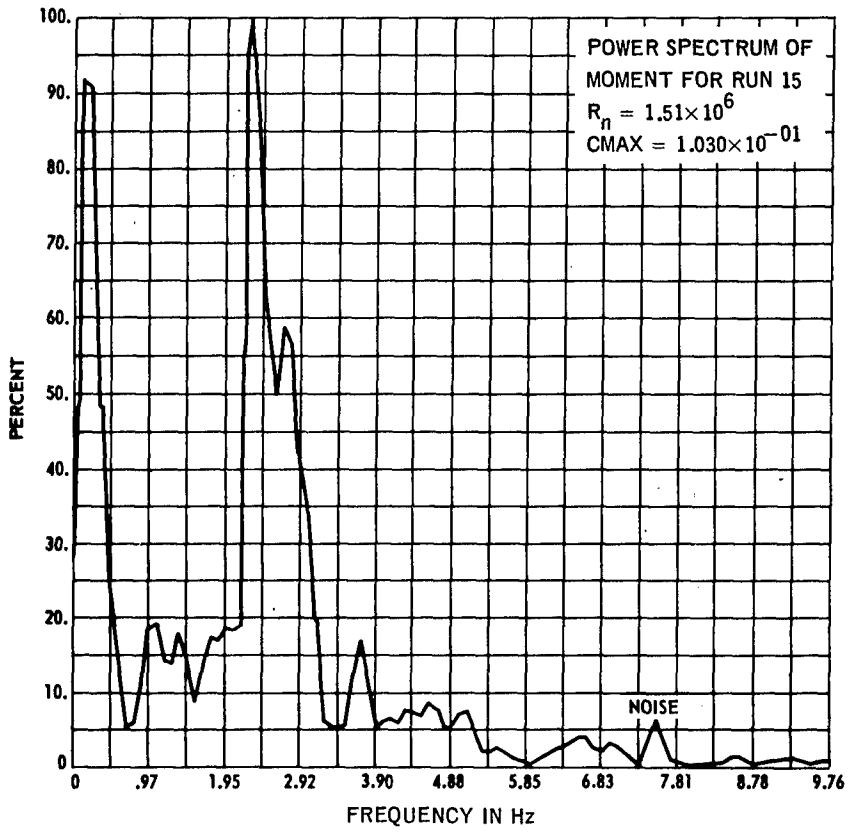
POWER SPECTRUM OF
MOMENT FOR RUN 15
$R_n = 1.51\times10^{6}$
CMAX = 1.030×10^{-01}
NOISE
PERCENT
100.
90.
80.
70.
60.
50.
40.
30.
20.
10.
0
0
.97
1.95
2.92
3.90
4.88
5.85
6.83
7.81
8.78
9.76
FREQUENCY IN Hz

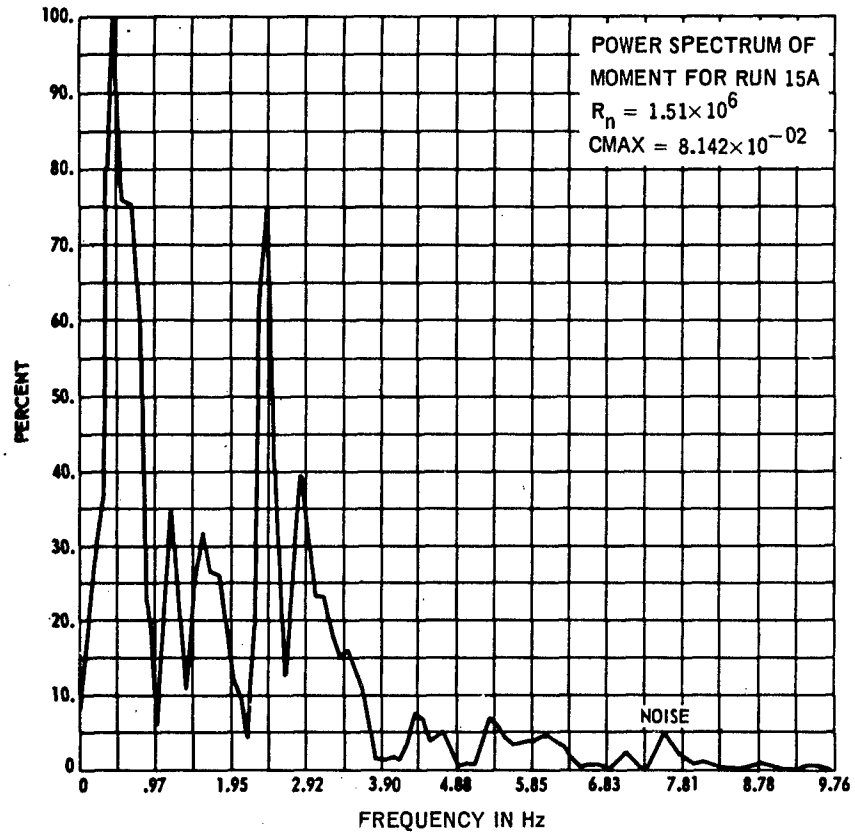
POWER SPECTRUM OF
MOMENT FOR RUN 15A
$R_n = 1.51\times10^{6}$
CMAX = 8.142×10^{-02}
PERCENT
100.
90.
80.
70.
60.
50.
40.
30.
20.
10.
0
NOISE
0
.97
1.95
2.92
3.90
4.88
5.85
6.83
7.81
8.78
9.76
FREQUENCY IN Hz

APPENDIX B

LIFT, DRAG, AND MOMENT COEFFICIENTS FOR THE NONOSCILLATING CYLINDER

$R_n \times 10^5$	$(C_L)_{p-p}$	$(C_L)_{p-p/c}$	$(C_L)_{p-p/s}$	$(C_L)_{rms}$	$(C_L)_{rms/c}$	$(C_D)_{ave}$
1.46	0.662(1)*	3.424	0.533	0.234(1)	0.480	---
1.95	0.388(1)	1.801	0.400	0.137(1)	0.265	---
2.43	0.135(2)	1.102	0.192	0.0365(2)	0.158	---
3.89	0.210(2)	0.583	0.125	0.0682(2)	0.0901	0.5707
4.86	0.573(2)	0.689	0.160	0.134(2)	0.1300	0.6326
5.84	0.493(4)	0.634	0.133	0.0920(4)	0.0964	0.6344
9.73	0.410(6)	0.440	0.160	0.0747(6)	0.0748	0.6875
15.10	0.707(8)	0.592	0.087	0.0998(8)	0.1024	0.6461
15.10	0.575(9)	0.435	0.097	0.0768(9)	0.0762	0.6237

*Numbers in parenthesis refer to number of components considered.

$(C_D)_{p-p}$	$(C_D)_{p-p/c}$	$(C_D)_{rms}$	$(C_D)_{rms/c}$	$(C_M)_{p-p} \times 10^3$	$(C_M)_{rms} \times 10^3$
---	---	---	---	---	---
---	---	---	---	---	---
---	---	---	---	---	---
0.122(3)	0.609	0.0265(3)	0.0802	0.686(1)	0.243(1)
0.162(5)	0.178	0.0265(5)	0.0534	1.690(3)	0.371(3)
0.180(7)	0.297	0.0250(7)	0.0391	1.987(5)	0.324(5)
0.207(9)	0.202	0.0253(9)	0.0315	2.386(8)	0.334(8)
0.234(9)	0.268	0.0320(9)	0.0391	2.912(9)	0.379(9)
0.199(7)	0.275	0.0286(7)	0.0367	2.360(8)	0.326(8)

$R_n \times 10^5$	S_{Li}	C_{Li}
1.46	0.195	0.331
1.95	0.195	0.194
2.43	0.234	0.0477
	0.000	0.0197
3.89	0.073	0.0960
	0.293	0.0090
4.86	0.137	0.140
	0.078	0.128
5.84	0.130	0.0849
	0.049	0.0827
	0.179	0.0523
	0.309	0.0120
9.73	0.176	0.0634
	0.127	0.0631
	0.029	0.0543
	0.283	0.0093
	0.322	0.0076
	0.410	0.0071
15.10	0.158	0.0970
	0.063	0.0561
	0.038	0.0537
	0.126	0.0379
	0.006	0.0361
	0.082	0.0267
	0.108	0.0243
	0.234	0.0216
15.10	0.076	0.0587
	0.019	0.0573
	0.107	0.0382
	0.183	0.0362
	0.151	0.0322
	0.133	0.0281
	0.227	0.0159
	0.271	0.0110
	0.246	0.0102

$R_n \times 10^5$	S_{Di}	C_{Di}
3.89	0.024	0.0309
	0.2686	0.0152
	0.2197	0.0150
4.86	0.0195	0.0212
	0.2539	0.0204
	0.0977	0.0162
	0.1953	0.0138
	0.3906	0.0093
5.84	0.098	0.0186
	0.228	0.0180
	0.326	0.0147
	0.147	0.0124
	0.016	0.0093
	0.440	0.0081
	0.472	0.0078
9.73	0.010	0.0186
	0.147	0.0143
	0.195	0.0128
	0.283	0.0111
	0.059	0.0109
	0.254	0.0100
	0.089	0.0100
	0.332	0.0082
	0.391	0.0072
15.10	0.013	0.0338
	0.183	0.0146
	0.139	0.0141
	0.297	0.0098
	0.253	0.0097
	0.095	0.0097
	0.316	0.0094
	0.063	0.0091
	0.278	0.0068
15.10	0.032	0.0254
	0.101	0.0182
	0.013	0.0146
	0.158	0.0142
	0.208	0.0109
	0.252	0.0082
	0.227	0.0082

$R_n \times 10^5$	S_{Mi}	$C_{Mi} \times 10^3$
3.89	0.073	0.343
4.86	0.117	0.417
	0.059	0.285
	0.391	0.143
5.84	0.114	0.283
	0.049	0.233
	0.244	0.164
	0.179	0.161
	0.326	0.154
9.73	0.010	0.290
	0.127	0.228
	0.176	0.207
	0.068	0.105
	0.254	0.102
	0.293	0.098
	0.215	0.091
	0.342	0.073
15.10	0.152	0.286
	0.013	0.273
	0.177	0.242
	0.070	0.137
	0.114	0.110
	0.240	0.109
	0.089	0.108
	0.126	0.107
	0.329	0.086
15.10	0.032	0.290
	0.158	0.189
	0.183	0.178
	0.101	0.166
	0.076	0.125
	0.221	0.105
	0.341	0.065
	0.278	0.063

APPENDIX C

LIFT, DRAG, AND MOMENT COEFFICIENTS FOR CYLINDER OSCILLATING IN HEAVE

STROUHAL NUMBER OF FORCED OSCILLATION (S_f)												
$R_n \times 10^5$		0.00	0.02	0.10	0.15	0.18	0.20	0.22	0.25	0.30	0.40	1.00
1.95	$(C_L)_{p-p}$	0.3880(1)*		0.2062(1)	0.1220(2)	0.6156(1)	0.6936(3)	0.5272(3)	0.4244(2)			
	$(C_L)_{rms}$	0.1372(1)		0.07289(1)	0.02189(2)	0.3253(1)	0.2261(3)	0.1980(3)	0.1591(2)			
	$(C_D)_{ave}$	0.6946		0.8490	0.9185	0.9799	0.9234	0.9237	0.9283	0.9441	0.9044	0.6781
4.86	$(C_L)_{p-p}$	0.573(2)			0.2974(4)	0.4948(3)	0.5962(5)	0.4726(4)	0.4244(4)			
	$(C_L)_{rms}$	0.134(2)			0.0861(4)	0.1654(3)	0.1393(5)	0.1554(4)	0.1591(4)			
	$(C_D)_{ave}$	0.6326			0.5044	0.4872	0.4786	0.4782	0.4891			
	$(C_D)_{p-p}$	0.196(6)			0.1699(10)	0.1892(10)	0.1669(10)	0.1289(8)	0.1273(9)			
	$(C_D)_{rms}$	0.0291(6)			0.02126(10)	0.02542(10)	0.02272(10)	0.01845(8)	0.1660(9)			
	$(C_M)_{p-p} \times 10^3$	1.6900(3)			1.8152(8)	2.2774(10)	1.2068(7)	2.6596(8)	2.9410(7)			
	$(C_M)_{rms} \times 10^3$	0.3712(3)			0.2516(8)	0.2729(10)	0.1424(7)	0.3722(8)	0.4897(7)			
9.73	$(C_L)_{p-p}$	0.410(6)		0.3224(4)	0.3246(4)	0.3946(5)	0.5148(4)	0.4884(3)	0.5510(4)			
	$(C_L)_{rms}$	0.0747(6)		0.0732(4)	0.0667(4)	0.0829(5)	0.1548(4)	0.1866(3)	0.1777(4)			
	$(C_D)_{ave}$	0.6875		0.5582	0.5659	0.6055	0.5804	0.5603	0.5662			
	$(C_D)_{p-p}$	0.207(9)		0.1516(12)	0.2218(15)	0.2614(15)	0.1967(16)	0.2426(14)	0.1920(16)			
	$(C_D)_{rms}$	0.0253(9)		0.01982(12)	0.02647(15)	0.02786(15)	0.02105(16)	0.02622(14)	0.01880(16)			
	$(C_M)_{p-p} \times 10^3$	2.3880(8)		1.6794(9)	1.845(9)	1.8908(7)	1.4916(8)	2.2724(9)	1.7348(6)			
	$(C_M)_{rms} \times 10^3$	0.3343(8)		0.2332(9)	0.2482(9)	0.2766(7)	0.2088(8)	0.3229(9)	0.2918(6)			

*Numbers in parenthesis refer to number of components considered.

$R_n \times 10^5$		0.00		0.02	0.10		
1.95	C_{Li} & S_{Li}	0.194	0.1953		0.1031	0.1709	0 0
	Lift Interaction Subtracted Out	0.0	0.0		0	0.10	0
4.86	C_{Li} & S_{Li}	0.140 0.128	0.137 0.078				0 0 0 0
	Lift Interaction Subtracted Out	0.0	0.0				0
4.86	C_{Di} & S_{Di}	0.0212 0.0204 0.0172 0.0162 0.0138 0.0093	0.0195 0.2539 3.691 0.0977 0.1953 0.3906				0 0 0 0 0 0 0 0 0 0
	Drag Interaction Subtracted Out	0.0	0.0				0
4.86	$C_{Mi} \times 10^3$ & S_{Mi}	0.417 0.285 0.143	0.117 0.059 0.391				0 0 0 0 0 0 0 0
	Moment Interaction Subtracted Out	0.0	0.0				0

STROUHAL NUMBER OF FORCED OSCILLATION (S_f)

	0.00		0.02	0.10		0.15		0.18		0.20		
	0.194	0.1953		0.1031	0.1709	0.1597	0.1465	0.4978	0.1709	0.3606	0.1953	0
						0.0313	0.0244			0.1361	0.0244	0
										0.0801	0.0977	0
ion t	0.0	0.0		0	0.10	0.130	0.15	0.190	0.18	0.230	0.20	0
	0.140	0.137				0.1651	0.1465	0.2794	0.1758	0.2713	0.1953	0
	0.128	0.078				0.0488	0.0781	0.0915	0.0977	0.0977	0.1563	0
						0.0343	0.0488	0.0665	0.0391	0.0632	0.1074	0
						0.0305	0.0195			0.0494	0.0684	0
										0.0465	0.0098	
ion t	0.0	0.0				0.130	0.15	0.190	0.18	0.230	0.20	0
	0.0212	0.0195				0.01721	0.1367	0.02490	0.0098	0.02287	0.0293	0
	0.0204	0.2539				0.01254	0.0098	0.01227	0.1270	0.01321	0.1172	0
	0.0172	3.691				0.01118	0.3223	0.01214	0.2148	0.01063	0.2246	0
	0.0162	0.0977				0.00812	0.1855	0.01096	0.3027	0.00990	0.3125	0
	0.0138	0.1953				0.00804	0.2246	0.00977	0.3613	0.00847	0.3809	0
	0.0093	0.3906				0.00761	0.0781	0.00956	0.1855	0.00712	0.1563	0
						0.00743	0.0391	0.00783	0.0879	0.00627	1.5918	0
						0.00653	0.3711	0.00645	1.5918	0.00619	1.4941	0
						0.00640	1.5918	0.00512	1.0938	0.00515	0.2637	
						0.00618	1.4941	0.00471	1.6211	0.00483	0.4297	
ion t	0.0	0.0				0.0063	0.15	0.0091	0.18	0.0112	0.20	0
Mi	0.417	0.117				0.1949	0.1367	0.1849	1.5918	0.1496	1.5918	0
	0.285	0.059				0.1607	1.5918	0.1564	0.0098	0.1315	0.0586	0
	0.143	0.391				0.1376	0.0488	0.1396	0.2051	0.1296	0.0977	0
						0.1241	1.4941	0.1351	0.0879	0.1253	1.4941	0
						0.1149	1.3672	0.1346	0.1270	0.1187	0.1953	0
						0.1071	1.6211	0.1322	1.6211	0.1053	0.0098	0
						0.0896	0.3027	0.1160	1.3867	0.1030	1.6211	0
						0.0879	0.0098	0.1070	1.0938			0
								0.1009	0.488			
								0.0988	0.1563			
ction t	0.0	0.0				0.1092	0.150	0.1668	0.180	0.2596	0.200	0

2

OSCILLATION (S_f)

	0.20		0.22		0.25		0.30		0.40		1.00	
9	0.3606	0.1953	0.3773	0.2197	0.4246	0.2441	0.5289	0.2930	0.8587	0.3906	5.753	0.9766
	0.1361	0.0244	0.1218	0.0244	0.2519	0.1709	0.2526	0.1709	0.1834	0.1709		
	0.0801	0.0977	0.0495	0.3662								
	0.230	0.20	0.285	0.22	0.360	0.25	0.5289	0.30	0.8587	0.40	5.753	1.0
8	0.2713	0.1953	0.3440	0.2148	0.4146	0.2441						
7	0.0977	0.1563	0.0788	0.0977	0.0586	0.0684						
1	0.0632	0.1074	0.0581	0.0391	0.0512	0.0879						
	0.0494	0.0684	0.0404	0.1563	0.0478	0.1172						
	0.0465	0.0098										
	0.230	0.20	0.285	0.22	0.360	0.25						
8	0.02287	0.0293	0.01487	0.0391	0.01358	0.1270						
0	0.01321	0.1172	0.01485	0.1367	0.01357	0.1758						
8	0.01063	0.2246	0.01123	0.2344	0.01282	0.0098						
7	0.00990	0.3125	0.00999	0.3125	0.01193	0.2539						
3	0.00847	0.3809	0.00992	0.4492	0.00779	0.2930						
5	0.00712	0.1563	0.00641	1.5820	0.00634	0.3613						
9	0.00627	1.5918	0.00556	0.3906	0.00520	0.4297						
8	0.00619	1.4941	0.00524	0.6055	0.00490	1.5918						
8	0.00515	0.2637			0.00482	0.4688						
1	0.00483	0.4297										
	0.0112	0.20	0.0136	0.22	0.0173	0.25						
8	0.1496	1.5918	0.3048	0.0586	0.5285	0.2441						
8	0.1315	0.0586	0.2991	0.2148	0.3816	0.0488						
1	0.1296	0.0977	0.2142	0.3711	0.2091	0.0098						
9	0.1253	1.4941	0.2061	1.5820	0.1818	0.3711						
0	0.1187	0.1953	0.1597	0.2930	0.1722	0.4980						
1	0.1053	0.0098	0.1555	1.3086	0.1608	0.0977						
7	0.1030	1.6211	0.1478	0.4492	0.1553	0.7520						
8			0.1284	0.5273								
3												
	0.2596	0.200	0.2856	0.220	0.3188	0.2500						

STROUHAL NUMBER OF FORCED OSCILLATION (S_f)																	
$R_n \times 10^5$		0.00		0.02		0.10		0.15		0.18		0.20		0.22		0.25	
9.73	C_{Li} & S_{Li}	0.0634	0.176	--	--	0.07113	0.1758	0.1293	0.1465	0.2017	0.1758	0.2950	0.1953	0.3722	0.2148	0.4212	0.2441
		0.0631	0.127			0.07082	0.1172	0.06616	0.0586	0.05932	0.1465	0.08595	0.0391	0.08393	0.0781	0.07759	0.0586
		0.0543	0.029			0.06138	0.0586	0.05067	0.1172	0.05122	0.0488	0.07316	0.1172	0.07310	0.1563	0.07008	0.0195
		0.0093	0.283			0.01594	0.2930	0.04608	0.0293	0.04775	0.0781	0.03316	0.1563			0.06661	0.1465
		0.0076	0.322							0.02730	0.0195						
		0.0071	0.410														
	Lift Interaction Subtracted Out	0.0	0.0			0.0	0.10	0.130	0.15	0.190	0.18	0.230	0.20	0.285	0.22	0.360	0.25
	C_{Di} & S_{Di}	0.0186	0.010	--	--	0.01766	0.0195	0.02426	0.0684	0.01724	0.1758	0.01741	0.0684	0.01838	0.0195	0.01627	0.0586
		0.0146	0.0147			0.01406	0.1367	0.01656	0.1465	0.01645	0.0098	0.01176	0.0977	0.01384	0.0488	0.01158	0.1172
		0.0128	0.195			0.00990	0.2734	0.01499	0.0098	0.01625	0.0488	0.01079	0.1855	0.01377	0.2344	0.00985	0.2441
		0.011	0.283			0.00796	0.2148	0.00827	0.3320	0.01383	0.0977	0.00906	0.2246	0.01345	0.1172	0.00951	0.2051
		0.0109	0.059			0.00710	0.4492	0.00774	0.2148	0.01381	0.1953	0.00906	0.4004	0.01197	0.2051	0.00915	0.1465
		0.0100	0.254			0.00411	0.3906	0.00731	0.2539	0.00978	0.2637	0.00796	0.0098	0.01138	0.1465	0.00834	0.3418
		0.100	0.089			0.00398	0.6055	0.00612	0.4297	0.00820	0.4297	0.00776	0.3418	0.01117	0.2637	0.00764	0.3711
		0.0082	0.332			0.00353	0.7422	0.00582	0.2832	0.00768	0.3125	0.00748	0.3125	0.00826	0.4395	0.00684	0.0195
		0.0072	0.391			0.00301	0.6836	0.00475	0.7324	0.00698	0.3516	0.00585	0.4688	0.00767	0.3223	0.00637	0.2832
						0.00251	0.9961	0.00425	0.5664	0.00568	0.5859	0.00426	0.5469	0.00749	0.3516	0.00601	0.1758
						0.00241	0.5469	0.00394	0.3809	0.00568	0.3809	0.00426	0.2832	0.00555	0.3906	0.00511	0.4980
						0.00237	0.8203	0.00383	0.5273	0.00518	0.5078	0.00333	0.8105	0.00489	0.5664	0.00427	0.4492
								0.00379	0.4688	0.00510	0.4688	0.00318	0.5078	0.00404	0.5078	0.00423	0.5566
								0.00309	0.6836	0.00488	0.6152	0.00286	0.7031	0.00302	0.8008	0.00332	0.7324
								0.00245	0.6152	0.00309	0.6543	0.00233	0.5859			0.00253	0.6543
												0.00220	0.6641			0.00230	0.6250
	Drag Interaction Subtracted Out	0.0	0.0			0.0028	0.10	0.0063	0.15	0.0091	0.18	0.0112	0.20			0.0173	0.25

STROUHAL NUMBER OF FORCED OSCILLATION (S_f)																	
$R_n \times 10^5$		0.00		0.02		0.10		0.15		0.18		0.20		0.22		0.25	
9.73	$C_{Mi} \times 10^3$ & S_{Mi}	0.290	0.10	--	--	0.2064	0.0195	0.2044	0.0586	0.1934	0.0586	0.1660	0.2148	0.3209	0.2148	0.2749	0.2441
		0.228	0.127			0.1439	0.1172	0.1581	0.1465	0.1901	0.1660	0.1417	0.0684	0.1831	0.1758	0.1932	0.1465
		0.207	0.176			0.1291	0.0781	0.1358	0.0293	0.1546	0.1953	0.1254	0.1270	0.1600	0.0195	0.1880	0.0586
		0.105	0.068			0.1102	0.1758	0.1121	0.0977	0.1542	0.0098	0.0960	0.0195	0.1264	0.1270	0.1359	0.1172
		0.102	0.254			0.0801	0.3125	0.1050	0.1855	0.1326	0.0977	0.0904	0.4004	0.1255	0.0879	0.1203	0.2051
		0.098	0.293			0.0714	0.3906	0.0895	0.3320	0.1112	0.3516	0.0875	0.3516	0.1054	0.3516	0.0987	0.2832
		0.091	0.215			0.0707	0.2539	0.0820	0.2539	0.1106	0.2930	0.0823	0.1563	0.0821	0.6543		
		0.073	0.342			0.0523	0.7422	0.0649	0.2832			0.0691	0.4688	0.0782	0.3027		
						0.0405	0.8008	0.0638	0.4980					0.0782	0.2637		
	Moment Interaction Subtracted Out	0.0	0.0			0.0649	0.100	0.0931	0.150	0.1013	0.180	0.1126	0.200	0.1236	0.220	0.1436	0.250

APPENDIX D

LIFT AND DRAG COEFFICIENTS FOR CYLINDER OSCILLATING IN PITCH

		STROUHAL NUMBER OF FORCED OSCILLATION (S_f)							
$R_n \times 10^5$		0.00	0.02	0.10	0.15	0.18	0.20	0.22	0
1.95	$(C_L)_{p-p}$	0.388(1)*	0.2988	0.2358	0.2038	0.3622	0.4212	0.1732	0
	$(C_L)_{rms}$	9.137(1)	0.0809	0.0647	0.0583	0.1280	0.0963	0.0613	0
	$(C_D)_{ave}$	0.6946	0.9363	0.8857	0.9799	1.060	0.9755	0.9249	0
4.86	$(C_L)_{p-p}$	0.573(2)	0.5952(7)	0.5624(7)	0.9892(6)	0.5758(8)	0.5452(6)	0.5158(6)	0
	$(C_L)_{rms}$	0.134(2)	0.0860(7)	0.0812(7)	0.1562(6)	0.0871(8)	0.0986(6)	0.0873(6)	0
	$(C_D)_{ave}$	0.6326	0.6338	0.6260	0.6794	0.6305	0.6370	0.6421	0
	$(C_D)_{p-p}$	0.196	0.1018(8)	0.0774(6)	0.1401(9)	0.0888(8)	0.0936(7)	0.0952(9)	0
	$(C_D)_{rms}$	0.0291(6)	0.02655(8)	0.02388(6)	0.03930(9)	0.02431(8)	0.02809(7)	0.02465(9)	0
9.73	$(C_L)_{p-p}$	0.410(6)	1.1492(14)	0.7428(7)	1.0400(16)	0.9010(13)	0.8996(13)	0.8118(11)	0
	$(C_L)_{rms}$	0.0747(6)	0.1205(14)	0.1917(7)	0.1075(16)	0.0977(13)	0.1004(13)	0.1006(11)	0
	$(C_D)_{ave}$	0.6875	0.7101	0.7151	0.6969	0.7179	0.6777	0.7015	0
	$(C_D)_{p-p}$	0.207(9)	0.2025(19)	0.1333(9)	0.1644(18)	0.1354(14)	0.1329(14)	0.1355(13)	0
	$(C_D)_{rms}$	0.0253(9)	0.03660(19)	0.03703(9)	0.02976(18)	0.02885(14)	0.02774(14)	0.03044(13)	0

*Numbers in parenthesis refer to number of components considered.

LLATION (S_f)							
	0.22	0.25	0.30	0.40	0.80	1.00	2.00
	0.1732	0.2394	0.2060	0.2586		0.5800	0.3830
	0.0613	0.0657	0.5192	0.0561		0.1769	0.1058
	0.9249	0.8418	0.8362	0.9045		1.055	0.8803
)	0.5158(6)	0.6574(5)	0.7170(5)	0.6292(5)	0.6028(5)		
)	0.0873(6)	0.1119(5)	0.1270(5)	0.1114(5)	0.1007(5)		
	0.6421	0.6385	0.6425	0.6604	0.6551		
)	0.0952(9)	0.0852(8)	0.1087(8)	0.0949(8)	0.0675(4)		
7)	0.02465(9)	0.02310(8)	0.02380(8)	0.02618(8)	0.03024(4)		
3)	0.8118(11)	0.7382(11)	0.8414(14)	0.8354(13)			
3)	0.1006(11)	0.0889(11)	0.0987(14)	0.0952(13)			
	0.7015	0.6913	0.6922	0.6939			
4)	0.1355(13)	0.1270(14)	0.1361(15)	0.1342(14)			
14)	0.03044(13)	0.02633(14)	0.02718(15)	0.02885(14)			

											STROU
$R_n \times 10^5$		0.00		0.02		0.10		0.15		0.18	
1.95	C_{Li} & S_{Li}	0.194	0.195	0.1058	0.1953	0.0857	0.1709	0.0793	0.1953	0.1811	0.19
				0.0436	0.0488	0.0322	0	0.0226	0.0244		
4.86	C_{Li} & S_{Li}	0.140	0.137	0.0720	0.0684	0.0711	0.1270	0.1422	0.0781	0.0748	0.06
		0.128	0.078	0.0627	0.1563	0.0533	0.0391	0.0971	0.0293	0.0660	0.12
				0.0440	0.1270	0.0441	0.0879	0.0834	0.1465	0.0474	0.00
				0.0366	0.0391	0.0368	0.1563	0.0801	0.1758	0.0456	0.15
				0.0345	0.1953	0.0289	0	0.0738	0.1270	0.0255	0.18
				0.0309	0.0098	0.0279	0.1855	0.0181	0.2441	0.0108	0.26
				0.0169	0.2539	0.0192	0.2344			0.0097	0.21
										0.0082	0.31
4.86	C_{Di} & S_{Di}	0.0212	0.0195	0.0172	0.1270	0.0195	0.0195	0.0379	0.0098	0.0181	0.05
		0.0204	0.2539	0.0165	0.0977	0.0165	0.0977	0.0278	0.0488	0.0154	0.19
		0.0172	3.691	0.0156	0.2637	0.0139	0.1660	0.0135	0.2539	0.0133	0.02
		0.0162	0.0977	0.0153	0.0195	0.0127	0.2734	0.0121	0.3125	0.0123	0.16
		0.0138	0.1953	0.0099	0.2344	0.0083	0.2441	0.0120	0.1074	0.0114	0.11
		0.0093	0.3906	0.0098	0.1953	0.0082	0.3613	0.0117	0.1660	0.0088	0.23
				0.0098	0.0488			0.0116	0.2051	0.0076	0.41
				0.0087	0.3320			0.0093	0.4590	0.0074	0.28
								0.0081	0.3613		
	Drag Interaction Subtracted Out	0	0	<0.001	0.02	0.0017	0.10	0.0039	0.15	0.0055	0.18

STROUHAL NUMBER OF FORCED OSCILLATION (S_f)

0.18		0.20		0.22		0.25		0.30		0.40		0.80	
811	0.1953	0.1193	0.1953	0.0866	0.2197	0.0870	0.1953	0.0585	0.1953	0.0643	0.1953		
		0.0539	0.0977			0.0327	0.0977	0.0444	0.0732	0.0372	0.0977		
		0.0374	0.0244							0.0279	0.3906		
748	0.0684	0.0965	0.0684	0.0975	0.0391	0.0928	0.0293	0.1321	0.0879	0.1109	0.0391	0.0990	0.1563
660	0.1270	0.0861	0.1563	0.0469	0.1563	0.0840	0.1563	0.0805	0.1367	0.0750	0.1270	0.0588	0.0293
474	0.0098	0.0431	0.1074	0.0387	0.1270	0.0785	0.0586	0.0669	0.0098	0.0693	0.1660	0.0579	0.1172
456	0.1563	0.0260	0.2344	0.0338	0.0977	0.0531	0.0977	0.0590	0.1758	0.0425	0.0977	0.0461	0.0586
255	0.1855	0.0111	0	0.0258	0.2148	0.0204	0.2441	0.0199	0.3027	0.0170	0.2539	0.0396	0.0879
108	0.2637	0.0099	0.3223	0.0154	0.1855								
097	0.2148												
082	0.3125												
181	0.0586	0.0245	0.0195	0.0172	0.2051	0.0142	0.0879	0.0323	0.0195	0.0289	0.4004	0.1201	0.7910
154	0.1953	0.0163	0.3027	0.0161	0.0098	0.0139	0.0488	0.0229	0.0586	0.0189	0.0488	0.0363	0.0195
133	0.0293	0.0162	0.1172	0.0130	0.1563	0.0133	0.1465	0.0161	0.1953	0.0174	0.2246	0.0169	0.1270
123	0.1660	0.0136	0.1465	0.0122	0.1172	0.0131	0.2441	0.0118	0.2441	0.0153	0.0977	0.0142	0.0977
114	0.1172	0.0122	0.2148	0.0102	0.3516	0.0127	0.2930	0.0115	0.1367	0.0131	0.0195		
088	0.2344	0.0108	0.0781	0.0101	0.0879	0.0112	0.0195	0.0114	0.2930	0.0119	0.1270		
076	0.4102	0.0070	0.3809	0.0094	0.3711	0.0109	0.2051	0.0109	0.3320	0.0098	0.2539		
074	0.2832			0.0080	0.3125	0.0079	0.4297	0.0078	0.3613	0.0086	0.2832		
				0.0074	0.0586								
055	0.18	0.0070	0.20	0.0084	0.22	0.012	0.25	0.016	0.30	0.029	0.40	0.12	0.80

	0.40		0.80		1.00		2.00	
3	0.0643	0.1953			0.2464	0.1953	0.1407	0.1953
2	0.0372	0.0977			0.0436	0.3174	0.0508	0.0488
	0.0279	0.3906						
)	0.1109	0.0391	0.0990	0.1563				
'	0.0750	0.1270	0.0588	0.0293				
3	0.0693	0.1660	0.0579	0.1172				
3	0.0425	0.0977	0.0461	0.0586				
'	0.0170	0.2539	0.0396	0.0879				
	0.0289	0.4004	0.1201	0.7910				
	0.0189	0.0488	0.0363	0.0195				
	0.0174	0.2246	0.0169	0.1270				
	0.0153	0.0977	0.0142	0.0977				
	0.0131	0.0195						
	0.0119	0.1270						
	0.0098	0.2539						
	0.0086	0.2832						
	0.029	0.40	0.12	0.80				

		STROUHAL NUMBER OF FORCED OSCILLAT									
$R_n \times 10^5$		0.00		0.02		0.10		0.15		0.18	
9.73	C_{Li} & S_{Li}	0.0634	0.176	0.0763	0.0879	0.0841	0.1758	0.0652	0.1660	0.0583	0.0586
		0.0631	0.127	0.0615	0.0537	0.0735	0.1270	0.0574	0.0195	0.0534	0.1709
		0.0543	0.029	0.0612	0.1514	0.0689	0.0684	0.0555	0.1025	0.0527	0.0293
		0.0093	0.283	0.0546	0.1270	0.0675	0.0293	0.0487	0.0781	0.0507	0.0830
		0.0076	0.322	0.0529	0.1660	0.0540	0.0977	0.0468	0.1807	0.0404	0.0098
		0.0071	0.410	0.0498	0.0244	0.0127	0.2734	0.0437	0.1465	0.0372	0.0977
				0.0451	0.0049	0.0108	0.2441	0.0416	0.0586	0.0350	0.1318
				0.0438	0.1123			0.0404	0.1270	0.0344	0.1514
				0.0418	0.1807			0.0365	0.0391	0.0338	0.1904
				0.0292	0.1953			0.0260	0.2002	0.0258	0.1123
				0.0170	0.2393			0.0187	0.2197	0.0124	0.2393
				0.0154	0.2686			0.0104	0.2832	0.0085	0.2539
				0.0153	0.2197			0.0078	0.2344	0.0080	0.3027
				0.0108	0.2832			0.0074	0.3076		
								0.0072	0.2637		
								0.0068	0.2490		
	C_{Di} & S_{Li}	0.0186	0.10	0.0240	0.0146	0.0380	0.0098	0.0174	0.0293	0.0235	0.0098
		0.0146	0.147	0.0223	0.0342	0.0167	0.3125	0.0121	0.1123	0.0131	0.1123
		0.0128	0.195	0.0146	0.0977	0.0165	0.0879	0.0133	0	0.0126	0.2148
		0.0111	0.283	0.0127	0.1221	0.0146	0.2148	0.0129	0.2344	0.0120	0.0781
		0.0109	0.059	0.0126	0.0830	0.0146	0.3516	0.0126	0.0537	0.0119	0.1514
		0.0100	0.254	0.0125	0.1416	0.0125	0.1563	0.0121	0.1563	0.0111	0.0586
		0.0100	0.089	0.0119	0.2686	0.0083	0.2637	0.0116	0.2783	0.0080	0.1758
		0.0082	0.332	0.0115	0.2002	0.0079	0.4102	0.0097	0.0879	0.0077	0.4004
		0.0072	0.391	0.0101	0.2490	0.0059	0.4688	0.0084	0.2148	0.0074	0.3613
				0.0097	0.0684			0.0083	0.1709	0.0071	0.3369
				0.0096	0.2295			0.0081	0.3223	0.0069	0.2393
				0.0092	0.0488			0.0073	0.3467	0.0069	0.2637
				0.0083	0.3418			0.0070	0.0732	0.0064	0.1904
				0.0067	0.4102			0.0067	0.3125	0.0063	0.2832
				0.0062	0.3223			0.0064	0.1367		
				0.0062	0.1855			0.0050	0.4248		
				0.0060	0.3662			0.0047	0.2979		
				0.0047	0.4443			0.0047	0.3809		
				0.0047	0.5078						
	Drag Interaction Subtracted Out	0	0	<0.001	0.02	0.0017	0.10	0.0039	0.15	0.55	0.18

R OF FORCED OSCILLATION (S_f)												
	0.18		0.20		0.22		0.25		0.30		0.40	
50	0.0583	0.0586	0.0771	0.0586	0.0679	0.0635	0.0662	0.1709	0.0902	0.1563	0.0595	0.1660
95	0.0534	0.1709	0.0574	0.0781	0.0580	0.1074	0.0532	0.0586	0.0509	0.1416	0.0527	0.1318
25	0.0527	0.0293	0.0493	0.1074	0.0536	0.1514	0.0513	0.1318	0.0478	0.0879	0.0505	0.0977
31	0.0507	0.0830	0.0418	0.1367	0.0525	0.0195	0.0466	0.0977	0.0441	0.0684	0.0491	0.0488
07	0.0404	0.0098	0.0391	0.1758	0.0525	0.1807	0.0413	0.0342	0.0389	0.0488	0.0489	0.0684
55	0.0372	0.0977	0.0355	0.1221	0.0461	0.0879	0.0221	0.2490	0.0300	0.0244	0.0458	0.0342
36	0.0350	0.1318	0.0320	0.0244	0.0363	0.0049	0.0217	0.0781	0.0271	0.0049	0.0332	0.1807
70	0.0344	0.1514	0.0317	0.1514	0.0168	0.2197	0.0188	0.2295	0.0233	0.1172	0.0250	0.0049
91	0.0338	0.1904	0.0294	0.0098	0.0080	0.2979	0.0184	0.0195	0.0159	0.2979	0.0166	0.2051
02	0.0258	0.1123	0.0269	0.1904	0.0078	0.2637	0.0159	0.0049	0.0154	0.2051	0.0116	0.2393
97	0.0124	0.2393	0.0147	0.2148	0.0063	0.2441	0.0136	0.2148	0.0120	0.2246	0.0095	0.3955
32	0.0085	0.2539	0.0076	0.2783					0.0108	0.2734	0.0081	0.2881
44	0.0080	0.3027	0.0073	0.2490					0.0075	0.2490	0.0073	0.2686
76									0.0069	0.3467		
37												
90												
93	0.0235	0.0098	0.0189	0.0098	0.0240	0.0098	0.0167	0.1221	0.0198	0.0098	0.0310	0.3995
23	0.0131	0.1123	0.0151	0.1953	0.0196	0.0488	0.0152	0.0098	0.0144	0.0342	0.0197	0.0049
	0.0126	0.2148	0.0132	0.0342	0.0129	0.0977	0.0140	0.2490	0.0135	0.2979	0.0159	0.0684
44	0.0120	0.0781	0.0116	0.3027	0.0120	0.2246	0.0127	0.2100	0.0132	0.1367	0.0123	0.1270
37	0.0119	0.1514	0.0111	0.1367	0.0112	0.2881	0.0103	0.2246	0.0108	0.1611	0.0113	0.1611
63	0.0111	0.0586	0.0105	0.0928	0.0100	0.1172	0.0096	0.2832	0.0106	0.1123	0.0112	0.0293
83	0.0080	0.1758	0.0099	0.2148	0.0095	0.1563	0.0093	0.1367	0.0089	0.0830	0.0111	0.1953
79	0.0077	0.4004	0.0095	0.1514	0.0085	0.3955	0.0087	0.0342	0.0088	0.0586	0.0086	0.2734
48	0.0074	0.3613	0.0084	0.0830	0.0085	0.2588	0.0080	0.3711	0.0087	0.3418	0.0085	0.3418
09	0.0071	0.3369	0.0073	0.0635	0.0081	0.2002	0.0074	0.3467	0.0080	0.2148	0.0076	0.3027
23	0.0069	0.2393	0.0065	0.4150	0.0068	0.1318	0.0072	0.1611	0.0080	0.2441	0.0075	0.0439
67	0.0069	0.2637	0.0062	0.2686	0.0067	0.1416	0.0072	0.0781	0.0076	0.3174	0.0071	0.2393
32	0.0064	0.1904	0.0059	0.3467	0.0061	0.3027	0.0064	0.0635	0.0070	0.2783	0.0060	0.2588
25	0.0063	0.2832	0.0058	0.2490			0.0063	0.4150	0.0065	0.1953	0.0054	0.4639
167									0.0063	0.1758		
148												
179												
309												
5	0.55	0.18	0.0020	0.20	0.0084	0.22	0.012	0.25	0.016	0.30	0.029	0.40

APPENDIX E

LIFT AND DRAG COEFFICIENTS FOR CYLINDER OSCILLATING IN PITCH AND HEAVE

STROUHAL NUMBER OF FORCED OSCILLATION (S_f)									
ϵ/D	$R_n \times 10^5$		0.10	0.15	0.18	0.20	0.22	0.25	0.30
+0.25	9.73	$(C_L)_{p-p}$	0.5624(8)	0.8390(12)	0.6508(6)	0.8502(11)	0.7708(5)	0.4534(6)	0.6018(7)
		$(C_L)_{rms}$	0.0882(8)	0.1135(12)	0.1065(6)	0.1094(11)	0.1287(5)	0.0806(6)	0.0920(7)
		$(C_D)_{ave}$	0.5680	0.6091	0.6107	0.5909	0.5904	0.5806	0.5948
		$(C_D)_{p-p}$	0.1870(14)	0.2190(14)	0.1890(14)	0.2798(19)	0.2164(11)	0.1961(15)	0.2020(14)
		$(C_D)_{rms}$	0.0217(14)	0.0242(14)	0.0217(14)	0.0259(19)	0.0304(11)	0.0222(15)	0.0239(14)
-0.25	9.73	$(C_L)_{p-p}$	0.4428(6)	0.5788(6)	0.7938(11)	0.6170(8)	0.6856(14)	0.8078(12)	0.7778(12)
		$(C_L)_{rms}$	0.0724(6)	0.0931(6)	0.0991(11)	0.0945(8)	0.0777(14)	0.0939(12)	0.0927(12)
		$(C_D)_{ave}$	0.5488	0.5709	0.5726	0.5599	0.5699	0.5653	0.5621
		$(C_D)_{p-p}$	0.1969(14)	0.2292(16)	0.2436(17)	0.1943(11)	0.2292(18)	0.2710(19)	0.2348(18)
		$(C_D)_{rms}$	0.0224(14)	0.0238(16)	0.0231(17)	0.0252(11)	0.0220(18)	0.0240(19)	0.0233(18)

STROUHAL NUMBER OF FORCED OSCILLATION (S_f)																
ϵ/D	$R_n \times 10^5$		0.10		0.15		0.18		0.20		0.22		0.25		0.30	
+0.25	9.73	C_{Li} & S_{Li}	0.07854	0.0488	0.09866	0.0195	0.08790	0.1758	0.06611	0.1660	0.09990	0.0684	0.07733	0.0684	0.06608	0.1465
			0.05577	0.1563	0.07037	0.1172	0.07570	0.0195	0.06330	0.0049	0.8010	0.0391	0.05799	0.1855	0.06194	0.2930
			0.04996	0.1172	0.06198	0.1462	0.06585	0.1074	0.06224	0.1904	0.07909	0.1367	0.04851	0.2441	0.05369	0.1074
			0.04139	0.0098	0.06002	0.0781	0.05512	0.2051	0.05647	0.0586	0.07519	0.0977	0.03786	0.1270	0.05158	0.0391
			0.03275	0.1953	0.05081	0.1953	0.04378	0.0488	0.05371	0.0684	0.07315	0.2148	0.02461	0	0.05016	0.1855
			0.009814	0.2344	0.01596	0.3711	0.01189	0.3125	0.05201	0.1074			0.008876	0.3613	0.04706	0.0098
			0.009232	0.3125	0.01527	0.2441			0.04986	0.1221					0.01140	0.2539
			0.008348	0.3418	0.01281	0.2930			0.01473	0.2246						
					0.01266	0.4102			0.01179	0.2588						
					0.01093	0.4688			0.007451	0.3174						
					0.01035	0.4395			0.005745	0.2930						
					0.009924	0.6348										
		Lift Interaction Subtracted Out	0.0046	0.10	0.0102	0.15	0.0148	0.18	0.0183	0.20	0.0220	0.22	0.0285	0.25	0.0410	0.30

STROUHAL NUMBER OF FORCED OSCILLATION (S_f)																
ϵ/D	$R_n \times 10^5$		0.10		0.15		0.18		0.20		0.22		0.25		0.30	
+0.25	9.73	C_{Di} & S_{Di}	0.01710	0.0098	0.01711	0.3320	0.01543	0.0586	0.01797	0.0098	0.03301	0.0098	0.01962	0.0098	0.01823	0.0195
			0.01330	0.1563	0.01456	0.1465	0.01409	0.1172	0.01409	0.0977	0.01275	0.2246	0.01342	0.0586	0.01819	0.2930
			0.01080	0.0781	0.01252	0.0879	0.01133	0.1660	0.01192	0.1172	0.01272	0.0684	0.01071	0.2637	0.01310	0.1270
			0.01053	0.3320	0.01247	0.2441	0.01018	0.2148	0.009949	0.0977	0.01142	0.0977	0.01005	0.1367	0.01270	0.1758
			0.008889	0.0977	0.008844	0.0488	0.009070	0.3223	0.009800	0.2100	0.01142	0.1465	0.00869	0.1074	0.009971	0.2148
			0.008423	0.2441	0.008532	0.1172	0.007986	0.2637	0.008264	0.0781	0.009138	0.2734	0.008181	0.2148	0.009083	0.0977
			0.005302	0.3809	0.007428	0.2734	0.007865	0.3613	0.008144	0.2881	0.008464	0.3027	0.007232	0.1855	0.008319	0.2539
			0.004407	0.4199	0.007131	0.0195	0.005982	0.5176	0.007827	0.1465	0.006543	0.3711	0.005906	0.3906	0.008098	0.4102
			0.003900	0.2051	0.005478	0.3906	0.004636	0.4297	0.007740	0.1660	0.004312	0.3418	0.004810	0.3516	0.004872	0.5078
			0.002684	0.4688	0.005237	0.4883	0.003417	0.5762	0.006044	0.0439	0.003722	0.4395	0.004168	0.3223	0.003484	0.4785
			0.002655	0.5176	0.004948	0.4395	0.002997	0.6250	0.006038	0.3027	0.002943	0.4980	0.003974	0.4883	0.002896	0.6055
			0.002564	0.6445	0.003602	0.6250	0.002454	0.6641	0.005972	0.2539			0.003959	0.5469	0.002484	0.8594
			0.002402	0.5566	0.003078	0.5469	0.002318	0.8008	0.005894	0.2734			0.002879	0.5859	0.002399	0.8203
			0.002216	0.7031	0.002357	0.7129	0.002247	0.7031	0.005543	0.0635			0.002571	0.6543	0.002637	0.7813
									0.005406	0.2393			0.002568	0.7324		
									0.004606	0.4248						
									0.004018	0.3955						
									0.003862	0.4492						
									0.003585	0.3760						
		Drag Interaction Subtracted Out	0.00167	0.10	0.00382	0.15	0.00550	0.18	0.00675	0.20	0.00820	0.22	0.0106	0.25	0.0152	0.30

STROUHAL NUMBER OF FORCED OSCILLATION (S_f)																
ϵ/D	$R_n \times 10^5$		0.10		0.15		0.18		0.20		0.22		0.25		0.30	
-0.25	9.73	C_{Li} & S_{Li}	0.06598	0.0586	0.06822	0.0293	0.08049	0.0684	0.07032	0.0586	0.05237	0.0488	0.05577	0.0684	0.06749	0.0293
			0.04636	0.0789	0.06672	0.1758	0.05006	0.1514	0.06567	0.0293	0.04620	0.0098	0.05278	0.0293	0.05369	0.0879
			0.04329	0.1563	0.06377	0.1367	0.04954	0.0977	0.06482	0.0977	0.03910	0.1074	0.04855	0.1904	0.04686	0.0098
			0.03983	0.0293	0.04804	0.0684	0.04870	0.1855	0.05278	0.1563	0.03826	0.0635	0.04647	0.1514	0.04472	0.2979
			0.02124	0.2051	0.04320	0.1074	0.04213	0.0049	0.03938	0.1953	0.03307	0.0928	0.04388	0.0830	0.04447	0.1563
			0.009286	0.2734	0.009631	0.3027	0.04100	0.0244	0.01463	0.2441	0.03242	0.1807	0.03887	0.0488	0.03995	0.0604
							0.03394	0.1270	0.01044	0.2832	0.03085	0.1611	0.03877	0.1172	0.03755	0.1318
							0.02896	0.1172	0.008768	0.3223	0.02744	0.2197	0.03813	0.1318	0.02809	0.1855
							0.02281	0.2197			0.02001	0.1367	0.03267	0.2490	0.02630	0.2051
							0.007508	0.3467			0.01371	0.2051	0.02175	0.2148	0.02533	0.1123
							0.006570	0.3125			0.009730	0.2490	0.007445	0.2686	0.008136	0.2686
											0.007905	0.2832	0.007281	0.3125	0.007337	0.2539
											0.007353	0.2686				
											0.006404	0.3076				
		Lift Interaction Subtracted Out	0.0046	0.10	0.0102	0.15	0.0148	0.18	0.0183	0.20	0.0220	0.22	0.0285	0.25	0.0410	0.30

STROUHAL NUMBER OF FORCED OSCILLATION (S_f)																
ϵ/D	$R_n \times 10^5$		0.10		0.15		0.18		0.20		0.22		0.25		0.30	
-0.25	9.73	C_{Di} & S_{Di}	0.01515	0.0293	0.01385	0.1172	0.01396	0.0146	0.02370	0.0098	0.01307	0.0098	0.01332	0.2490	0.01765	0.0098
			0.01514	0.0879	0.01339	0.0098	0.01159	0.0879	0.01240	0.2148	0.01204	0.2100	0.01249	0.0293	0.01754	0.2979
			0.01193	0.2734	0.01170	0.2051	0.01144	0.1416	0.01239	0.0391	0.01156	0.0435	0.01083	0.0049	0.01264	0.1270
			0.01063	0.1953	0.01140	0.0391	0.01000	0.0635	0.01077	0.1367	0.01062	0.1221	0.01079	0.0488	0.009725	0.1953
			0.008722	0.1367	0.01093	0.2637	0.009355	0.2197	0.01031	0.1074	0.009858	0.0977	0.008975	0.2295	0.008403	0.0488
			0.008452	0.1660	0.01077	0.1465	0.009017	0.1660	0.009582	0.3125	0.009532	0.0635	0.008927	0.0635	0.008343	0.0977
			0.008357	0.3711	0.01075	0.1855	0.008064	0.0293	0.007727	0.1758	0.006829	0.1514	0.008400	0.3125	0.007186	0.1514
			0.004546	0.4590	0.006728	0.3320	0.007966	0.2637	0.004841	0.3516	0.006265	0.3223	0.007799	0.1318	0.007140	0.2441
			0.003853	0.4395	0.005500	0.3906	0.006945	0.1953	0.004400	0.6152	0.006001	0.1904	0.007676	0.1611	0.005629	0.3857
			0.003082	0.6934	0.004302	0.5371	0.006618	0.2881	0.004292	0.4590	0.005947	0.1660	0.007428	0.1855	0.005598	0.3467
			0.002906	0.6055	0.003836	0.4980	0.005544	0.1074	0.003499	0.4102	0.005095	0.1367	0.007143	0.3564	0.005415	0.3174
			0.002812	0.7910	0.003429	0.4297	0.005318	0.3174			0.004784	0.2686	0.006971	0.1123	0.005284	0.0684
			0.002381	0.5371	0.003302	0.4688	0.004817	0.3467			0.004500	0.3076	0.006455	0.2051	0.004777	0.3320
			0.002162	0.5762	0.003104	0.6445	0.004538	0.4443			0.004149	0.2393	0.006381	0.0928	0.004296	0.6152
					0.002738	0.5762	0.004319	0.3027			0.003249	0.4932	0.006108	0.2881	0.004085	0.2148
					0.002730	0.7910	0.004129	0.3760			0.003198	0.3418	0.004382	0.3857	0.003074	0.4541
							0.003707	0.4053			0.003125	0.7080	0.004232	0.1465	0.002914	0.4688
											0.003013	0.4053	0.004048	0.4395	0.002901	0.4150
													0.003779	0.3955		
		Drag Interaction Subtracted Out	0.00167	0.10	0.00382	0.15	0.00550	0.18	0.00675	0.20	0.00820	0.22	0.0106	0.25	0.0152	0.30

REFERENCES

1. Morkovin, M.V., "Flow around Circular Cylinder--A Kaleidoscope of Challenging Fluid Phenomena," ASME Symposium on Fully Separated Flows (May 1964).

2. Marris, A.W., "A Review on Vortex Streets, Periodic Wakes, and Induced Vibration Phenomena," ASME Paper 62-WA-106 (1962).

3. "Instruction Manual: Pitch-Heave Oscillator," Prepared for Consolidated Systems Corporation, TM 3-3081, David Taylor Model Basin (15 Apr 1964).

4. Keefe, R.T., "An Investigation of the Fluctuating Forces Acting on a Stationary Circular Cylinder in a Subsonic Stream and of the Associated Sound Field," University of Toronto Institute of Aero. Physics, UTIA Report 76 (Sep 1961).

5. Macovsky, M.S., "Vortex-Induced Vibration Studies," David Taylor Model Basin Report 1190 (Jul 1958).

6. Sommerville, D.E. and D.R. Kobett, "Research and Development Services Covering Wind Induced Oscillations of Vertical Cylinders," Midwest Research Institute, Contract DA-23-072-ORD-1264, Phase Report 2, MRI Project 2190-P (Apr 1959).

7. Graham, C., "A Survey of Correlation Length Measurements of the Vortex Shedding behind a Circular Cylinder," MIT Engineering Projects Lab Report 76028-1, Prepared under Contract Nonr. 3963(25) (Oct 1966).

8. Luistro, J.A., "Lift and Drag Coefficients for a Smooth Circular Cylinder at High Reynolds Numbers," David Taylor Model Basin Report 1405 (Nov 1960).

9. Warren, W.F., "An Experimental Investigation of Fluid Forces on an Oscillating Cylinder," Ph.D. Thesis, University of Maryland (1962).

10. Cahn, R.D., "The Nature of Flow Separation from a Circular Cylinder Near the Critical Reynolds Number," Masters Thesis, University of Maryland, Aeronautical Engineering Department (1963).

11. Schenck, H., "Theories of Engineering Experimentation," McGraw-Hill Book Company, Inc., New York (1961).

12. Sretensky, L.N., "Motion of a Cylinder under the Surface of a Heavy Fluid," NACA TM 1335 (Aug 1953).

13. Wang, H.T., "Survey of the Magnitude and Correlation of the Lift Force Acting on a Nonoscillating Circular Cylinder," NSRDC Report 3335 (in review).

14. Coder, D.W., "Location of Separation on a Circular Cylinder in Crossflow as a Function of Reynolds Number," NSRDC Report 3647 (Nov 1971).

15. Fung, Y.C., "Fluctuating Lift and Drag Acting on a Cylinder in a Flow at Supercritical Reynolds Numbers," IAS Paper 60-6 (Jan 1960).

16. Bishop, R.E.D. and A.Y. Hassan, "The Lift and Drag Forces on a Circular Cylinder Oscillating in a Flowing Fluid," Proc. of the Royal Society, A, Vol. 277, pp. 51-75 (1963).

INITIAL DISTRIBUTION

Copies	
1	Waterways Exp Station Research Center Lib
3	CHONR 1 Boston 1 Chicago 1 Pasadena
3	NRL 1 Code 2027, Lib 1 Charles Votaw 1 Dr. G.H. Koopman
3	USNA 1 Lib 1 Dr. Bruce Johnson 1 Prof P. Van Mater
3	USNPGSCOL 1 Lib 1 Prof J. Miller 1 Dr. T. Sarpkaya
1	USNROTC, MIT
1	NAVWARCOL
5	NAVSHIPSYSCOM 1 SHIPS 2052 1 SHIPS 03412 1 SHIPS 0342 1 SHIPS 037 1 PMS 381
1	NAVFACENGCOM FAC 0321
1	NAVORDSYSCOM ORD 035
2	NADC 1 Tech Lib 1 J.R. Dale
1	NELC Lib
1	NUC San Diego Dr. A. Fabula
1	NUC Pasadena Dr. J. Hoyt
1	NWC Code 753

Copies	
1	NCEL Code L31
1	NCSL Lib
1	NUSC
1	NAVSHIPYD BOSTON Lib
1	NAVSHIPYD CHARLESTON Lib
3	NAVSHIPYD HUNTERS PT 1 Tech Lib 1 Code 250 1 Code 1301L
1	NAVSHIPYD NORFOLK Lib
1	NAVSHIPYD PEARL HARBOR Code 246-P
1	NAVSHIPYD PHILADELPHIA Code 240 ABCF
1	NAVSHIPYD PORTSMOUTH Lib
1	NAVSHIPYD PUGET SOUND Eng Lib
8	NAVSEC 1 SEC 6034B 1 SEC 6053B 1 SEC 6110 1 SEC 6114D 1 SEC 6136 1 SEC 6140 1 SEC 6144G 1 SEC 6660, D.L. Blount
1	AFOSR/SREM
1	AFFDL/FDDS, J. Olsen
12	DDC
1	Bureau of Standards Fluid Mechanics Br Dr. G.B. Schaubauer
2	COGARD 1 Div of Merchant Marine Safety

Copies	
1	Lib of Congress
1	NASA
1	Nat'l Sci Foundation
1	Univ of Bridgeport Bridgeport, Conn. 06602 Attn: Prof. Earl Uram Mech Engr Dept
1	Brown Univ Providence, R.I. 02912 Attn: Div of Applied Math
4	Univ of Calif, Berkeley Naval Architecture Dept College of Engr Attn: 1 Lib 1 Prof J.R. Paulling 1 Prof J.V. Wehausen 1 H.A. Schade
1	Univ of Calif, Scripps La Jolla, Calif 92038 1 J. Pollock
1	Univ of Calif at San Diego Dept of Applied Mechanics La Jolla, Calif 92038 Attn: Dr. Albert T. Ellis
3	Calif Inst of Technology Pasadena, Calif 91109 Attn: 1 Dr. A.J. Acosta 1 Dr. T.Y. Wu 1 Dr. M.S. Plesset
1	Colorado State Univ Dept of Civil Engr Fort Collins, Colorado 80521 Attn: Prof. M. Albertson
1	Univ of Connecticut Box U-37 Storrs, Connecticut 06268 Attn: Prof. V. Scottron Hydraulic Research Lab
1	Cornell Univ Graduate School of Aerospace Engr Ithaca, New York 14850 Attn: Prof. W.R. Sears

Copies	
1	Harvard Univ 2 Divinity Avenue Cambridge, Mass 02138 Attn: Prof. G. Birkhoff Dept of Mathematics
1	Harvard Univ, Pierce Hall Cambridge, Mass 02138 Attn: Prof. G.F. Carrier
2	Univ of Ill. College of Engr Urbana, Ill 61801 Attn: 1 Dr. J.M. Robertson Theoretical & Applied Mechs Dept 1 Dr. Ben Chie Yen Hydrosystems Lab
2	Univ of Iowa Iowa City, Iowa 52240 Attn: 1 Dr. Hunter Rouse 1 E.O. Macagno
2	Univ of Iowa Iowa Inst of Hydraulic Res Iowa City, Iowa 52240 Attn: 1 Dr. L. Landweber 1 Dr. J. Kennedy
1	JHU, Mechanics Dept Baltimore, Md. 21218 Attn: Prof. O.M. Phillips
1	Kansas State Univ Engr Experiment Station Seaton Hall Manhattan, Kansas 66502 Attn: Prof. D.A. Nesmith
1	Univ of Kansas Lawrence, Kansas 60644 Attn: Chm Civil Engr Dept
1	Lehigh Univ Bethlehem, Pa. 18015 Attn: Fritz Lab Lib
1	Long Island Univ Graduate Dept of Marine Sci 40 Merrick Ave East Meadow, N.Y. 11554 Attn: Prof. David Price

Copies	
3	Univ of Md. Mechanical Engr Dept College Park, Md. Attn: 1 Dr. C.L. Sayre 1 Dr. J.E. John 1 Dr. F. Buckley
1	MIT, Hydrodynamics Lab Cambridge, Mass. 02139 Attn: Prof. A.T. Ippen
7	MIT, Dept of Naval Arch & Marine Engr Cambridge, Mass. 02139 Attn: 1 Dr. A.H. Keil, Head Dept of Engr 1 Prof. P. Mandel 1 Prof. J.R. Kerwin 1 Prof. P. Leehey 1 Prof. M. Abkowitz 1 Prof. F.M. Lewis 1 Dr. J.N. Newman
3	Univ of Michigan Dept of Naval Arch & Marine Engr Ann Arbor, Michigan 48104 Attn: 1 Dr. T.F. Ogilvie 1 Prof. H. Benford 1 Dr. F.G. Michelsen
5	Univ of Minnesota St. Anthony Falls Hydra Lab Mississippi River at 3rd Ave. S.E., Minneapolis, Minn. 55414 Attn: 1 Director 1 Dr. C.S. Song 1 Mr. J.M. Killeen 1 Mr. F. Schiebe 1 Mr. J.M. Wetzel
1	Newark College of Engr 323 High Street Newark, N.J. 07102 Attn: Dr. W.L. Haberman
1	New York Univ Univ Heights Bronx, New York 10453 Attn: Prof. W. Pierson, Jr.
2	New York Univ Courant Inst of Math Sci 251 Mercier Street New York, N.Y. 10012 Attn: 1 Prof A.S. Peters 1 Prof. J.J. Stoker
3	Univ of Notre Dame Notre Dame, Indiana 46556 Attn: 1 Dr. A. Strandhagen 1 Dr. J. Nicolaides 1 Prof. A.A. Szewczyk
1	Ohio Northern Univ College of Engr Ada, Ohio Attn: Dr. R.J. Glass
1	Penn State Univ Ordnance Research Lab Univ Park, Pa. 16801 Attn: Director
1	Princeton Univ James F. Res Cen Dept of Aerospace & Mechanical Sci Attn: Prof. G. Mellor
1	St. Johns Univ Dept of Mathematics Jamaica, N.Y. 11432 Attn: Prof. Jerome Lurye
3	Stanford Univ Stanford, Calif 94305 Attn: 1 Prof H. Ashley Dept Aeronautics & Astronautics 1 Prof. R. Street 1 Prof. B. Perry Dept Civil Engr
3	SIT, Davidson Lab 711 Hudson Street Hoboken, N.J. 07030 Attn: 1 Dr. J.P. Breslin 1 Dr. S. Tsakonas 1 Library
1	Univ of Texas Defense Research Lab P.O. Box 8029 Austin, Texas 78712 Attn: Director

Copies

1 Utah State Univ
College of Engr
Logan, Utah 84321
Attn: Dr. Roland W. Jeppson

1 Univ of Washington
Applied Physics Lab
1013 N.E. 40th Street
Seattle, Wash 98105
Attn: Director

1 WHOI, Woods Hole, Mass 02543
Attn: Reference Rm ABCDF

1 Worcester Polytechnic Inst
Alden Research Labs
Worcester, Mass 01609
Attn: Director

1 Aerojet-General Corp
1100 W. Hollyvale Street
Azusa, Calif 91702
Attn: Mr. J. Levy
Bldg 160, Dept 4223

1 Bethlehem Steel Corp
Central Technical Div
Sparrows Point Yard
Sparrows Point, Md. 21219
Attn: Mr. A. Haff,
Technical Director

1 Bolt Beranck & Newman, Inc.
1501 Wilson Blvd
Arlington, Va. 22209
Attn: Dr. F. Jackson

1 Cambridge Acoustical
Associates, Inc
129 Mount Auburn Street
Cambridge, Mass 02138
Attn: Mr. M.C. Junger

1 Cornell Aeronautical Lab
Applied Mechanics Dept
O.O. Box 235
Buffalo, N.Y. 14221

1 Eastern Research Group
P.O. Box 222
Church Street Station
New York, N.Y. 10006

Copies

1 Esso International
15 West 51st Street
Mew York, N.Y. 10019
Attn: Mr. R.J. Taylor,
Manager R&D Tanker Dept

1 Gen Applied Sci Labs, Inc.
Merrick & Stewart Avenues
Westbury, L.I., N.Y. 11590
Attn: Dr. F. Lane

1 General Dynamics/
Electric Boat, Groton,
Connecticut 05340
Attn: Mr. V. Boatwright, Jr.

1 Gibbs & Cox, Inc.
21 West Street
New York, N.Y. 10006
Attn: Tech Lib

1 Grumman Aircraft Engr Corp
Bethpage, L.I., N.Y. 11714
Attn: Mr. W. Carl

2 Hydronautics, Inc
Pindell School Road
Laurel, Md. 20810
Attn: 1 Mr. P. Eisenberg
1 Mr. M. Tulin

2 McDonnell Douglas Aircraft
Douglas Aircraft Div
3855 Lakewood Blvd
Long Beach, Calif 90801
Attn: 1 Mr. John Hess
1 Mr. A.M.O. Smith

1 Measurement Analysis Corp
10960 Santa Monica Blvd
Los Angeles, Calif 90025
DF

1 NNSB & DD Co
Newport News, Va. 23607
Attn: Tech Lib Dept

1 North American Rockwell, Inc
Space & Info Systems Div
12214 Lakewood Blvd
Downey, Calif 90241
Attn: Mr. B.H. Ujihara

Copies	
1	Oceanics, Inc. Tech Industrial Park Plainview, L.I., N.Y. 11803 Attn: Dr. Paul Kaplan
1	SNAME, 74 Trinity Place New York, N.Y. 10006
2	Southwest Research Inst 8500 Culebra Road San Antonio, Texas 78206 Attn: 1 Dr. H. Abramson 1 Applied Mechanics Review
1	Stanford Research Inst Menlo Park, Calif 94025 Attn: Lib
1	Systems Technology, Inc. 13766 South Hawthorne Blvd Hawthorne, Calif 90250 Attn: Ms. Arlene Muise, Lib.
1	Robert Taggart, Inc. 3930 Walnut Street Fairfax, Va. 22030 Attn: Mr. R. Taggart
1	Tracor, Inc. 6500 Tracor Lane Austin, Texas 78721

CENTER DISTRIBUTION

Copies	Code	Copies	Code
1	15	1	1556
1	1502	1	156
1	1504	1	1564
1	1506	1	1843
1	152	1	1942
1	154	1	1962
1	1541	1	1966
1	1542		
1	1544		
1	1548		
1	1552		

UNCLASSIFIED
Security Classification

DOCUMENT CONTROL DATA - R & D

(Security classification of title, body of abstract and indexing annotation must be entered when the overall report is classified)

1. ORIGINATING ACTIVITY *(Corporate author)*
Naval Ship Research and Development Center
Bethesda, Maryland 20034

2a. REPORT SECURITY CLASSIFICATION
None

2b. GROUP

3. REPORT TITLE
HYDRODYNAMIC FORCES ON OSCILLATING AND NONOSCILLATING SMOOTH CIRCULAR CYLINDERS IN CROSSFLOW

4. DESCRIPTIVE NOTES *(Type of report and inclusive dates)*
Final Report

5. AUTHOR(S) *(First name, middle initial, last name)*
David W. Coder

6. REPORT DATE
October 1972

7a. TOTAL NO. OF PAGES
89

7b. NO. OF REFS
16

8a. CONTRACT OR GRANT NO.

b. PROJECT NO.
54611 010

c Task 11098

d.

9a. ORIGINATOR'S REPORT NUMBER(S)
3639

9b. OTHER REPORT NO(S) *(Any other numbers that may be assigned this report)*

10. DISTRIBUTION STATEMENT
APPROVED FOR PUBLIC RELEASE: DISTRIBUTION UNLIMITED

11. SUPPLEMENTARY NOTES

12. SPONSORING MILITARY ACTIVITY
Naval Ship Systems Command
Washington, D.C. 20360

13. ABSTRACT

A 12-in.-diameter, 6-ft-long cylinder was towed horizontally 4 ft beneath the water surface and perpendicular to the flow. The cylinder was towed at a constant velocity under the following conditions: nonoscillating, oscillating in heave, oscillating in pitch (around the axis of the cylinder), and simultaneously oscillating in pitch and heave. Experimental data on lift, drag, and moment were obtained for Reynolds numbers from about 10^5 to above 10^6. The results show that the oscillations can significantly influence the magnitude of the lift, drag, and moment.

DD FORM 1 NOV 65 1473 (PAGE 1)
S/N 0101-807-6801

UNCLASSIFIED
Security Classification

14. KEY WORDS	LINK A		LINK B		LINK C	
	ROLE	WT	ROLE	WT	ROLE	WT
Lift, Drag, and Moment Coefficients						
Experimental Hydrodynamics						
Oscillating Cylinder						
Strouhal Number						
Reynolds Number						

GPO 938-240